

Effect of cholesterol on the interaction of charged lipids with alkali metal salts

**Thesis Submitted to Jadavpur University
for the Degree of Doctor of Philosophy (Science)**

by

Kalyan Kumar Banerjee

Index No. 68/20/Phys./27

Supervisor:

Prof. Sanat Karmakar



Department of Physics

Jadavpur University

Kolkata – 700 032

India

2025



শাদতপুত্র বিশ্ববিদ্যালয়
JADAVPUR UNIVERSITY

Prof. (Dr.) Sanat Karmakar

Professor

Department of Physics

CERTIFICATE FROM THE SUPERVISOR

This is to certify that the thesis entitled “**Effect of cholesterol on the interaction of charged lipids with alkali metal salts**” submitted by **Mr. Kalyan Kumar Banerjee** who got his name registered on 25.11.2020 for the award of **Ph.D. (science)** degree of **Jadavpur University**, is absolutely based upon his own work under the supervision of **Prof. Sanat Karmakar** and that neither this thesis nor any part of it has been submitted for either any degree / diploma or any other academic award anywhere before.

Sanat Karmakar



Prof. Sanat Karmakar
Department of Physics
Jadavpur University
Kolkata-700032, India

Prof. Sanat Karmakar

(Signature of the Supervisor, date with official seal)

Telephone: +91 33 24572879 (O);

9477507538 (M)

Email: sanat.karmakar@jadavpuruniversity.in / sanatkarmakar@gmail.com

Web: <https://sites.google.com/site/sanatkarmakar/>

Dedicated to Maa and Bapi ...

DECLARATION

I hereby declare that the work reported in this thesis is entirely original. I have composed this thesis independently at Jadavpur University under the supervision of Prof. Sanat Karmakar and all the literature has been properly cited. The work presented in this thesis has not been used previously for the award of any degree, diploma, membership, associate ship, fellowship or any other similar title of any university or institution.



Prof. Sanat Karmakar

Soft Matter and Bio-physics laboratory

Department of physics

Jadavpur University

Kolkata- 700 032

INDIA

(Kalyan Kumar Banerjee)

ACKNOWLEDGEMENT

My research work will remain incomplete if I do not offer my regards and thanks to those people, who helped me during this course.

First of all, I would like to express my deepest gratitude to my supervisor Prof. Sanat Karmakar for giving me the opportunity to work under his supervision. His invaluable guidance, advice and constant encouragement inspired me throughout my research tenure and that will help also for my future academic career.

I am extremely thankful to my collaborator Dr. Krishnananda Chattopadhyay at CSIR-IICB, Kolkata, for academic discussions and for allowing me to use his laboratory and instruments whenever required. Without his help and support I could not be able to complete my work within time. I also thankful to all lab members of his group.

I want to express my sincere thanks to honourable Vice-Chancellor, Mahatma Gandhi University Prof. Sourangshu Mukhopadhyay sir for his constant encouragement throughout my Ph.D journey.

I record my sincere thanks to HOD physics Prof. Nabin Baran Manik, Prof. Sukhen Das Prof. Kalyan Kumar Chattopadhyay, Prof. Joydeep Chowdhury, Prof. Partha Pratim Ray, Prof. Pabitra Kumar Pal, Prof. Chittaranjan Sinha, Dr. Saubhik Halder and other faculty members of the Department of Physics, Jadavpur University.

The peaceful atmosphere and free environment of Jadavpur University made every day of my research tenure very much pleasant. I thank everyone in the administrative department and gratefully acknowledge Jadavpur University for providing me the infrastructural facilities for my research.

I am thankful to my lab colleague Pabitra da, Animesh da, Subir Da, Surajit Da, Ranajoy, Debjita for academic, non-academic discussions and making my days enjoyable.

I remember my indebtedness to Amit da, Sandip da, Souvik da and all the staff members of this department for their help in various official work.

Special thanks to Dyutiman Da, Anupam da of fellowship section and Azizur da, Subhadeep da and Mona da of PhD cell for their constant help in my official work. My sincere thanks to

all security staff, canteen staff, hostel staff and everyone at Jadavpur University for making my stay enjoyable.

I thank the Govt. of West Bengal and Jadavpur University for my fellowship.

Whatever I am and whatever I intend to be in future are because of the goodwill and unstinted encouragements that I have received from my parents. No words are enough to acknowledge them. They are the source of my inspiration.

Last but not the least I must extend my deepest respect to my grandfather late Suryanarayan Banerjee, uncle late Sankar Prosad Banerjee and also grateful to my uncle Shiba Prosad Banerjee, brother Rajarshi and Sudip, sister Mousumi and Sudipa , brother in law Anupam, my beloved niece Asmita and rest of the family members for their constant encouragement. I thank all my friends, teachers, relatives and well-wishers for their support, whom I could not mention by name.

CONTENTS

Chapter 1: Introduction	1-15
1.1 Brief introduction to amphiphilic molecules	2
1.2 Lipids and their classifications	3
1.3 Self-assembly of amphiphilic molecules	4
1.4 Phase behaviour of lipid-water system	7
1.5 Lipid bilayer as a model system of biological membrane	10
1.6 Importance of ions in biological membrane	11
1.7 Influence of cholesterol on biological membranes	12
Chapter 2: Experimental Techniques	16-35
2.1 Introduction	16
2.2 Preparation of small unilamellar vesicles (SUV)	16
2.3 Preparation of large unilamellar vesicles (LUV)	17
2.4 Characterization of Vesicles	18
2.4.1 Size measurement using dynamic light scattering (DLS)	18
2.4.2 Zeta potential	21
2.5 Fluorescence spectroscopy	24
2.5.1 Origin of fluorescence	24
2.6 Isothermal titration calorimetry	25
2.6.1 Surface potential model	26
2.7 Small Angle X-ray Scattering (SAXS)	28
2.8 Preparation of giant unilamellar vesicles (GUV)	30
2.9 Phase contrast optical microscopy	31
Chapter 3: Studies on effect of cholesterol on the ion-membrane interaction in unsaturated phospholipids	36-53
3.1 Introduction	36
3.2 Earlier studies	36
3.3 Experimental results and discussions	38
3.3.1 Size distributions of vesicles containing cholesterol: Effect of NaCl	38

3.3.2 Effect of cholesterol on the ion-membrane interaction: Zeta potential	40
3.3.3 Electrostatics of the membrane: Gouy Chapman model	42
3.3.4 Binding of ions as evidenced from fluorescence spectroscopy	44
3.3.5 Discussion	45
3.4 Conclusion	49

Chapter 4: Interaction of sodium salt with DMPC/DMPG membrane: Effect of cholesterol **54-73**

4.1 Introduction	54
4.2 Earlier studies	55
4.3 Results	57
4.3.1 Interaction of NaCl with membranes composed of saturated lipids DMPC: ITC study	57
4.3.2 Effect of cholesterol on the ion-membrane interaction	58
4.3.2.1 Interaction of NaCl with binary mixture of DMPC and cholesterol	58
4.3.2.2 Effect of Na ⁺ ions on the ternary mixture of DMPC, DMPG and cholesterol	58
• Size distribution of LUV as observed from DLS	58
• Binding of cations with the anionic membrane containing cholesterol: Zeta potential study	60
4.3.3 Effect of cholesterol on the ion-membrane interaction: Fluorescence spectroscopy study	62
4.3.4 Fluorescence Correlation Spectroscopy	66
4.3.5 Discussion	67
4.4 Conclusion	70

Chapter 5: Interaction of alkali metal salts with membranes made up of lecithin and cholesterol **74-87**

5.1 Introduction	74
5.2 Earlier studies	74
5.3 Experimental Results	76
5.3.1 Effect of various alkali metal ions on the size distribution of small unilamellar vesicles: Dynamic light scattering experiment	76
5.3.2 Effect of alkali metal ions on zeta potential	77

5.3.3 Effect of cholesterol on vesicle size and zeta potential distribution	78
5.4 Effect of cholesterol in ion binding in membrane: Gouy Chapman theory	79
5.5 Discussion	83

Chapter 6 Effect of cholesterol on the interaction of alkali metal salt with cationic vesicles **88-100**

6.1 Introduction	88
6.2 Earlier Studies	89
6.3 Results	90
6.3.1 Effect of monovalent sodium salts on the size distributions of cationic vesicles	90
6.3.2 Effect of cholesterol on zeta potential: Binding of ion with vesicles	91
6.3.3 Phase contrast microscopy of GUV exposed to various concentration of ion: Effect of cholesterol	94
• Formation of transmembrane pores induced by cholesterol: Kinetics of pore formation	94
6.3.4 Small angle X-ray scattering (SAXS) studies	96

Preface

This thesis deals with the studies on effect of cholesterol on the interaction of alkali metal ions with charged biological membranes. Cholesterol is a ubiquitous component of all animal cell membranes. It plays an important role in many cellular events and is known to regulate the functional activity of protein and ion-channel. Cholesterol can also significantly alter the electrostatic behaviour of the membrane. Again structure, dynamics and physicochemical properties of lipid membranes are modulated by ionic strength, composition, temperature, pH etc. of the surrounding aqueous medium. Therefore, studies on effect of cholesterol on the ion-membrane interaction in lipid membranes is important to match physiological conditions. Biological membranes are complex in nature and regulated by various proteins, so it is difficult to study *in vivo*. Our motivation is to gain some insight about how cholesterol affects structure, dynamics and other physiological functions of cell membrane in presence of ions.

We have systematically investigated the effect of cholesterol on the interaction of various alkali metal monovalent ions with large unilamellar vesicles and small unilamellar vesicles using a variety of experimental techniques such as dynamic light scattering, zeta potential, isothermal titration calorimetry (ITC) and phase contrast fluorescence microscopy etc. To prepare vesicles (model membrane), we have used various lipids such as DOPC, DOPG, DMPC, DMPG, DPPC and DOTAP etc. Small unilamellar vesicles were made from ultrasonic probe sonicator for lipid DPPC and surfactants like DDAB. Here unsaturated lipids DOPC, DOPG and DOTAP represents charge state as neutral, negative and positive respectively. Whereas saturated lipid DMPC and DPPC are zwitterionic in nature. The intrinsic binding constant of Na^+ for different cholesterol concentration has been estimated from measured zeta potential using Gouy Chapman theory. We have also obtained the binding constant from the fit using hill equation and compared with the result obtained from zeta potential study. We have used membrane sensitive lipophilic fluorescence probe, Nile red to study ion-membrane interaction as significant quenching of fluorescence intensity in presence of Nile red implies existence of ion in the core of the membrane. Change in binding with the increase in cholesterol concentration implies that presence of cholesterol significantly affects the binding affinity of the bio-membrane. Small angle x-ray scattering (SAXS) is employed to gain insight into molecular or structural changes in biological membranes.

In chapter 1, we have given a brief introduction to lipids and to the various lamellar phases exhibited by them in aqueous solutions. A summary of earlier studies on the ion-membrane interactions and the effect of cholesterol is also given.

Amphiphiles in aqueous solution form a variety of self-assembled structures. Lipid bilayer is the basic building block of all cell membranes. Generally, lipids are amphiphilic molecules, consisting of two parts; a polar hydrophilic head and a non-polar hydrophobic hydrocarbon chain. All lipids have a chain melting transition temperature (T_m) above which they undergo a transition from gel phase to liquid phase. As model membranes, unilamellar vesicles can be classified into three categories like small (SUV), large (LUV) and giant (GUV) unilamellar vesicles. Different monovalent and divalent metal ions like Na^+ , K^+ , Ca^{2+} , Mg^{2+} , Fe^{2+} etc. plays important roles in many biological systems. Among all the ions present in the intracellular and extracellular media, Na^+ and K^+ ions are the most abundant cations in the human body. Na^+ ions having high concentration ($>100\text{mM}$) mostly found outside cell in the body and control the body fluids, whereas K^+ ions found mostly inside the cell and regulate many cellular processes. As a counter ion of sodium, Cl^- is mainly found in extra cellular fluid maintaining hydration and balancing cations in the fluid. Other anions, such as Br^- and I^- are also found in all organisms and essential part of biological functions. Structure and physiochemical properties of membranes are modulated by the ionic strength. In bio-membrane, cholesterol plays a vital role in maintaining structure and regulating functions and properties of membranes. Cholesterol is also responsible for the stability of vesicle. So, studies on effect of cholesterol on the interaction of ions with membranes are important in order to match the physiological conditions. Inhomogeneous distribution of cholesterol, so called rafts has led to large number of studies in lipid-cholesterol membranes. Membrane cholesterol and partitioning of cholesterol into the membrane domain are also known to regulate ion-channel. Activity of the ion-channel is highly influenced by the level of membrane cholesterol. Earlier studies have shown that activity of ion-channel is highly influenced by the level of membrane cholesterol. For example, increase in cholesterol level leads to suppression in ion-channel activity. Besides ion transport, ions in the membrane regulate the surface charge, which in turn affect the efficiency of the drug delivery using liposome. Studies on the effect of alkali metal ions on the phospholipid membrane has received a significant attention in view of understanding the ion transport and other biological functions.

A variety of experimental techniques as well as computer simulation has been employed in order to gain insight into the ion-membrane interaction. Ion-membrane

interaction has an important role in restructuring macromolecules such as proteins, peptides etc. It is important to note that most of the work has been done in order to investigate effect of alkali metal ions with model membranes. The systematic study on the effect of cholesterol on the interaction of charged lipids with alkali metal salts is overlooked in literatures. As cholesterol largely affects the ion transports across the membrane, we intend to investigate effect of cholesterol on ion-membrane interaction for better understanding of much more complex biological membranes.

In chapter 2, we describe various experimental methods employed by us for studying effect of cholesterol on ion-membrane interaction. Basic principles of these techniques and detailed methodology are also discussed below.

SUVs were prepared from ultrasonic homogenizer (probe sonicator) method and LUVs were made from extrusion method. Size of SUVs and LUVs were confirmed by dynamic light scattering experiment. Owing to a larger size, GUVs were prepared from the electroformation method. These vesicles can be observed under phase contrast fluorescence microscope. It was difficult to study on GUV under normal microscope. In this thesis, SUVs and LUVs were used to study ion-membrane interaction. The zeta potential is used to estimate the surface charge, surface potential of the vesicles and to determine the electrophoretic mobility, isoelectric point, binding of ions with charged membranes in an electrolyte solution. We have found the binding constant using well known Gouy Chapman theory from the measured zeta potential of the biomembrane.

The fluorescence spectroscopy technique is widely used to determine the structure and dynamics of the lipid membrane. Quenching constants of environment sensitive probe Nile red was estimated from Stern Volmer equation. The thermodynamics of lipid-ion interaction and binding kinetics of ions have been probed using ITC. The nature of interaction in terms of exothermic and endothermic reaction can directly be envisaged from ITC heat flow. The integrated heat flow at injection provides the isotherm which can be fitted to an appropriate model in order to obtain binding parameters, such as K , ΔH , ΔS etc. As the one site binding model provided by *Microcal Origin* does not fit well, we have adopted a partition model to fit the data. SAXS (small angle X-ray scattering) is a powerful technique which can provide rich information about the structure of biological macromolecules in terms of their size, shape and flexibility etc. This technique is extremely useful to extract structural information from non-crystallographic complex samples in contrast to the X-ray crystallography technique that requires samples to be highly crystalline.

In chapter 3, we present results of effect of cholesterol on the interaction of sodium chloride with negatively charged phospholipid membranes (DOPC-DOPG on 4:1 ratio) at physiological pH 7.4. We have used a ternary system composed of DOPC, DOPG and cholesterol. The experiments have done systematically by keeping fixed the molar ratio of DOPC-DOPG at 4:1 and varying the cholesterol concentration from 0 to 20 mol%. Size distributions of LUV have been confirmed from dynamic light scattering experiment (DLS). We have measured the size distributions by titrating with NaCl solution at different concentrations varying from 0 mM to 100 mM. For a particular cholesterol concentration, we have observed decrease in hydrodynamic radius of vesicles with increasing ion concentration. It can be explained from the fact that adsorption of ions into the membrane causes compression of electrostatic double layer which results in a decrease in the hydrodynamic radius of the vesicle. Decrease in average size of LUV is faster at higher cholesterol conc. (>15mol%) than the lower conc. (<10 mol%). It is also important to mention that average vesicle diameter decreases with cholesterol concentration even in the absence of NaCl. Concentration dependent size distribution has been presented by a single exponential decay curve in fig. 1. Beside average size, polydispersity index (PDI) is one of the important factors to consider in illustration of effect of cholesterol in size distribution. PDI of all measurements are found to be within 0.1 and does not alter with salt or cholesterol concentrations.

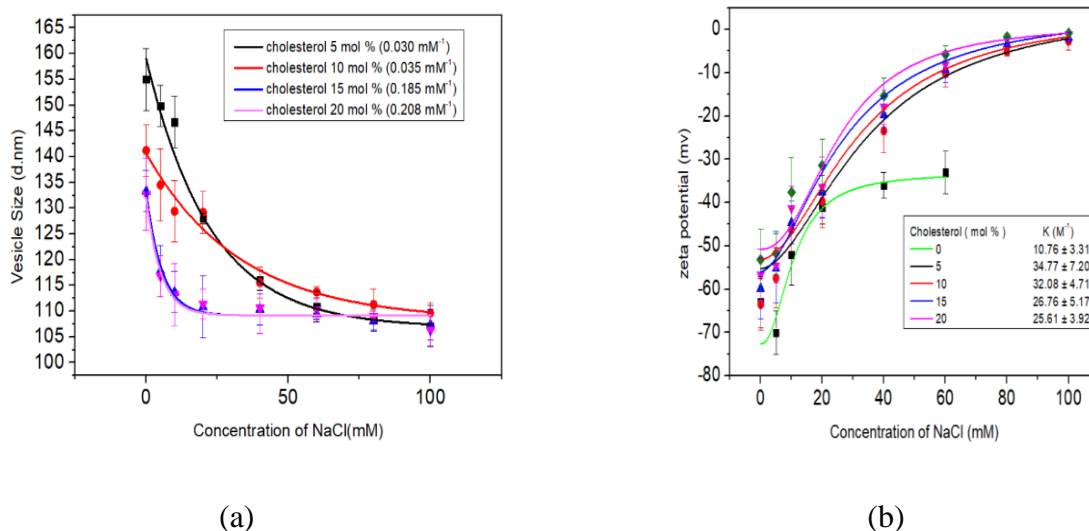


Fig. 1 (a) Exponential decay fit of average size distribution of ternary mixture DOPC-DOPG (4:1), NaCl and cholesterol. (b) Hill fit of zeta potential measurement of negatively charged phospholipid DOPC-DOPG (4:1) in presence of cholesterol.

Zeta potential and effective charges per vesicle in the presence of NaCl and cholesterol have been estimated from the measured electrophoretic mobility using the modified Henry function. We have determined the intrinsic binding constant from the electrostatic double layer theory. From the results of experiments, it is clearly evident that zeta potential shows high negative value in the absence of NaCl for all cholesterol concentrations. The zeta potential increases with increasing salt concentration and this potential value saturates to zero but never exceeds zero. The underlying partial charge compensation has been discussed in chapter 3 in detail. Vesicle solution after zeta potential measurement shows colour change, which is due to electrolysis in the electrode of zeta cuvette. We have measured the intrinsic binding constant from the measured zeta potential using Gouy Chapman model. From the results we can observe that the value of binding constant is increasing with the increase of cholesterol concentration. The effective area per molecule decreases with the cholesterol concentration, which leads to reduction in the surface charge density of the membrane.

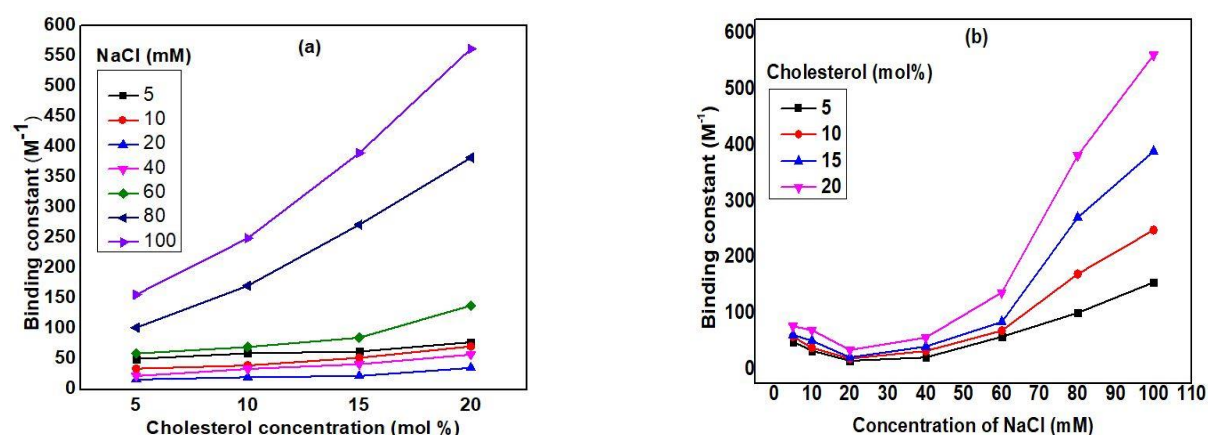


Fig. 2 (a) Intrinsic binding constant as a function of cholesterol concentration for different NaCl concentrations indicated in the figure legend. (b) Binding constant was plotted with NaCl concentration for different cholesterol concentration.

We have found higher binding affinity of Na^+ with cholesterol concentration as estimated from the electrostatic double layer theory. This is due to decrease in the negative value of surface charge density. This underpins the fact that cholesterol increases the ion binding with the membrane. These values (fig. 2) are in agreement with the values obtained from the fit (Fig. 1) of Hill equation. The binding of ions is not purely electrostatic; there are also entropic contribution due to release of water in the hydration layer of the membrane upon adsorption of ions. Intrinsic binding occurs due to the competition between screening effect

and binding phenomenon. Therefore, at higher concentration of salts, it is expected to dominant screening effect over binding of ions. Further cholesterol in the membrane alters the intrinsic concentration hence we observe concentration dependent binding constant.

In chapter 4, we present a systematic study of effect of cholesterol on the interaction of alkali metal ions with negatively charged saturated phospholipid. We have used dynamic light scattering, zeta potential, fluorescence correlation spectroscopy (FCS), fluorescence spectroscopy and isothermal titration calorimetry (ITC) to study binding thermodynamics, chain saturation and lipid phase state etc. Binding thermodynamics of ion-membrane interaction was determined from isothermal titration calorimetry experiments. We have also compared the results of unsaturated lipid discussed in chapter 1. Ion-membrane interaction significantly depends on the phase state of lipid bilayer and cholesterol can significantly affect the binding thermodynamics of the membrane. Here we have used ternary mixture of saturated phospholipid DMPC-DMPG (4:1), cholesterol and alkali metal salt (NaI). Size distributions of SUV are measured by titrating with NaCl and NaI from 0 to 100 mM at different cholesterol concentration 0, 10 and 20 mol %. Presence of ion in the medium can in principle alter the hydrodynamic radius of the LUV by changing the thickness of electrostatic double layer. Here we can observe that for both NaCl and NaI vesicle size is increasing with increasing ion concentration from 0 to 150 mM for cholesterol concentration up to 10 mol % but after 10 mol % (i.e 20 mol %) vesicle size is decreasing from 20 mM concentration. If the cholesterol concentration further increased i.e 20 mol% cholesterol, we have observed that vesicle size is increasing initially with increasing NaI concentration but at a particular concentration of NaI (40 mM) vesicle size decreases and reaches to ~ 60 nm. Average vesicle size for 20 mol % cholesterol is very high i.e 109 nm. The increase in vesicle size with increasing ion is faster in higher cholesterol than lower cholesterol. It is important to mention that increase in vesicle size with cholesterol occurs even in the absence of ions.

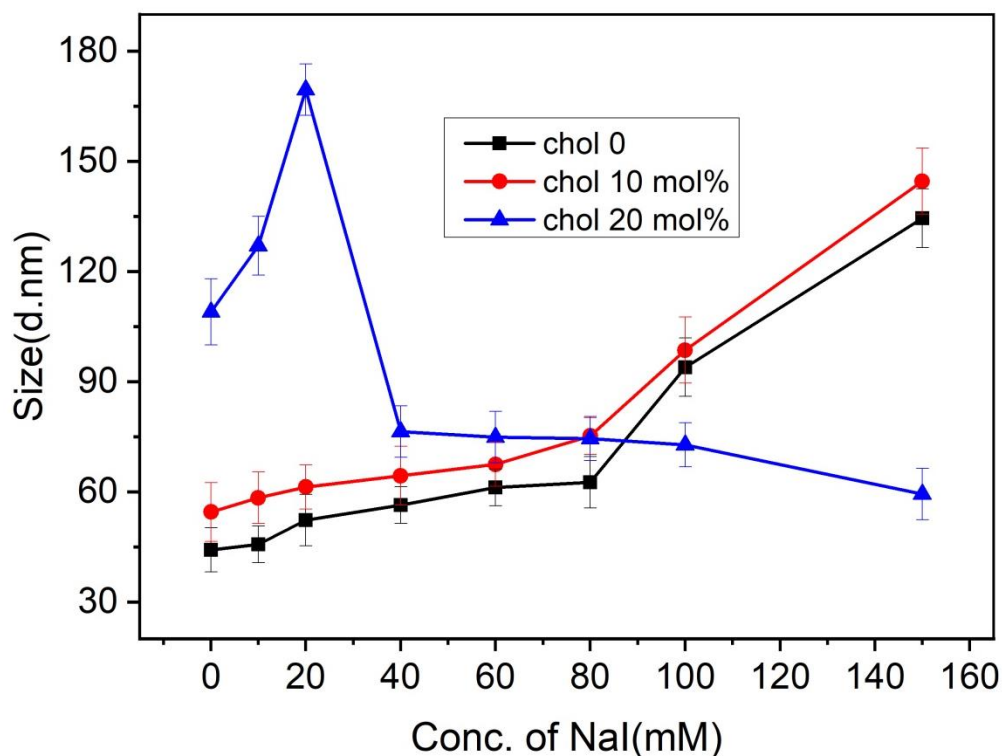


Fig.3 Variation of average size of SUVs prepared from saturated phospholipid DMPC-DMPG with different NaI concentrations (0 to 150 mM) for different cholesterol concentrations (indicated in the figure legend). Error is determined from the average value of three different measurements.

Zeta potential (ζ) was measured for small unilamellar vesicles (SUV), composed of mixture of saturated lipid DMPC-DMPG (4:1) and cholesterol. It is clear from the result that zeta potential shows high negative value (-48 mv) in the absence of NaI for all cholesterol concentration. Now if we increase the ion concentration gradually, zeta potential becomes less negative (negative value decreases), which means zeta potential increases with the increase of ion concentration. For zero cholesterol concentration, value of zeta potential is -48 mv and with increasing ion concentration it increases to -7.5 mv at 150 mM NaI concentration. Similarly, for sample with 10 mol% and 20 mol% cholesterol at 150 mM NaI concentration zeta potential increases to -6.5 mv and -5 mv respectively. Interestingly zeta potential value saturates close to zero but never exceeds zero. The underlying cause of partial charge compensation will be discussed later.

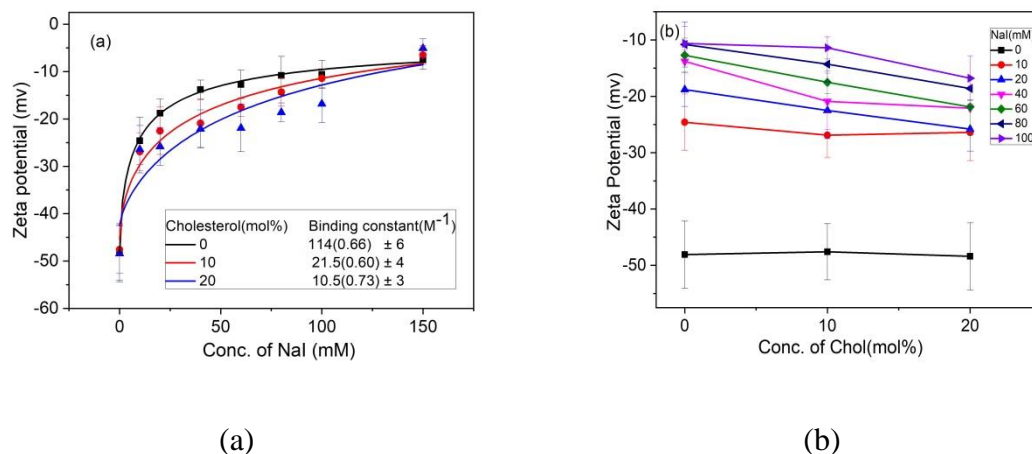


Fig. 4 Variation of zeta potential of DMPC-DMPG vesicles with NaI concentrations at two different cholesterol concentration. Solid lines in (a) are obtained from fit using Hill equation, describing the binding phenomenon. The binding constant obtained from the fit are presented in the inset of the fig a. The number within the bracket represent the cooperativity index. Fig. (b) is derived from the fig (a) to show the effect of cholesterol concentration at a fixed salt concentration.

We have compared the effect of cholesterol on the saturated lipid with that of unsaturated negatively charged lipid and we observed that effect of cholesterol is completely opposite in saturated lipid to that of unsaturated lipid.

Table 1: Electrostatic parameters obtained at 20 mM NaI concentration using the Gouy Chapman theory from the measured zeta potential of small unilamellar vesicles (SUV) for different cholesterol concentration. SUVs are prepared from binary mixture of saturated phospholipid DMPC-DMPG(4:1) and cholesterol.

Chol (mol%)	Surface potential (ψ_0) (mV)	Surface Charge (σ) (C/m^2)	Intrinsic concentration C_0 (M)	Binding constant (K) (M^{-1})	ΔG (KJ/mol)
0	-21 ± 4	-0.0068 ± 0.0008	0.045 ± 0.007	124 ± 8	-22 ± 6
10	-25 ± 5	-0.0083 ± 0.0009	0.053 ± 0.008	84 ± 6	-21 ± 5
20	-26 ± 3	-0.0096 ± 0.0007	0.060 ± 0.006	60 ± 7	-20 ± 7

The intrinsic binding of ion with membranes are calculated with the help of Gouy Chapman theory. In contrary to unsaturated lipid, in case of saturated lipid intrinsic binding of ions with membrane decreases with increasing of cholesterol concentration.

We have also systematically investigated the effect of cholesterol on the fluorescence intensity of Nile red labeled DOPC lipid vesicles at 25° C and DMPC at 15° C. Typical variation of maximum emission peak with increasing cholesterol concentration at no salt condition is shown in fig. 5.

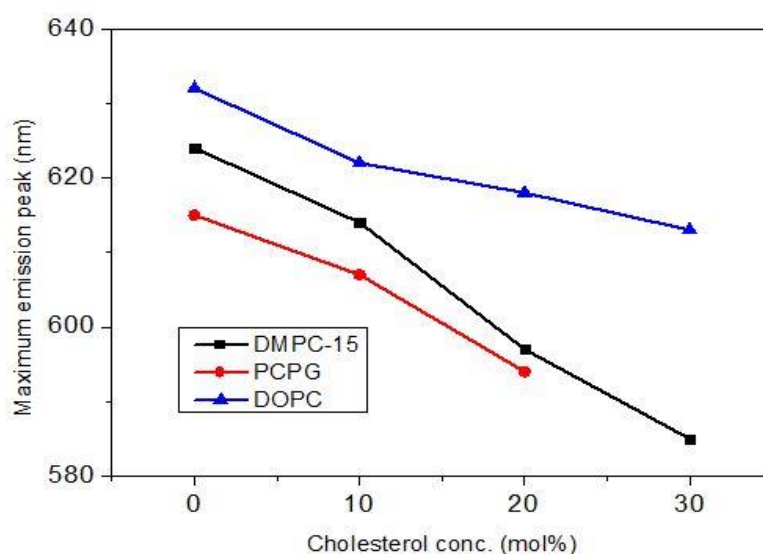


Fig.5 Variation of maximum emission peak with cholesterol concentration for DMPC-DMPG(4:1), DOPC and gel phase of DMPC.

Relative intensity of Nile red in the presence of different NaI concentration varying from 0 mM to 100 mM in presence of cholesterol (10, 20, 30 mol%) has been plotted using Hill equation for both gel and fluid phase of DMPC. For gel phase binding is more higher than the fluid phase of DMPC and the value of binding obtained from the fit has good resemblance with the result obtained from partition fit.

In chapter 5, we have systematically studied the effect of cholesterol on the interaction of sodium salts (NaCl and NaI) with saturated phospholipid egg lecithin. Electrostatic parameters like surface zeta potential, surface charge density, intrinsic binding obtained without cholesterol and with cholesterol are compared for both the counterions I^- and Cl^- . Variation of vesicle size with NaCl concentration in presence of cholesterol (0, 10, 20 mol%) is given in fig.6. From this result we can see that, in the absence of cholesterol vesicle size decreases with increasing ion concentration but if we increase the cholesterol concentration,

for both 10 and 20 mol% cholesterol concentration vesicle size increases with the increase of NaCl concentration. An identical result has been found, when the experiment has been repeated with NaI.

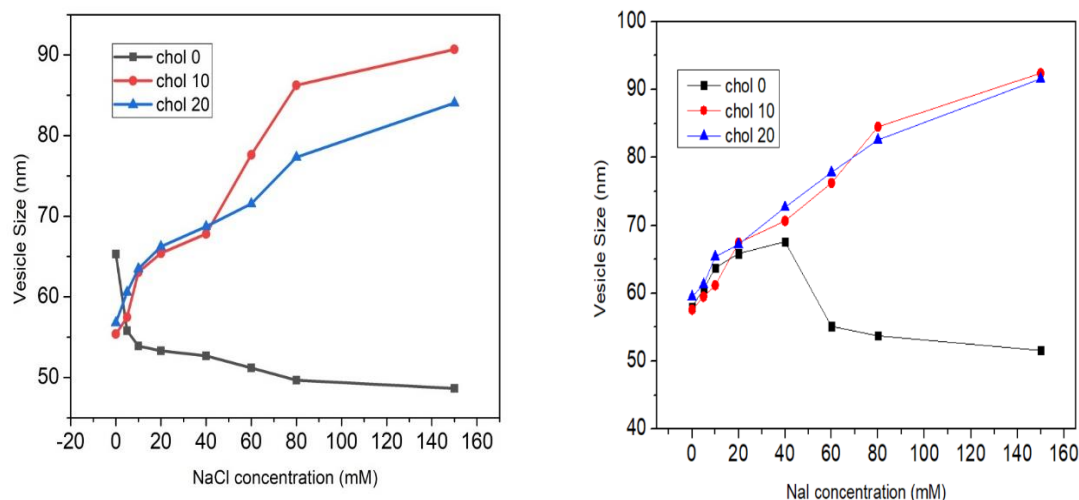


Fig. 6 Variation of vesicle size with different NaCl and NaI concentration in presence of cholesterol as indicated in the figure legend.

Zeta potential of small unilamellar vesicles (SUV) was measured for mixture of egg lecithin and ions (both NaCl and NaI) in presence of cholesterol. From the figure it is clearly evident that zeta potential shows high negative value at all X_C (cholesterol concentration) in the absence of NaCl or NaI. Now, if we increase the salt concentration zeta value increases (becomes less and less negative) for all X_C . Interestingly, zeta value saturates close to zero, but never exceeds zero.

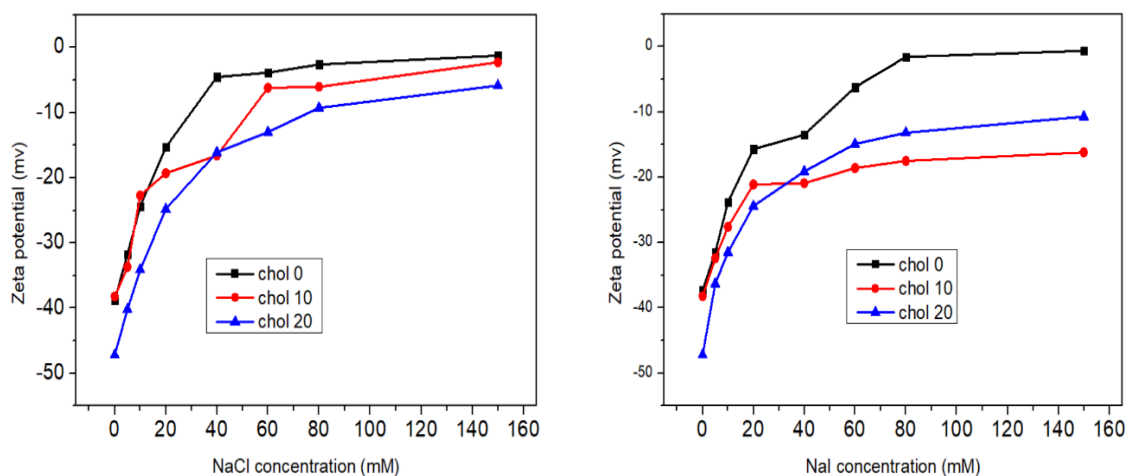


Fig. 7 Variation of zeta potential of egg lecithin for different NaCl and NaI concentration in presence of cholesterol as indicated in the figure legend.

Table 2 Electrostatics parameters obtained at 20 mM NaCl (a) and NaI (b) concentration for Egg lecithin using the Gouy Chapman theory from the measured zeta potential of small unilamellar vesicles (SUVs) for different cholesterol concentration.

NaCl				
Chol (mol%)	Surface potential (ψ_0) (mV)	Surface Charge (σ) (C/m^2)	Intrinsic concentration C_0 (M)	Binding constant (K) (M^{-1})
0	-16 \pm 4	-0.0011 \pm 0.0007	0.012 \pm 0.003	654 \pm 13
10	-21.2 \pm 3	-0.0070 \pm 0.0009	0.046 \pm 0.007	118 \pm 9
20	-27.3 \pm 5	-0.0092 \pm 0.0008	0.081 \pm 0.008	67 \pm 5
NaI				
Chol (mol%)	Surface potential (ψ_0) (mV)	Surface Charge (σ) (C/m^2)	Intrinsic concentration C_0 (M)	Binding constant (K) (M^{-1})
0	-16.5 \pm 3	-0.0026 \pm 0.0008	0.017 \pm 0.007	747 \pm 9
10	-23.2 \pm 5	-0.0077 \pm 0.0005	0.049 \pm 0.006	168 \pm 8
20	-26.9 \pm 4	-0.0091 \pm 0.0007	0.057 \pm 0.009	69 \pm 6

From the above results (table 2), it is clear that when there is no cholesterol, intrinsic binding of Cl^- is more than I^- . But in the presence of cholesterol, binding of I^- is more prominent than Cl^- . So cholesterol has great influence on the binding of sodium salt with membranes. For better understanding of the result, we have also obtained the binding constant from the fit using hill equation. These results has well resemblance with the result obtained from the Gouy Chapman theory.

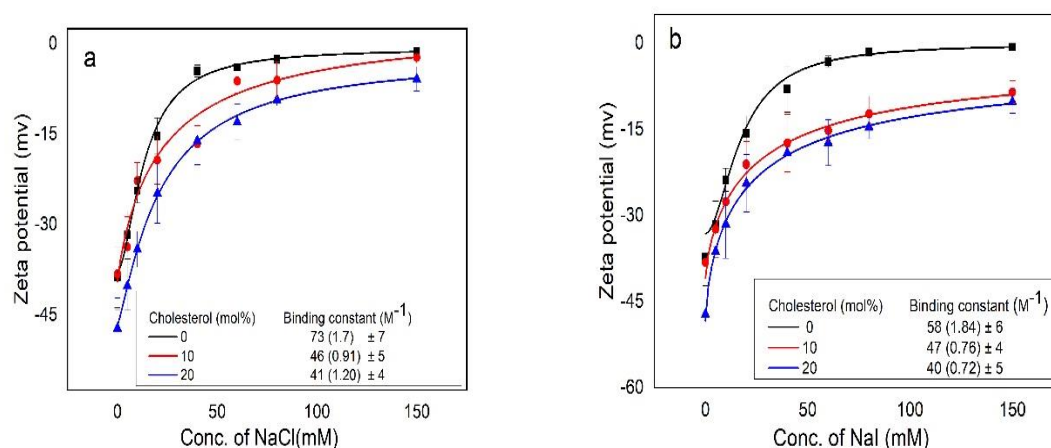


Fig. 8 Variation of zeta potential with different NaCl and NaI concentration for different cholesterol concentration as indicated in the figure legend. Solid line is obtained from the fit using hill equation. Binding constant (K) obtained from the fit also indicated in the figure legend.

In Chapter 6, we have systematically studied the effect of cholesterol on the interaction of sodium salts (NaCl and NaI) with cationic unsaturated phospholipid DOPC-DOTAP (4:1). The size distribution of SUV composed of DOPC-DOTAP (4:1) and cholesterol mixture for two different sodium salts NaCl and NaI increases with the increase of ion concentrations, when there is no cholesterol. Now if we increase the cholesterol concentration to 5, 10 mol%, vesicle size decreases for both NaCl and NaI. So, presence of cholesterol seems to inhibit the aggregation.

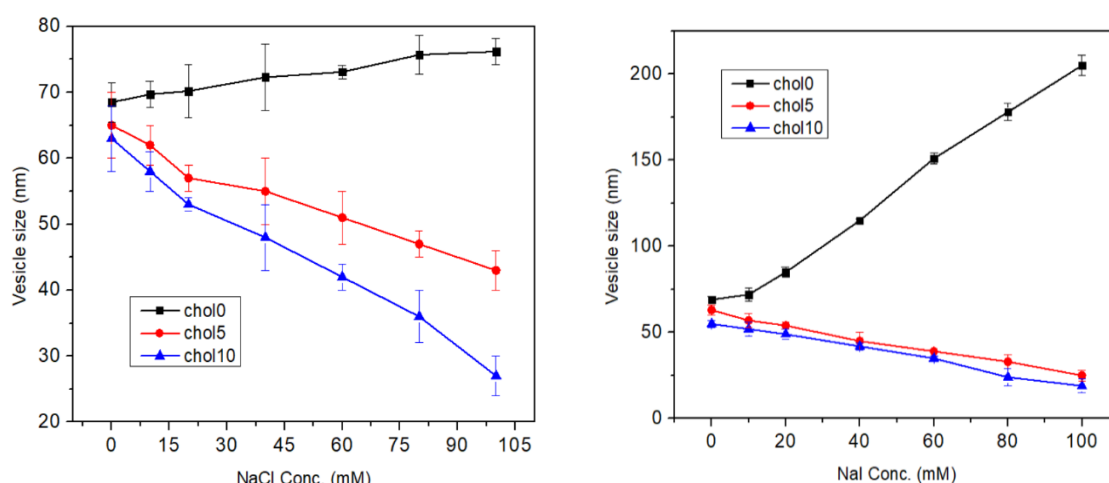


Fig. 9 Variation of vesicle size with NaCl and NaI concentration in presence of cholesterol concentration as indicated in the figure legend. SUVs are prepared from binary mixture of DOPC-DOTAP (4:1) and cholesterol.

From the variation of zeta potential of vesicles with NaCl and NaI concentration in presence of cholesterol, we can observe that when there is no cholesterol, zeta potential decreases with increasing ion concentration for both NaCl and NaI. Interestingly, for NaI zeta potential goes to negative at higher ion concentration ($>100\text{mM}$) at zero cholesterol. But if we increase the cholesterol concentration, zeta potential increases with increasing ion concentration for both NaCl and NaI.

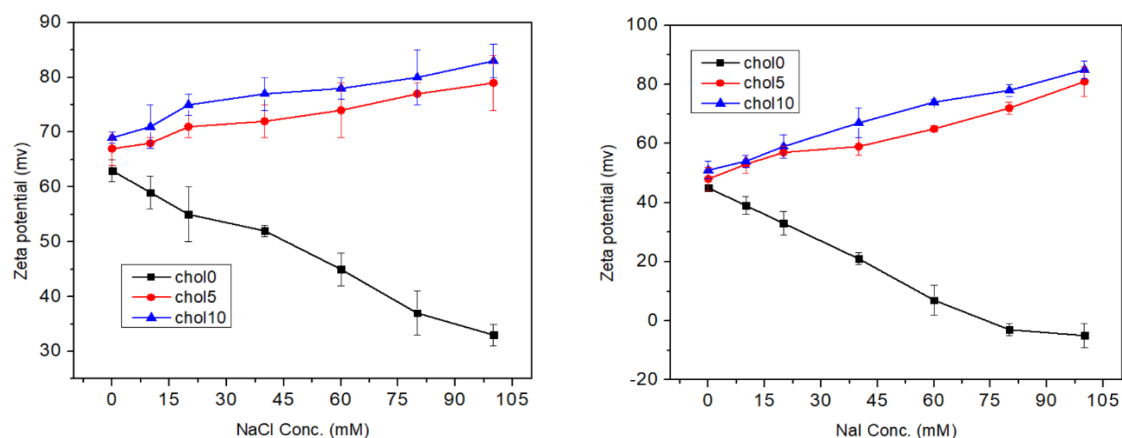


Fig.10 Variation of zeta potential of small unilamellar vesicles with NaCl and NaI concentration in presence of cholesterol concentration as indicated in the figure legend.

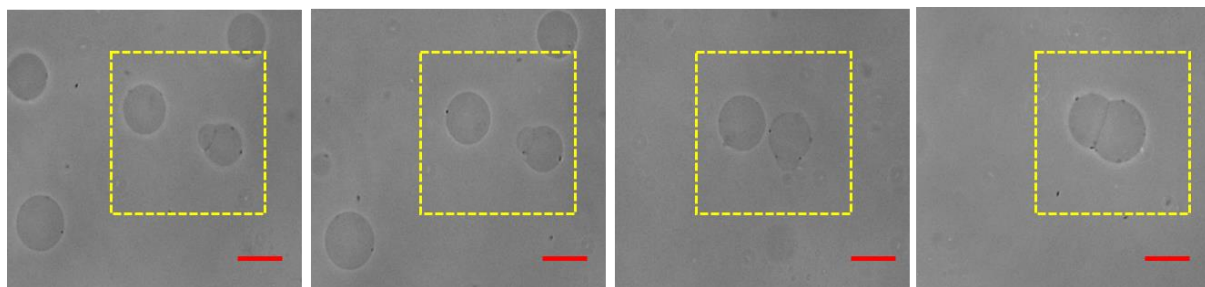
Table 3 Electrostatic parameters obtained from Gouy Chapman theory from the measured zeta potential for DOPC:DOTAP (4:1) in presence of cholesterol at a particular NaCl and NaI concentration 20 mM. SUVs are prepared from binary mixture of DOPC-DOTAP (4:1) and cholesterol.

NaCl				
Chol (mol%)	Surface potential (ψ_0) (mV)	Surface Charge (σ) (C/m^2)	Intrinsic concentration C_0 (M)	Binding constant (K) (M^{-1})
0	59	0.029	0.34	15.6
05	77	0.038	0.45	33.4
10	88	0.049	0.59	48.2
NaI				
Chol (mol%)	Surface potential (ψ_0) (mV)	Surface Charge (σ) (C/m^2)	Intrinsic concentration C_0 (M)	Binding constant (K) (M^{-1})
0	38	0.011	0.21	71.3
05	65	0.018	0.39	125.7
10	77	0.023	0.51	279.6

From this table 3, it is clear that, for unsaturated cationic phospholipid intrinsic binding of ion is increasing with increasing cholesterol concentration and I^- binds more with the membrane than Cl^- . In this novel work we have explored effect of cholesterol on the lipid composition DOPC-DOTAP with the help of fluorescence microscopy images. For this we have made giant unilamellar vesicles (GUV) as SUVs can't be observable through fluorescence

microscope. Phase contrast microscopy images of giant unilamellar vesicles (GUV) for without cholesterol and with cholesterol is given in fig. 9. As pure DOTAP vesicles got turbid at particular ion concentration, we have also observed any structural or morphological changes in the sample at particular ion concentration with the help of small angle x-ray scattering (SAXS) techniques.

(a) Without cholesterol



(b) With cholesterol

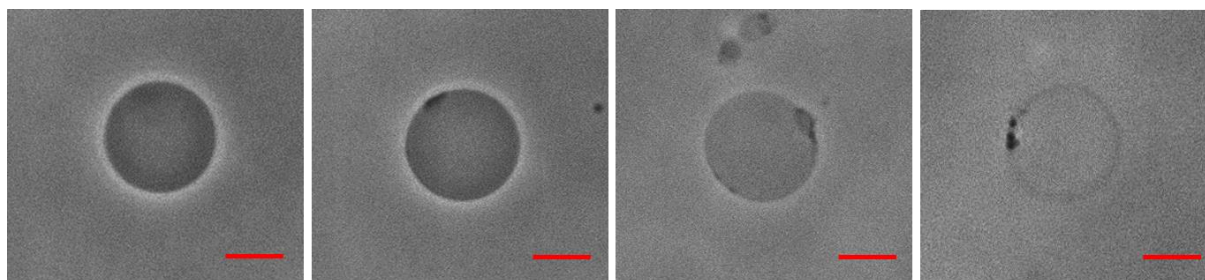


Fig.11 Phase constant micrographs of GUV composed by DOPC-DOTAP (4:1) for cholesterol concentration (a) 0 (b) 5 mol% for NaI concentration 40 mM. Scale bar is 30 μ m.

In this thesis, we have studied in detail the effect of cholesterol on the interaction of ion with phospholipids. Our study revealed that cholesterol significantly affects the charge state and binding affinity of both saturated and unsaturated lipid. Interestingly, the ion-membrane interaction of saturated lipids exhibits a completely reverse trend with unsaturated lipids i.e cholesterol modulates the surface charge density of the membrane and alters the binding affinity of ions differently in saturated and unsaturated phospholipid membranes. However, there is no significant counterion effect on the anionic membrane containing cholesterol. The binding affinity and distributions of ions at membrane-water interfaces are of great

importance in the formation of electrical double layers and provide insights into the ion-transport process in the cellular membrane. For cationic membrane, both zeta potential and average vesicle size show an opposite trend in presence of cholesterol. Microscopy of GUV revealed that presence of cholesterol inhibits vesicle aggregation. Presence of cholesterol suggests the adsorption of Na^+ on to the membrane and prevents the binding of halide ions. Further studies are underway to understand the role of cholesterol in ion-membrane interaction.

Chapter 1

Introduction

Lipid bilayer is the building block of all biological membranes. Biological membranes are complex, assembled structures that mainly consist of phospholipids, proteins and cholesterol. Their compositions and distributions are regulated differently for different membranes (1). The composition of lipids and proteins varies significantly depending on the membrane types and their functions. Lipids are distributed asymmetrically between the outer and inner leaflets of the membrane. The biological membrane in cells provides a barrier between the inside and outside environments and is involved in a variety of cellular functions, such as cell-cell communication, recognition, signal transduction, substance exchange. etc. (2). In physiological environments, biological membranes are immersed in solutions of salt ions, mainly including Na^+ , K^+ , Ca^{2+} , Mg^{2+} and Cl^- , that are considered the most important biologically relevant salt ions. Phosphatidylcholine (PC) lipids are major constituents in the outer leaflet, whereas the inner leaflet is mostly composed of phosphatidylethanolamines (PE). The structure and functions of biological membranes are greatly influenced by the different types of monovalent and divalent ions present in extra- and intracellular fluid at a particular concentration and at physiological pH. These ions play important roles in maintaining and regulating many cellular functions such as ion channels, membrane fusion, phase transition. etc.

The unilamellar vesicle is an enclosed lipid bilayer cell and serves as an excellent model system for biological membranes. Apart from model systems of biological membranes, these vesicles can also be used as microreactors for enzymatic RNA synthesis (3) and also to form nanoparticles of controlled size distributions. Vesicles are also extensively used as carriers of bioactive agents including drugs, vaccines and cosmetics. A variety of experimental as well as theoretical studies has been employed in order to gain insights into the ion-membrane interaction. Cholesterol is a type of lipid that performs many essential jobs in our body. It is the principal sterol of all higher animals, distributed in body tissues, especially the brain and spinal cord, and in animal fats and oils. The structure, dynamics and stability of lipid membranes are strongly influenced by the presence of cholesterol.

The cell membrane is a very complex system due to the wide variety of lipids and proteins present in it, as well as the various active processes taking place at the cell surface. It is often useful to study effect of cholesterol on the ion membrane interaction in the model system in order to obtain some sights into the physical mechanism of many biological phenomena. In this thesis, we present systematic investigations on the effect of cholesterol on the interaction of various types of alkali metal salts with charged model phospholipid membranes using variety of experimental techniques like dynamic light scattering (DLS), zeta potential, fluorescence spectroscopy, phase contrast microscopy, isothermal titration calorimetry and small angle x-ray scattering (SAXS) etc. We believe that the present study will be helpful for a better understanding on appropriate physiochemical condition of cholesterol and ions in our human body. A few relevant topics in connection with the present thesis will be discussed now.

1.1 Brief introduction to amphiphilic molecules

Amphiphilic molecules, such as surfactants, lipids consist of a polar (hydrophilic) part, usually called the head group, attached to a nonpolar (hydrophobic) part consisting of one or more hydrocarbon chains (Fig. 1.1). Lipids are amphiphilic molecules of biological origin. An example of a synthetic surfactant molecule is cetyltrimethylammonium bromide (CTAB) and dipalmitoyl phosphatidylcholine (DPPC) is a lipid found in bio-membranes. Negatively charged ion carboxylates, sulfonates, phosphate and positively charged ion amines can be taken as examples. The Most common examples of amphiphilic molecules are lipid, polymer, proteins and surfactants etc.

Due to surface activity, when any amphiphilic molecule interacts with water, it's hydrophobic part tries to minimize contact with water whereas it's hydrophilic part tries to separate out from each other as far as possible. Artificial double-chain cationic surfactant didodecyldimethylammonium bromide (DDAB) and single-chain cationic surfactant Cetyl Trimethyl Ammonium Bromide (CTAB) are examples of surfactants. These surfactant molecules are extensively used in cleaning products, foods, cosmetics, detergents etc. (4, 5). Lipids, mainly found in bio-membrane are another important amphiphiles which is discussed briefly in the next section.

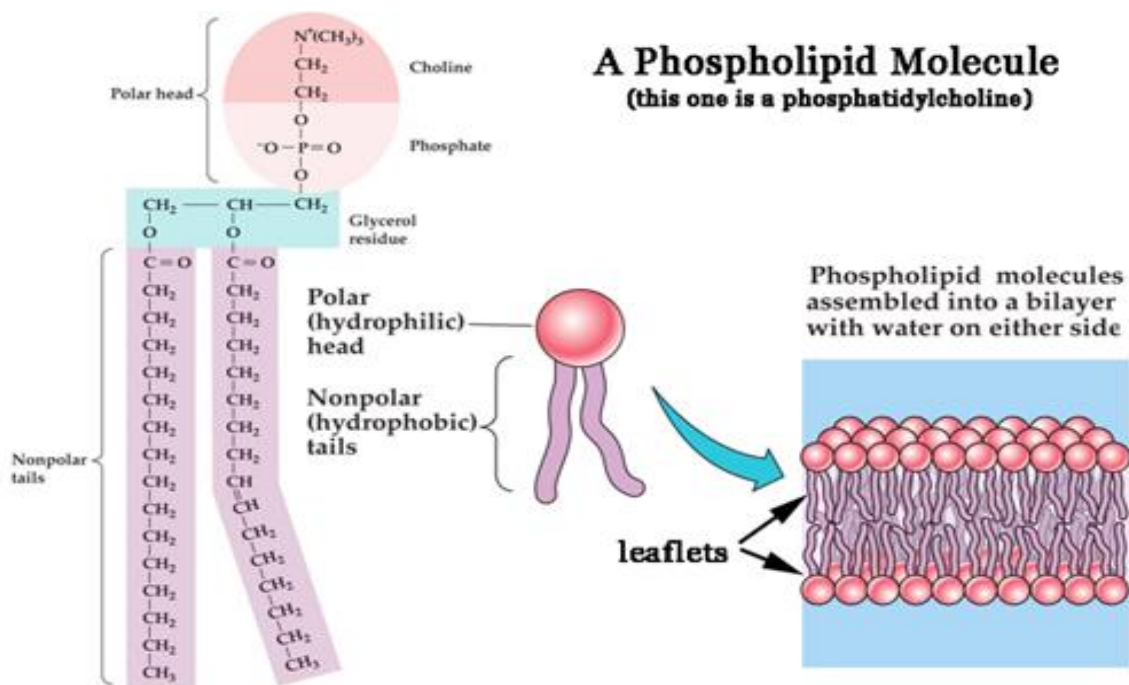


Fig 1.1 Structure of phosphatidylcholine and lipid bilayer.

1.2 Lipids and their classifications

Lipids are fatty acids and their derivatives which are the major constituent of all biological membranes. The fatty acid chain differs in length and contains carbon atoms from 4 to 28. There are two different type of fatty acids, saturated and unsaturated. If there are only single bonds between neighbouring carbons in the hydrocarbon chain, it is saturated (Fig. 1.2) fatty acid and if there is one or more double covalent bond in the fatty acid chain, it is said to be unsaturated. The double bond in unsaturated fatty acids can exist in either *cis* or *trans* configuration. In the *cis* configuration (Fig. 1.2), the two hydrogens associated with the bond are on the same side and generates a kink or bend in the fatty acid. In the *trans* configuration, hydrogens are on opposite side (fig. 1.2).

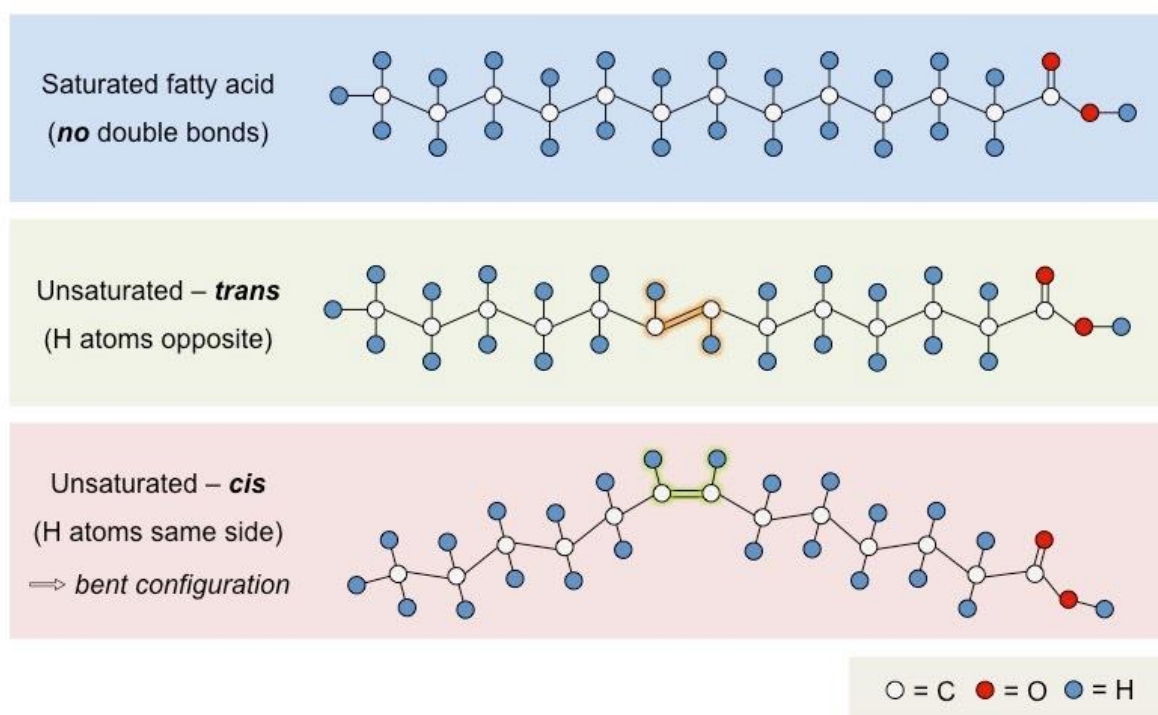


Fig 1.2 Structure of saturated and unsaturated lipids

Lipids play diverse roles in organisms. Primary functions of lipids include storing energy, signalling and acting as structural components of the cell membrane (6). Lipids have applications in nanotechnology as well as in the cosmetics and food industries. Among all lipids, phospholipids are widely studied as they are the major components of the plasma membrane. They are made of fatty acid chains attached to a backbone of glycerol. Phospholipids are classified into several groups depending on the chemical structure of the head group. Phosphatidylcholines (PCs), phosphatidylethanolamines (PEs) and phosphatidylserines (PSs) are common phospholipids found in the plasma membranes. These lipids may be charged or neutral. Neutral lipids that possess a dipole moment in aqueous solution are called zwitterionic.

1.3 Self-assembly of amphiphilic molecules

By virtue of self-association, amphiphilic molecules can associate into a variety of structure like micelles, bilayers in an aqueous solution. Hydrogen bonding, hydrophobic effects, electrostatic interaction and Van der Waals forces are the main reason behind the self-association. The strength of underlying forces (5 KJ/mole – 120 KJ/mole) are much less than that of covalent bonds (400 KJ/mole) but strong enough to maintain the stability of amphiphiles in solution (7, 8). When the amphiphilic molecules self-aggregate then there is

an enthalpy gain in solution due to the formation of hydrogen bond and entropic gain of the bulk water due to hydrophobic effect. Hydrogen bonds are critical for structures and interaction of biological macromolecules. Together with the hydrogen bonds, the hydrophobic effect leads to self-assembly of amphiphiles which plays an important role in many biological processes like formation of lipid membranes, protein folding etc.

The aggregates of various structures can transform from one to another by changing the solution conditions such as electrolytic or lipid concentration, pH or temperature. At very low concentrations, amphiphilic molecules form a monolayer at the air water interface. Above a certain concentration, called critical micellar concentration (CMC), amphiphiles aggregate into a variety of structures like rods, disc, spherical, cylindrical, bilayers and vesicle shown in table 1.1.


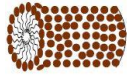


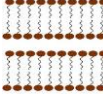
Packing parameter	Structure name	Structure
• $<1/3$	spherical micelles	
• $1/3-1/2$	cylindrical micelles	
• $1/2-1$	vesicles	
• $1/3-1/2$	hexagonal phase	
• ~ 1	lamellar phase	

Table 1.1 Summary of aggregated structures that can be predicted from the critical packing parameter

The different aggregates of amphiphilic molecules are in thermodynamic equilibrium. This equilibrium claims that the chemical potential (μ) of all identical amphiphile has to be same in all aggregates, i.e, $\mu_1 = \mu_2 = \mu_3 = \dots = \mu_N$. This may be written as

$$\mu = \mu_1^0 + k_B T \log X_1 = \mu_2^0 + \frac{k_B T}{2} \log \frac{X_2}{2} = \mu_3^0 + \frac{k_B T}{3} \log \frac{X_3}{3} = \dots \quad 1.1$$

or

$$\mu_N = \mu_N^0 + \frac{k_B T}{N} \log \left(\frac{X_N}{N} \right) = \text{Constant} \quad 1.2$$

Where, $N = 1$ corresponds to monomer, $N=2$ corresponds to dimer and so on. μ_N is the mean chemical potential of a molecule in an aggregate of aggregation number N , μ_N^0 is the standard chemical potential corresponding to the interaction free energy per molecule in aggregates of aggregation number N , X_N is the total concentration of amphiphile in aggregate of size N . The second term in the equation 1.2 arises from entropy of mixing. The total concentration (X) of the system considered to be small, i.e,

$$X = \sum_{N=1}^{\infty} X_N \ll 1 \quad 1.3$$

From $\mu_N = \mu_1$, we get

$$X_N = N [X_1 \exp\{(\mu_1^0 - \mu_N^0)/k_B T\}]^N = N(X_1 e^{\alpha})^N \quad 1.4$$

where $\alpha = \frac{\mu_1^0 - \mu_N^0}{k_B T}$. The essential condition for the formation of aggregates of size N is $\mu_N^0 < \mu_1^0$. When $X_1 \ll 1$, $X_1 e^{\alpha} < 1$ and we must have $X_N \ll X_1$ for sufficiently low monomer concentrations. Therefore, $X \approx X_1$ and the isolated monomers in solution will be the favoured state. As X_1 is increased $X_1 e^{\alpha}$ approaches unity. Since $X_N < 1$, X_1 never exceed a value of the order of $e^{-\alpha}$. Therefore, the monomer concentration should saturate at a value $\sim e^{-\alpha}$. Beyond which, aggregates are formed. This concentration is known as the critical micellar concentration (CMC). It is given by

$$CMC = (X)_c \approx (X_1)_c \approx e^{-(\mu_1^0 - \mu_N^0)/k_B T} \quad 1.5$$

The CMC is measured experimentally by many microscopic and macroscopic techniques such as conductivity (for ionic surfactant) and surface tension. The typical value of CMC of a CTAB surfactant is $\sim 10^{-3}$ M and that of a lipid, such as DPPC, is $\sim 10^{-12}$ M. Usually the CMC decreases with increasing the length of hydrocarbon chain (9).

According to Israelachvili (10) the structure of the aggregate can be predicted from the critical packing parameter (p), which is defined as

$$p = \frac{v}{a_0 l_c}$$

Where v is the effective volume occupied by hydrophobic chains in the aggregate core, l_c is the critical acyl chain length and a_0 is the effective hydrophilic head group surface area at the aggregate-solution interface.

Preparation of unilamellar vesicles will be described in details in the next chapter. Lipids with head group of larger cross-sectional area relative to chain cross-section area such as, DOPC, DOPG and DOTAP generally form bilayer in aqueous solution at a sufficient concentration above CMC. Surfactant like CTAB usually forms spherical micelles just above CMC. At higher concentrations of amphiphiles the self-assembled structures form a variety of liquid crystalline phases. The most common examples are the hexagonal and lamellar phases. The hexagonal phase consists of cylindrical micelles arranged on a two-dimensional hexagonal lattice and the lamellar phase consists of a stack of bilayers separated by water.

In the presence of water, the phospholipid structure (comparable area of between head and chain) prevents the formation of micelles because of two unsaturated fatty acid chains that prevent the aggregation into a tight sphere. These are usually formed vesicles at room temperature in which are bilayer sac of phospholipid molecules. All lipids have a transition temperature (T_m) at which they undergo a transition from gel phase to liquid phase. In gel phase, hydrophobic chains are highly ordered and rigid such that mobility is very less. In the liquid phase, chains are very flexible and freely diffuse in the bilayer. T_m is dependent on the number of carbon atoms, number of double bonds in the hydrocarbon chain, number of carbon atoms and also nature of the head group. The conformational state (*cis/trans*) in the hydrocarbon chain drastically changes the transition temperature. *Cis* configuration has a significantly lower transition temperature compare to *trans*. The transition temperature also plays an important role on the structure and phase behaviour of lamellar phase.

1.4 Phase behaviour of lipid-water system

Phospholipids are the main constituents of plasma membranes and they form the structural basis of these membranes. Phospholipid molecules spontaneously form bilayers when placed in water. Due to the hydrophobic effect, phospholipid molecules reorient in such a way that their head groups towards water and shield their fatty acid tails from water. Fluidity i.e. relative mobility of individual lipid molecules is an important property of lipid bilayers. This relative mobility is greatly influenced by the temperature. As the temperature changes mobility of the lipid molecule also changes. This response is known as the phase behaviour of the lipid bilayer. Self-assembly of lipids in an aqueous solution above critical micelle concentration leads to the formation of lamellar phases, consisting of a stack of bilayers separated by water. Depending upon the nature of the head group and temperature they exhibit a variety of lamellar phases (11). Above the transition temperature (T_m), hydrocarbon chains of lipid are completely molten and disordered a fluid phase, known as L_α phase.

Typical lateral diffusion constant and bilayer bending modulus in this phase are $\sim 10^{11} \text{ m}^2\text{s}^{-1}$ and $\sim 10^{-19} \text{ J}$ ($\sim 10\text{-}20 \text{ K}_B\text{T}$), respectively. On decreasing the temperature below T_m , fluid phase transforms into a gel phase where hydrocarbon chains are fully stretched (all trans conformation). There are two types of gel phases found in lipid, are known as L_β phase and $L_{\beta'}$ phase. In the L_β phase, the hydrocarbon chains are parallel to the bilayer normal i.e. zero tilt. Some lipids with larger head group exhibit the $L_{\beta'}$ phase where chains are tilted with respect to bilayer normal. The cholesterol influences the main transition temperature (T_m) of lipid bilayer. T_m decreases with increasing concentration of cholesterol. It indicates that cholesterol transforms the gel phase into a fluid phase (12). At a particular concentration of cholesterol ($\sim 20 \text{ mol } \%$) below T_m , liquid ordered phase (l_o) is formed which indicates that coexistence of the gel ($L_{\beta'}/L_\beta$) with a cholesterol-rich phase (13). Above T_m it transforms into the coexistence of l_o with another fluid phase, known as liquid disordered phase (l_d) [14]. At higher cholesterol concentration typically $> 20 \text{ mol } \%$, the main transition completely disappears and the gel phase replaced by the l_o phase. Lipid diffusion or mobility is decreased in the fluid phase and increased in the gel phase, as cholesterol concentration is increased (15). T_m of few lipids are listed in table 1.2.

Table 1.2. This is a list of lipids used in the present work. All these lipids have two identical chains. The number of carbon atoms in the chains and the number of double bonds is also given. The position of the double bond along the chain (starting from ester group) and its conformation are indicated in the bracket. T_m is the chain melting transition temperature discussed above.

Lipids	Abbreviation	Charge	Lipid chains	T_m (°C)
1, 2-dioleoyl-sn-glycero-3-phosphocholine	DOPC	Zwitterionic	18:1(cis-9)	-18.3
1,2-dioleoyl-sn-glycero-3-phospho-(1'-rac-glycerol) (sodium salt)	DOPG	Negative	18:1(cis-9)	-18
1,2-dioleoyl-3-trimethylammonium-propane (chloride salt)	DOTAP	Positive	18:1(cis-9)	-11.9
1,2-dimyristoyl-sn-glycero-3-phosphocholine	DMPC	Zwitterionic	14:0	24
1,2-dipalmitoyl-sn-glycero-3-phosphocholine	DPPC	Zwitterionic	16:0	42
1,2-dimyristoyl-sn-glycero-3-phospho-(1'-rac-glycerol) (sodium salt)	DMPG	Negative	18:1	23.3

A model based on thermodynamics of lipid-cholesterol interaction has been used to calculate the phase diagram in binary lipid-cholesterol mixtures (31). Two basic conformational states; an ordered state (all trans) and a disordered state were used in the model. Entropic contribution comes from the conformational difference between the two states and from the ideal mixing of the states. Relative populations of the two conformational states were obtained by minimizing the free energy with respect to relative population subjected to the constraint that the sum of the two populations equals unity. The coexistence of two fluids (l_o and l_d) phases was obtained for reasonable range of values of model parameters. Introducing a solid phase with long range molecular packing within the bilayers, a temperature-concentration phase diagram has been determined. A microscopic model also provides a similar phase behavior.

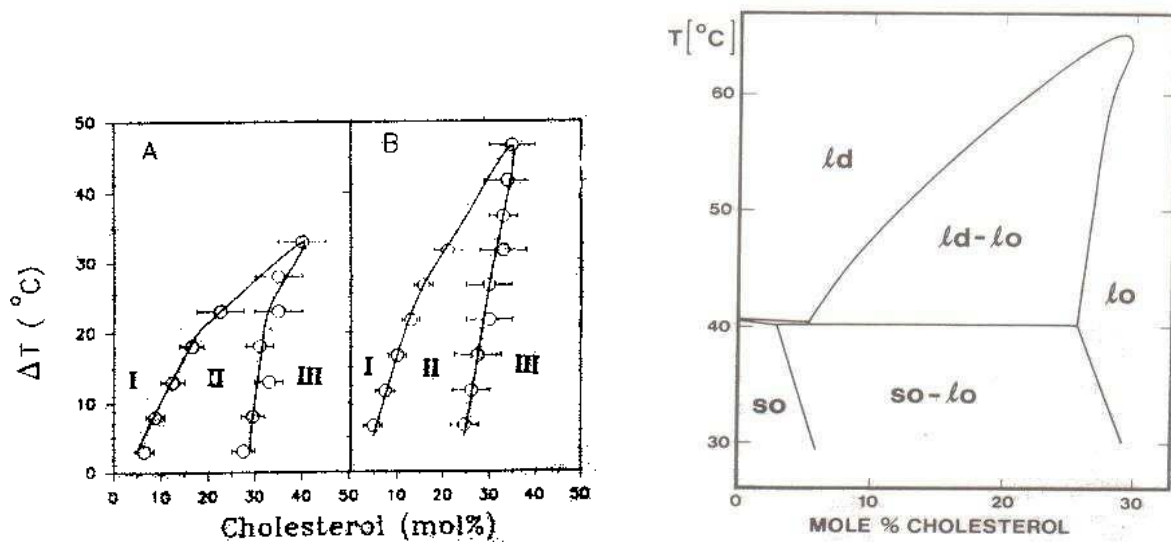


Figure 1.3: (a) Partial phase diagram of binary mixtures of cholesterol with DPPC (A) and sphingomyelin (B) obtained from ESR study [29]. ΔT is the difference between the temperature of measurement and the corresponding main transition of pure lipid. I: l_d phase; II: $l_d + l_o$; III: l_o phase. (b) Theoretical phase diagram calculated from microscopic model [31].

In this model, each monolayer is modeled as a triangular lattice where each lattice site is occupied either by acyl chain of the lipids or cholesterol. As in the case of the thermodynamic model, two conformational states, the ordered state and the disordered state, were considered for the acyl chains. Crystalline domains can develop in the plane of the bilayer with different orientations of the lattice. This is taken into account in the model by

assigning a Potts variable to the PC molecules with ordered chain conformations. Hamiltonian for lipid-cholesterol mixtures was constructed by taking into account interaction energy between acyl chains and between acyl chain and cholesterol molecules using a mean field approximation. Minimizing the free energy derived from the Hamiltonian a phase diagram was obtained (Fig. 1.3 b) which is in agreement with the experimental phase diagram (Fig. 1.3 a) (see ref. [31] for details).

1.5 Lipid bilayer as a model system of biological membrane

The biological membranes are complex, regulated by various active processes occurring on the cell surface. It is often useful to study the artificial lipid bilayer as a bio-mimetic system in order to gain insights into the structures and functions of membranes. So, the lipid bilayer can be used as an excellent model system for all biological membranes. In our study we use unilamellar vesicles to investigate the fundamental properties of biological membrane at physiological condition. Vesicles are also extensively used as carriers of bioactive agents, including drugs, vaccines and cosmetics (16). When a small amount of dehydrated lipid is dissolved into water and vortex then multilamellar vesicles are formed. To make unilamellar vesicle there are so many methods such as sonication, extrusion through a membrane and electro formation depending to their average size, unilamellar vesicles are classified into three categories. Vesicles have diameter between 10-100 nm called small unilamellar vesicle (SUV), between 100-250 nm called large unilamellar vesicle (LUV) and between 5-50 μm called giant unilamellar vesicle (GUV). SUV can usually be prepared by high energy (power >150 watt) probe sonication method and LUV are made by the extrusion method which are discussed in chapter 2. Both the size of SUV and LUV are confirmed by dynamic light scattering measurement. GUVs are prepared from the electro formation first described by Angelova et al (17). Owing to their large size these vesicles can be observed under phase contrast or fluorescence microscopy. Therefore, any morphological change of GUV can directly be envisaged using optical microscopy. Fig. 1.4 represents schematic representation of unilamellar vesicles.

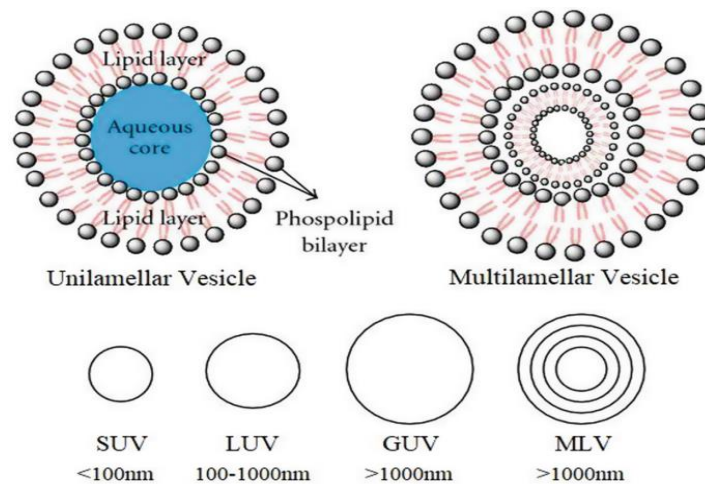


Fig.1.4 Schematic representation of multilamellar, giant, large and small unilamellar vesicles.

1.6 Importance of ions in biological membranes

Different monovalent and divalent ions, such as Na^+ , K^+ , Ca^{2+} , Mg^{2+} , Fe^{2+} etc. play important roles in many biological systems. Ions are present in the intra and extra cellular fluid (fig. 1.5). Among all the ions present in the cellular media, Na and K are the most abundant cations in human body. Sodium ions with higher concentration ($>100 \text{ mM}$) are mostly found in extra cellular fluid and maintains level of body fluids. Potassium ions are mostly found inside cell and responsible for many cellular processes like nerve impulses, heartbeats and level of body fluids etc. As counter ions of sodium, Cl^- is mainly found in extra cellular fluid maintaining hydration and balancing cations in the fluid. Other anions, such as Br^- and I^- are also found in all organisms and essential part of biological functions. Ca^{2+} plays a crucial role in many cellular processes.

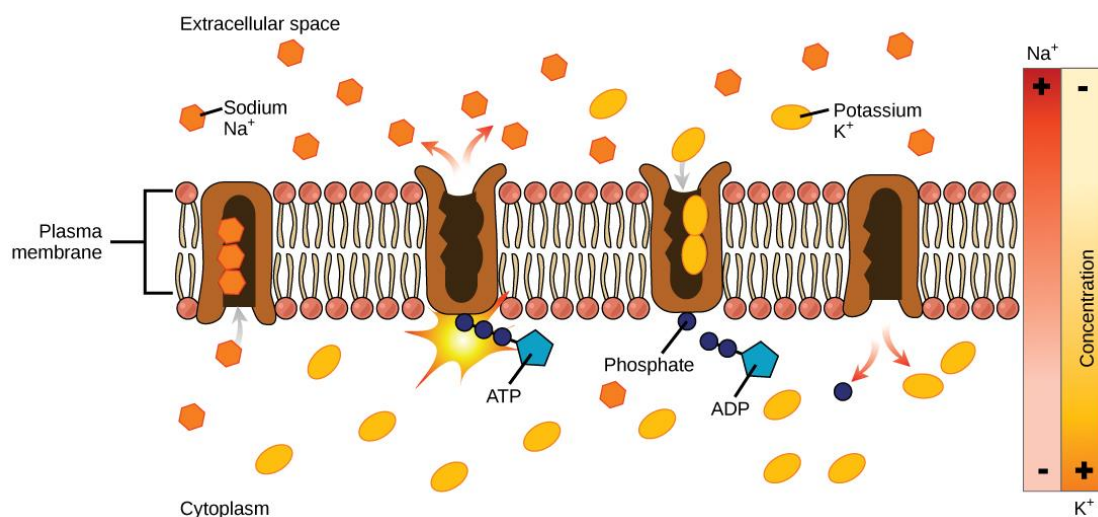


Fig. 1.5 Schematic representation of different ions in the intracellular and extracellular fluid

Ion channels are formed via pore formation through the membrane protein in the cell membrane. It established a resting membrane potential, shaping action potential and control other electrical signals by passing ion through the channel pore (20). The Na^+ and K^+ -ATP phase also known as ion pump that creates an ion concentration gradient between inside and outside the cell.

1.7 Influence of cholesterol on biological membranes

Cholesterol is a ubiquitous and major sterol component of all animal cell membranes. It plays an important role in maintaining membrane structure and the physiochemical properties of membrane. The structure of cholesterol is shown in the figure 1.6. Cholesterol is an amphipathic molecule like phospholipids and form a hydrogen bond with neighbouring lipid molecule especially with sphingomyelin. Presence of cholesterol is believed to be responsible for lateral organization of lipids in the membranes. Cholesterol provides rigidity and integrity to the plasma membrane and helps to maintain the fluidity.

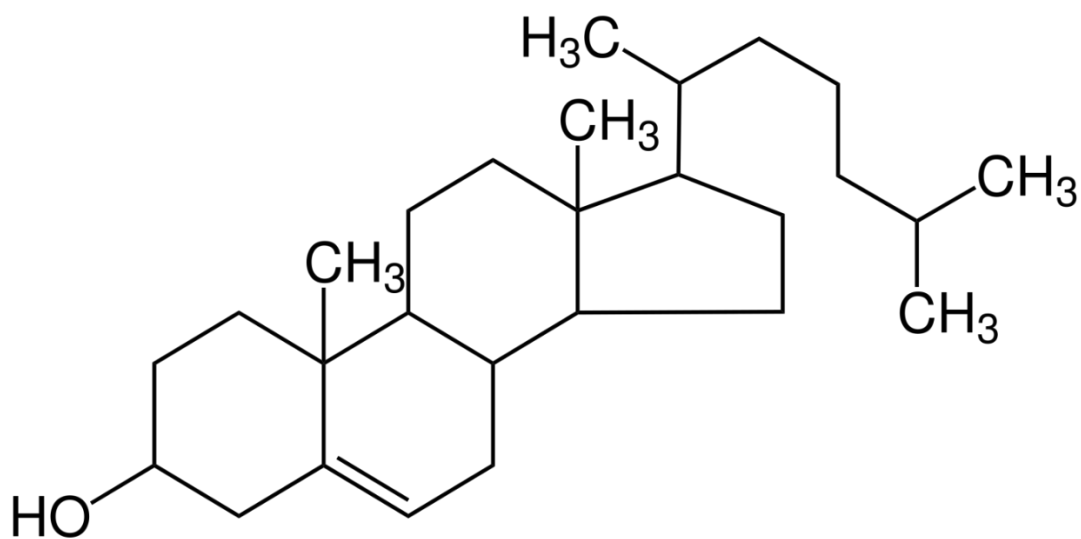


Fig. 1.6 Structure of cholesterol

Cholesterol is present in bio membranes of all animal cells, but its content varies in different parts of organisms. In particular, a high content of cholesterol can be found in the brain, which contains about 25% of the whole cholesterol of a human body (1). Cholesterol influences the main transition temperature (T_m) and the pre transition temperature (T_p) of lipid bilayer. These temperatures (T_m, T_p) of lipid bilayers has been determined by DSC experiments. The main transition temperature decreases with increasing concentration of cholesterol indicating that cholesterol transforms the gel phase into a fluid phase (18, 20). In

the cholesterol containing membrane, bilayer thickness depends only on the chain length and phase state of the lipid. Bilayer thickness is increased in the gel phase of PC bilayers for chain length from 12 to 16 carbons, as cholesterol is known to remove the chain tilt. However, for longer chain lengths, the bilayer thickness is decreased in the gel phase (21). Bilayer thickness of fluid phase of cholesterol containing membrane also increases but at low cholesterol concentration this effect is not significant (22). Cholesterol induces non-lamellar phases in lipids, such as PEs and unsaturated PCs (23, 24). Cholesterol also facilitates the formation of the L_C phase in PE bilayers (25) which in general occurs after long incubation at 4^o C. At a particular concentration of cholesterol (~ 20 mole %) below T_m , liquid ordered phase (L_O) is formed which indicates that coexistence of the gel ($L_{\beta'}/L_{\beta}$) with a cholesterol-rich phase (26). Above T_m it transforms into the coexistence of with another fluid phase, known as liquid disordered phase (L_d) (27). At higher cholesterol concentration typically > 20 mole %, the main transition completely disappears and the gel phase replaced by the L_O phase. Lipid diffusion or mobility is decreased in the fluid phase and increased in the gel phase, as cholesterol concentration is increased (28). In general, cholesterol has greater affinity for saturated lipids than for unsaturated ones. This is due to the fact that cholesterol cannot pack efficiently in the lipid bilayers if the molecules possess a *cis*-double bond, creating a kink in the chain. Among phospholipids, affinity for cholesterol increases in order of PC > PS > PE (19). However, sphingomyelin has more affinity for cholesterol than PC (29). This could be due to the ability of the -OH group of cholesterol to form hydrogen bond with the neighbouring sphingomyelin molecules. Rafts probably exist in membrane in the liquid order (L_O) phase. The coexistence of the cholesterol-rich liquid-ordered (L_O) phase and cholesterol-poor liquid-disordered (L_d) phase below the transition temperature (T_m) of the saturated lipid, is believed to be relevant for the formation of rafts in plasma membranes. Cholesterol is known to alter significantly the elastic properties and permeability (30) of the membrane. Therefore, cholesterol is expected to change the surface charge and hence the electrostatic behaviour of the membrane. Recently many computer simulation studies have been revealed that cholesterol affects the surface charge of the membrane in the presence of ions (1). In brief, cholesterol has significant effect on vesicle size, zeta potential, membrane binding and electrostatics of the membrane. A variety of simulation and experimental studies have been done before to investigate the effect of cholesterol mostly on neutral membranes. Therefore, in our work we have given attention to study effect of cholesterol on charged phospholipid membranes.

References: -

1. L. Mao, L. Yang, Q. Zhang, H. Jiang and H. Yang, *Biochim. Biophys. Res. Comm.*, 1-2, 125-129 (2015)
2. M. Edidin, *Molecular Cell Biology*, 5, 414-418 (2003)
3. A. Fischer, A. Franco and T. Oberholzer, *ChemBioChem*, 5, 409-417 (2002)
4. K. Holmberg, B. Jonsson, B. Kronberg, and B. Lindman, John Wiley & Sons, Chichester, UK, 2nd edition, 2002
5. M. J. Rosen, Wiley, New York, NY, USA, 2nd edition, 1989.
6. D. J. Murphy, *Progress in Lipid Research*, 32, 247-280 (1993).
7. P. Horowicz, A. L. Hodgkin, *J. physiol.*, **153**, 404-412 (1960)
8. X. Cui, S. Mao, M. Liu, H. Yuan, and Y. Du, *Langmuir*, vol. 24, no. 19, 10771–10775 (2008).
9. C. J. Marzzacco, B. Peterson, *The Chemical Educator*, 12, 80-84 (2007)
10. J. N. Israelachvili, *Intermolecular and Surface Forces*, Academic Press, New York, NY, USA, 2nd edition, 1992.
11. E. Sackmann, R. Lipowsky, *Structure and Dynamics of Membranes From Cells to Vesicles*, (Elsevier Science B. V, 1, 1995)
12. T. P. W. McMullen, R. N. A. H. Lewis, and R. N. McElhaney, *Biochemistry*, 32, 516–522 (1993)
13. K. Mortensen, W. Pfeiffer, E. Sackmann and W. Knoll. *Biochim. Biophys. Acta*, 945, 221-245 (1988)
14. T. E. Thompson, M. B. Sankaram, *Biochemistry*, 29, 10670 (1990)
15. A. Filippov, G. Or'add, G. Lindblom, *Biophys. J.*, 86, 891–896 (2004)
16. V. P. Torchilin, *Nat. Rev. Drug Discov*, 4, 145-160 (2005).
17. M. I. Angelova, S. Soleau, P. Meleard, J.F. Faucon and P. Bothorel, *Prog. Colloid Polym. Sci.*, 89, 127 (1992).
18. M. Cascio, T. S. Tillman, *Cell Biochem Biophys*, 38, 161-190 (2003)
19. T. P. W. McMullen and R. N. McElhaney, *Biochemistry* 36, 4979 (1997).

20. T. P. W. McMullen, R. N. A. H. Lewis, and R. N. McElhaney, *Biochemistry* 32, 516 (1993).
21. T. J. McIntosh, *Biochim. Biophys. Acta* 513, 43 (1978).
22. S. W. Hui and N. B. He, *Biochemistry* 22, 1159 (1983).
23. R. M. Epand, D. W. Hughes, B. G. Sayer, N. Borochoy, D. Bach, and E. Wachtel, *Biochim. Biophys. Acta* 1616, 196 (2003).
24. H. Takahashi, K. Sinoda, and I. Hatta, *Biochim. Biophys. Acta* 1289, 209 (1996).
25. T. P. W. McMullen, R. N. A. H. Lewis, and R. N. McElhaney, *Biochim. Biophys. Acta* 1416, 119 (1999).
26. K. Mortensen, W. Pfeiffer, E. Sackmann and W. Knoll. *Biochim. Biophys. Acta*, 945, 221-245 (1988).
27. T. E. Thompson, M. B. Sankaram, *Biochemistry*, 29, 10670 (1990).
28. A. Filippov, G. Oradd, G. Lindblom, *Biophys. J.*, 86, 891–896 (2004).
29. M. B. Sankaram and T. E. Thompson, *Biochemistry* 29, 10670 (1990).
30. Cholesterol Stiffening of Lipid Membranes. Fathima T. Doole, Teshani Kumarage, Rana Ashkar & Michael F. Brown, 255, 385–405 (2022).
31. J. H. Ipsen, G. Karlström, O. G. Mouritsen, H. Wennerström, and M. J. Zuckermann, *Biochim. Biophys. Acta*, 905, 162 (1987).

Chapter 2

Experimental Techniques

2.1 Introduction

In this chapter, we have described briefly the experimental techniques which are used to study the effect of cholesterol on the interaction of ions with phospholipid membrane. Section 2.2 describes the extrusion technique which was used to prepare large unilamellar vesicles. In section 2.3 we have discussed the preparation of small unilamellar vesicles using sonication method. The average size of the lipid vesicles was confirmed by dynamic light scattering measurement and principle of zeta potential, which is discussed in section 2.4. Section 2.5 describes the fluorescence spectroscopy techniques. We have discussed isothermal titration calorimetry in section 2.6. Isotherms obtained from ITC data were fitted using surface partition model. Small angle x-ray scattering technique (SAXS) to study morphology and structural properties of LUV and SUV is discussed in section 2.7. Phase contrast microscopy was used to observe morphological changes in giant unilamellar vesicles (GUVs). We have discussed electroformation method for preparation of GUV and basic principles of phase contrast microscopy in section 2.8.

2.2 Preparation of large unilamellar vesicle (LUV)

There are several techniques for the preparation of large unilamellar vesicles, reported in the literatures [1, 2]. However, most convenient and widely used method is the extrusion method. During the preparation of vesicles, it is important to keep the temperature above the chain melting transition temperature (T_m) of lipid i.e vesicles form only in the fluid lamellar phase of the hydrated lipid film. In the gel phase, the membranes are rigid and stiff. It costs more energy to bend the bilayer and hence it prevents the formation of vesicles. Large unilamellar vesicles were prepared using an extrusion technique as described by Hope et al. [2]. An appropriate amount of lipid in chloroform (concentration of stock solution is 10 mg/ml) was transferred to a 5 ml glass bottle. Organic solvent was removed by gently passing dry nitrogen gas. The traces of the solvent were then removed by placing the sample in a desiccator, connected to a vacuum pump for a couple of hours.

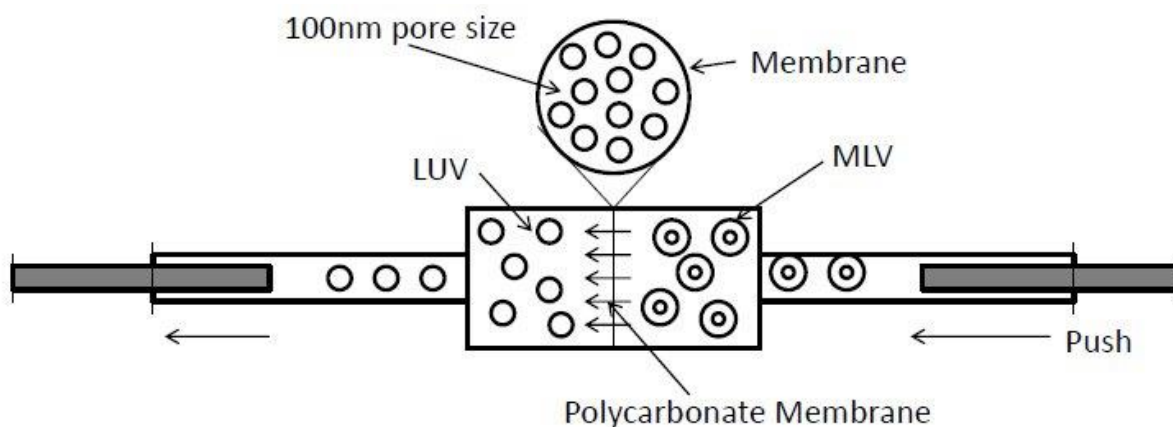


Fig. 2.1 Schematic diagram of extruder which showing the formation of MLV to LUV.

Required volume of previously prepared buffer (HEPES-1mM) was added to the dried lipid film so that the final desired concentration (1.2 mM) was obtained. The lipid film with the buffer was kept overnight at 4°C to ensure the better hydration of phospholipid heads. Vortexing of hydrated lipid film for about 30 minutes produces multilamellar vesicles (MLV). LUVs were prepared by extruding the MLV with LiposoFast from AVESTIN (Canada). MLV suspensions were extruded through polycarbonate membranes of pore diameters 100 nm. This results in a formation of well-defined size of LUV (average diameter ~ 100 nm), as measured by dynamic light scattering. In order to avoid the artifact caused by air bubbles, vesicle solution was degassed prior to all measurements.

2.3 Preparation of small unilamellar vesicles (SUV):

Small unilamellar vesicles (SUV) can also be prepared by extrusion method using polycarbonate membrane of smaller diameter (~ 50 nm). In this case, the pore diameter of the polycarbonate membrane was taken as 50 nm. MLV suspension successively was extruded through polycarbonate membrane of 50 nm pore diameter and the mean size of the SUVs obtained less than 100 nm which was confirmed by DLS experiment. The size of the SUV was around 60 nm. In this method we could not reduce the size below 60 nm. Besides extrusion method, SUV can be produced using sonication method [3]. Prior to sonication, MLV needs to be prepared. MLV preparation is already discussed in previous section. For the formation of SUV, the MLV was sonicated gently using probe sonicator, QSONICA-SONICATORS (125W, 20 kHz) (Fig. 2.2).



Fig. 2.2 Qsonica Ultrasonic Homogenizer

Probe sonicator delivers high energy into the lipid suspension. Power delivery was controlled as percentage amplitude (20%, 30% & 40%). After sonication for 30 min, a clear suspension of SUVs was obtained. We extruded the sonicated vesicles one-time through 100 nm polycarbonate membrane as a filtration step. Also, due to the high degree of curvature of these membranes, SUV are inherently unstable and will spontaneously fuse to form larger vesicles when stored below their phase transition temperature.

2.4 Characterization of Vesicles

2.4.1 Size measurement using dynamic light scattering (DLS)

Dynamic light scattering (DLS) is the most popularly used technique for the measurement of particle size in the submicron to nanometre range. We first discuss the principle of DLS technique. When particles are dispersed in a liquid they move randomly in all directions. This motion is known as Brownian motion. The principle of Brownian motion is that particles are constantly colliding with solvent molecules. These collisions cause a certain amount of energy to be transferred, which induces particle movement. The energy transfer is more or less constant and therefore has a greater effect on smaller particles. As a result, smaller particles are moving at higher speeds than larger particles. If all other parameters are known which have an influence on particle movement, we can determine the hydrodynamic diameter by measuring the speed of the particles. In a typical experimental setup, scattered light can be detected at both 90° as well as 173° scattering angle. The backscattered light intensity (173°) is better than 90° scattered for more accuracy of size measurement (Fig. 2.4). This is because

the scattered light from unwanted big particles or dust particles in the solution can be minimized by the backscattered mechanism since there are known to scattered by the dust particle in forward direction [8]. It is also important that the rotational diffusion coefficient can be ignored when the scattered light is detected at 173° compared to the detection at 90° . Therefore, by detecting the back scattered light, the translational diffusion D can be obtained. The back scattered light is detected and sent to digital signal processing correlator.

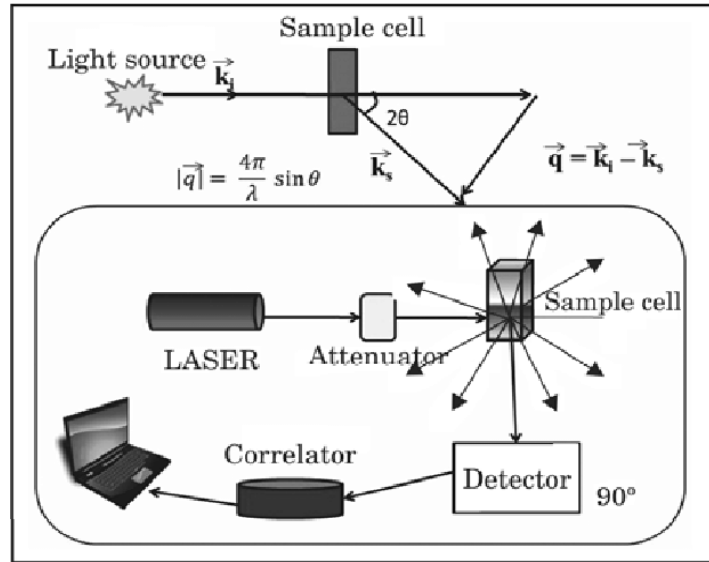


Fig. 2.4 Schematic diagram of experimental set up of dynamic light scattering (DLS).

The scattering wave vector (\vec{q}) is defined as

$$|\vec{q}| = |\vec{k}_s - \vec{k}_i| = \frac{4\pi \sin \theta}{\lambda} \quad (2.1)$$

Where \vec{k}_i and \vec{k}_s are the incident and scattering vector respectively.

The intensity fluctuations measured at two different time points t and $t + \tau$, where τ is the correlation time of the measured intensities and it is much smaller than the characteristic time of fluctuation. The correlation function is defined as

$$G(\tau) = \langle I(t) I(t + \tau) \rangle = \lim_{T \rightarrow \infty} \left\{ \frac{1}{T} \int_0^T I(t) I(t + \tau) dt \right\} \quad (2.2)$$

The translational diffusion coefficient (D) of the particles can be determined from autocorrelation by fitting the equation

$$G(\tau) \sim e^{-q^2 D \tau} \quad (2.3)$$

The hydrodynamic radius (R_H) of the vesicles can be determined from the diffusion coefficient using the Stokes-Einstein relation.

$$R_H = \frac{k_B T}{6\pi\eta D} \quad (2.4)$$

Where k_B is Boltzmann constant, T is absolute temperature, η is the viscosity of the medium in which LUV are dispersed D is the diffusion constant and other symbols have their usual meaning. Hydrodynamic radius (R_H) refers to the radius of the sphere that diffuses with the same velocity as that of the particle. The major assumption in DLS is that we assume the spherical shape of LUV. Therefore, the information of shape changes or fluctuations of the vesicles does not determine by the DLS experiment i.e. it always consider the spherical shape during the measurement [9]. DLS measures the hydrodynamic radius which includes both solvent (hydro) and shape (dynamic) effects. Polydispersity index (PDI) is a measure of dispersion or the standard deviation of size distribution. PDI indicates the extent of Polydispersity of the size distribution. The slope of the correlogram and width of the size distribution provide the idea of Polydispersity of the sample. Smooth exponential decay of intensity correlation curve indicates no aggregation or coagulation process occurring in the system. It is known that $PDI > 0.7$ usually indicates that sample is highly polydisperse and probably not suitable for the DLS measurement. $PDI < 0.05$ is purely monodisperse.

Using dynamic light scattering (DLS), the size distribution was measured at room temperature ($\sim 25^\circ\text{C}$) with Zetasizer Nano ZS (Malvern Instruments, UK). Zetasizer Nano uses 4 mW He Ne Laser of wavelength 632.8 nm and power 2 – 4 mW. A transparent quartz cuvette was used for the size measurement. In each measurement, we have performed 10-100 consecutive runs. The disposable zeta cuvette is also used to measure size distribution. Typical size distribution of LUV has been shown in fig. 2.5.

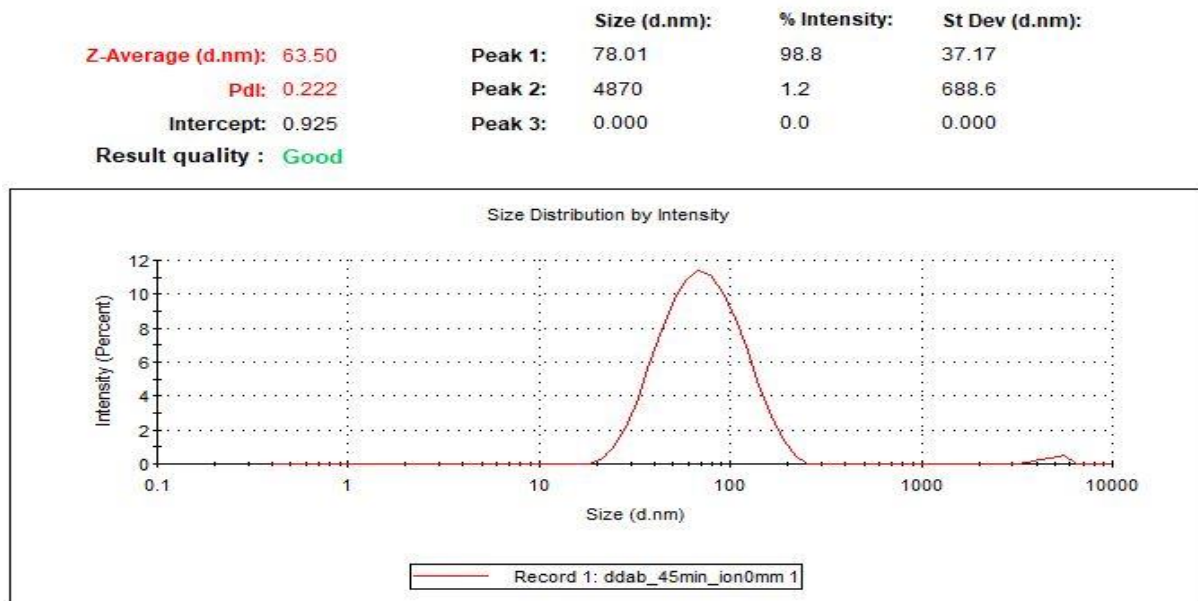


Fig. 2.5 size distribution measurement of SUV made from DDAB surfactant

2.4.2 Zeta potential

This technique of zeta potential is widely used to estimate the surface charge, surface potential of the vesicles and to determine the electrophoretic mobility, isoelectric point of charge system. When charged LUVs are embedded in aqueous solution containing ions, the oppositely charged ions form electrostatic double layer around the LUV and some ions are free to diffuse. Thus, electrostatic double layer exists around each vesicle. The scientists Derjaguin, Landau, Verwey, and Overbeek (DLVO) developed a theory in the 1940s which dealt with the stability of colloidal systems. DLVO theory suggests that the stability of a particle in solution is dependent upon its total potential energy function V_T .

$$V_T = V_A + V_R + V_S \quad (2.5)$$

V_S is the potential energy due to the solvent. V_A and V_R , these are the attractive and repulsive contributions. They potentially are much larger and operate over a much larger distance.

$$V_A = -A/12\pi D^2 \quad (2.6)$$

Where A is the Hamaker constant and D is the particle separation. The repulsive potential V_R is a far more complex function.

$$V_R = 2\pi\epsilon a\zeta^2 \exp(-\kappa D) \quad (2.7)$$

Where a is the particle radius, ϵ is the solvent permeability, κ is a function of the ionic composition and ζ is the zeta potential.

DLVO theory suggests that the stability of a colloidal system is determined by the sum of these van der Waals attractive (V_A) and electrical double layer repulsive (V_R) forces that exist between particles as they approach each other due to the Brownian motion they are undergoing. If the particles have a sufficiently high repulsion, the dispersion will resist flocculation and the colloidal system will be stable. However, if a repulsion mechanism does not exist then flocculation or coagulation will eventually take place. Zeta potential is a physical property which is exhibited by any particle in suspension, macromolecule or material surface. It can be used to optimize the formulations of suspensions and protein solutions and also predict the interaction with the surfaces. This technique is widely used to estimate the surface charge, surface potential of the particle and to determine the electrophoretic mobility, isoelectric point of charge system. When charged LUVs are embedded in aqueous solution containing ions, the oppositely charged ions form electrostatic double layer around the LUV. Thus, electrostatic double layer exists around each vesicle. Ions are strongly bound surrounding the vesicles and form the first liquid layer is called stern layer. From the stern layer ions are loosely bound with the vesicles and free to diffuse and form diffuse layer. The boundary of the diffuse layer is called shear or slipping plane. When the vesicle moves, ion within the boundary of slipping plane move with it. The electrostatic potential that exists in the shear or slipping plane is known as zeta potential. Therefore, zeta potential can be a good approximation of the surface potential of LUV.

The ζ -potential was measured from the electrophoretic mobility by laser Doppler velocimetry using the Helmholtz-Smoluchowski equation (10, 11).

$$\zeta = \frac{3\mu\eta}{2\epsilon f(\kappa a)} \quad (2.8)$$

Where η and ϵ are the coefficient of viscosity and the permittivity of the aqueous medium, respectively. $f(\kappa a)$ is the Henry function, which depends on the inverse Debye length (κ) and the radius (a) of the vesicle, the change in the size distribution of the vesicles does not alter the zeta potential significantly. This is due to the fact that zeta potential depends on the formation of electrostatic double layer. In Smoluchowski approximation, the maximum value of the function $f(\kappa a)$ is equal to 1.5 when particles are in aqueous media [9]. However, when

the particles are suspended in a nonaqueous medium, the value of $f(\kappa a)$ would be 1 (Huckel approximation). We have used $f(\kappa a) = 1.5$ to calculate the ζ -potential from measured electrophoretic mobility. The average ζ -potential was obtained using three successive measurements. Each measurement included 10–100 runs.

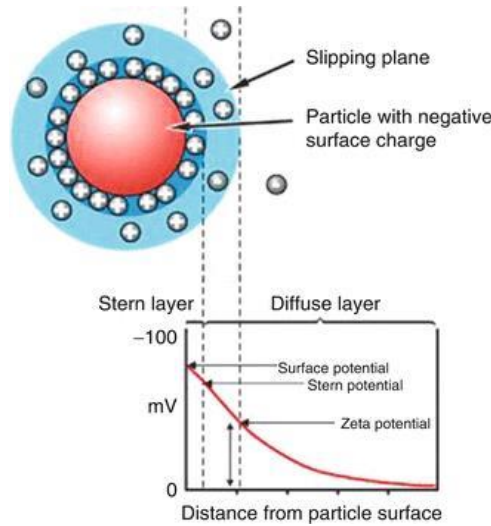


Fig. 2.6 Formation of electric double layer due to charged vesicles and zeta potential measurement at the slipping plane.

Effective charge, Q_{eff} , of the vesicles has also been estimated from the measured electrophoretic mobility according to equation

$$\mu = \frac{Q_{\text{eff}}}{6\pi\eta a_{\text{eff}}} \quad (2.9)$$

a_{eff} is the effective radius of the vesicle including stern layer and it can be obtained from dynamic light scattering.

In this study, the average ζ potential and size were obtained from 3 to 4 successive measurements. The same cuvette is used for both ζ potential and DLS measurements. All experiments were performed at 25 °C. Typical zeta potential distribution curve of SUV is shown in Fig. 2.7

	Mean (mV)	Area (%)	St Dev (mV)
Zeta Potential (mV): 51.0	Peak 1: 51.0	100.0	5.22
Zeta Deviation (mV): 5.22	Peak 2: 0.00	0.0	0.00
Conductivity (mS/cm): 1.46	Peak 3: 0.00	0.0	0.00
Result quality : Good			

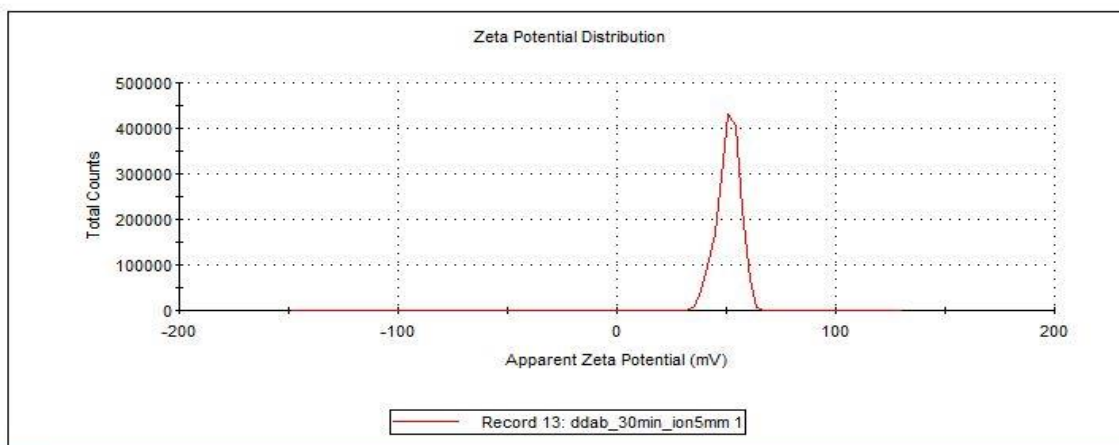


Fig. 2.7 Zeta potential distribution of SUV made from DDAB surfactant

2.5 Fluorescence spectroscopy:

2.5.1 Origin of fluorescence

Fluorescence spectroscopy analyses fluorescence from a molecule based on its fluorescent properties. Fluorescence spectroscopy uses a beam of light that excites the electrons in molecules of certain compounds and causes them to emit light. That light is directed towards a filter and onto a detector for measurement to identify the molecule or change in the molecule. When molecules are excited by a constant source of light i.e. fixed wavelength, emit fluorescence detected as a function of wavelength called steady state fluorescence spectra. A fluorescence emission spectrum is when the excitation wavelength is fixed and the emission wavelength is scanned to get a plot of intensity emission wavelength. Typically, the emission spectrum occurs at higher wavelength (lower energy) than the excitation spectrum. The spectral intensity or peak wavelength may alter with the change of temperature, concentration or interaction with other molecules. Some fluorophores are sensitive to solvent environment properties such as pH, polarity and ion concentration. Some intrinsically fluorescent molecules are chlorophyll and amino acid residue tryptophan (Trp) phenylalanine (Phe) and tyrosine (Tyr). Others synthesized molecules used as stable organic dyes to tag non-fluorescent system. The fluorescence spectroscopy technique is widely used to determine the structure and dynamics of the lipid membrane [12, 13]. Nile red (9-diethylamino-5H-

benzo (α) phenoxazine-5-one), is one such environment sensitive probe and is widely used to monitor the membrane organization and dynamics [14]. It emits fluorescence in the presence of lipid membrane [15]. However, its fluorescence is significantly quenched in the aqueous or polar environment. Therefore, the Nile red is used on living cells as a fluorescence stain for the detection of intracellular lipid droplets if the proper spectral condition is chosen.

We have measured the steady state fluorescence emission intensity of Nile red labelled large unilamellar vesicles composed of various lipids and lipid-cholesterol mixtures. Fluorescence measurements were carried out using a PTI Quantamaster 400 spectrofluorimeter (Horiba-PTI, Canada). We have measured the absorption spectrum of Nile red and optimum excitation wavelength was found to be at 550 nm. Therefore, excitation wavelength has been kept fixed at 550 nm and emission spectra of Nile red were monitored for different lipids and at different cholesterol concentration. We have kept the emission and excitation band pass filters at 5 nm for all measurements. Spectra were also observed at different cholesterol concentration at temperatures below and above the chain melting transition for saturated lipids. The effect of temperature on the emission spectrum has also been investigated.

2.6 Isothermal titration calorimetry:

Isothermal Titration Calorimetry (ITC) is widely used to investigate the thermodynamics of binding kinetics by measuring heat of reaction between ligand and macromolecules [16]. The thermodynamic parameters such as binding constant (K), reaction stoichiometry (N), binding enthalpy (ΔH), Gibbs energy and entropy (ΔS) are quantitatively determined from the ITC and provides the mechanism of interaction between biomolecules.

ITC experiments were performed with a VP ITC unit (Microcal, Northampton, USA) at fixed temperature as per the requirement. ITC sample cell of volume 1.414 ml was filled with LUV in 1 mM HEPES buffer. 300 μ L of salt solution (300 mM) in the same HEPES buffer (pH = 7.4) was loaded in the ITC syringe. The rotating speed of syringe was maintained at 300 rpm. Reference cell was filled with buffer only. All solutions were degassed prior to filling the syringe and the ITC cell to eliminate air bubble formation under vacuum (140 mbar, 8 min) using the Microcal's thermovac unit. A series of 28 injections, each of 8 μ L, was introduced into the sample cell at 300 sec intervals. All experiments were performed at 25 °C. Each injection produces a characteristic heat signal, arising from the released or absorbed heat from the system, leading to exothermic or endothermic peaks. Heat

of dilution was measured by injecting LUV into the buffer. Net heat per injection was obtained by subtracting the heat of dilution from the actual measurement. Although the heat of dilution was found to be small as compared to the actual measurement. ITC data have been analysed without altering the lipid concentration. This would ensure that the ions interact with both monolayers of the membrane. All dilution measurements show exothermic signal. The binding constant (K) and binding enthalpy (ΔH) and Gibbs free energy ($\Delta G = -RT \ln(55.5K)$) and entropic contributions ($T\Delta S = \Delta H - \Delta G$) of the binding kinetics can be obtained from the model, as described by Domingues et al (17). Here, the concentration of water 55.5 M was used to correct the unit of K to molar fraction. The shape of the ITC isotherm is determined by the equation $c = n C_{micro} K$, where C_{micro} is the concentration of macromolecules in the sample cell (LUV in the present experiment), K is the association constant and n being the stoichiometry. For the very low value of c (< 0.1), the isotherm is almost parallel to the concentration axis. Therefore, not much information about thermodynamics of binding kinetics can be inferred. A summary of the model is described below.

2.6.1 Surface partition model:

The binding fraction x_b is defined as $x_b = \frac{C_L^b}{C_{ion}}$ (2.10)

Where C_L^b and C_{ion} are the molar concentrations of bound lipids and total ion concentration, respectively, referred to the same cell volume (V_{cell}). Now we define binding constant or partition constant K from the relation $x_b = K C_L^f$, where C_L^f is the free lipid concentration in the volume of V_{cell} . Using the conservation of mass balance equation $C_L^0 = C_L^b + C_L^f$, we have

$$C_L^b = \frac{K C_L^0 C_{ion}}{1 + K C_{ion}} \quad (2.11)$$

In the ITC experiment, we have fixed the lipid concentration in the ITC cell and increased the ion concentration in each successive injection. Taking the derivative of Eq. 2.38, with respect to ion concentration, we obtain

$$\delta C_L^b = \frac{K C_L^0 \delta C_{ion}}{(1 + K C_{ion})^2} \quad (2.12)$$

Heat of reaction in i th injection is given by $\delta h_i = \delta C_L^b V_{cell} \Delta H$. Each injection produces a heat of,

$$\delta h_i = \frac{K C_L^0 \delta C_{ion}}{(1+K C_{ion})^2} V_{cell} \Delta H \quad (2.13)$$

Here, the δC_{ion} , C_{ion} and current volume of V_{cell} of sample chamber are known from the experiment. Fitting the experimental data with Eq. 2.40, we can obtained apparent binding constant, K_{app} and molar enthalpy change ΔH . The dilution effect of C_L^0 and C_{ion} are included during the fit [27]. “One set of sites” model given by Microcal Origin is also widely used to obtain the binding parameters by fitting the isotherm. However, this model was not practically possible to find out the binding parameters for low binding heat of interaction.

2.7 Small Angle X-ray Scattering (SAXS)

SAXS is a powerful technique which can provide rich information about the structure of biological macromolecules in terms of their size, shape and flexibility etc. (19, 20). This technique is extremely useful to extract structural information from non-crystallographic complex samples in contrast to the X-ray crystallography technique (21, 22) that requires samples to be highly crystalline. Also, it is advantageous over NMR which is limited only to small protein molecules (22, 23). In a conventional SAXS instrument macromolecules like protein, nucleic acid or lipids are exposed in aqueous form to incident X-ray radiation and the elastically scattered intensity (I) is measured with respect to scattering angle (θ). Again, the scattering angle (θ) is related to the scattering vector (q) through the equation (22)

$$q = \frac{4\pi \sin \theta}{\lambda} \quad (2.14)$$

The scattered intensity $I(q)$ for monodisperse systems is expressed as (23)

$$I(q) = n V_p^2 (\Delta \rho)^2 P(q) S(q) \quad (2.15)$$

Where V_p is the volume of scattering molecule, n is the volume fraction, $\Delta \rho$ is the difference in scattering length density between macromolecules (lipid) and solvent (buffer), $P(q)$ and $S(q)$ are the related structure factor and form factor of protein/lipid/nucleic acids. In general structure factor $S(q)$ gives information about interaction between the molecules in solution, on the other hand form factor $P(q)$ gives idea about the morphology of molecules. When the system is diluted, we can take interactions between molecules as negligible. So, taking $S(q) = 1$, we can get the simplified expression of $I(q)$ (23)

$$I(q) = nV_p^2(\Delta\rho)^2 P(q) \quad (2.16)$$

For small angles the form factor $P(q)$ can be approximated from the Guinier equation (45) and expressed as (25)

$$P(q) \cong I(q) = I(0) \exp\left(-\frac{1}{3}q^2 R_g^2\right) \quad (2.17)$$

Where R_g is the radius of gyration of the macromolecular systems/complex under study and $I(0)$ is the zero-angle scattered intensity of the beam at $q \rightarrow 0$. This approximation is valid only for $qR_g < 1.3$, where the Guinier plot shows the linear variation of $\ln I(q)$ as a function of q^2 . We can extract information about R_g in reciprocal space and $I(0)$ from the linear regression plot. Interestingly, variation of $q^2 I(q)$ as a function of q yields the ‘Kratky’ plot that gives crucial information about the conformations of the macromolecules like lipids in general and unfolded/misfolded states of proteins in particular.

Radius of gyration R_g can be best estimated by considering the entire q range as opposed to low q values like in the Guinier approximation. R_g in real space can be obtained from the following equation: (23)

$$R_g = \frac{\int_0^{D_{max}} r^2 p(r) dr}{2 \int_0^{D_{max}} p(r) dr} \quad (2.18)$$

Here r is the interatomic distance, $p(r)$ is the pair distribution function and D_{max} corresponds to maximum particle dimension. Pair distribution function $p(r)$ can be reproduced from direct Fourier transformation of the scattered intensity $I(q)$ and is mathematically expressed as (22):

$$p(r) = \frac{r^2}{2\pi^2} \int_0^\infty q^2 I(q) \frac{\sin(qr)}{qr} dq \quad (2.19)$$

The distribution function gives information about the shape of macromolecules under study. While globular, oblate, or prolate, ellipsoidal particles show ideal bell-shaped distributions, skewed profiles and shoulders often indicate cylindrical geometries of the molecules and the presence of dimers or higher-order aggregated domains, respectively (22, 23). However, in practice, there are difficulties in enumerating $p(r)$, as data for $I(q)$ can only be collected in a limited range. Direct Fourier transforms from the limited data points may not be reliable for generating realizable distribution functions. In this regard, indirect Fourier transformation, as proposed by Glatter et al., is considered (24), where $p(r)$ is expressed as linear combination of

orthogonal functions in the interval $[0, D_{max}]$ with a defined D_{max} value. Detailed analysis has been reported elsewhere (23, 24). In fact, the evaluation of $p(r)$ helps to estimate $I(0)$ from the real space data and is mathematically linked through the following equation (21)

$$I(0) = 4\pi \int_0^{D_{max}} p(r) dr \quad (2.20)$$

The value of $I(0)$, as obtained either from the pair distribution function in real space or from the Guinier plot in reciprocal space, can be utilized to obtain the particle volume (V_p), and hence the molecular weight of the molecules under study. As proposed by Porod (28) V_p of the particle, Porod volume, can be estimated from the following equation (23):

$$V_p = \frac{2\pi^2 I(0)}{Q} \quad (2.21)$$

Where Q is the Porod invariant obeying the following equation

$$Q \equiv \int_0^\infty (I(q) - k) q^2 dq \quad (2.22)$$

Where k is a constant that is being subtracted to assure the asymptotic intensity decay to follow the power law that scales with q^{-4} . In fact, the Porod volume can be further utilized to estimate the molecular weight (MW) of molecules using the following relation: (24)

$$MW = \frac{V_p}{1.66} \quad (2.23)$$

In our work, SAXS studies have been explored from X-ray scattering system, D8 Bruker advance, Germany. The obtained SAXS data were fitted using an Ab initio structure modelling as executed in the DAMMIF modelling tool of ATSAS 2.7.1 software suite (26). The fitted DATA were further analysed by estimating parameters like shape, radius of gyration (R_g), volume (V_p) and molecular weight (MW) of the lipid sample. The pair distribution function $p(r)$ was estimated applying the inverse Fourier transform (IFT) method using the GNOM tool (27) of ATSAS 2.7.1 software package.

2.8 Preparation of giant unilamellar vesicle (GUV):

Giant unilamellar vesicles (GUV) are prepared using well known the electroformation method, first described by Angelova et al [4, 5, 6]. This method is a popular and widely used to prepare GUV. Electroformation of vesicles produces mainly unilamellar vesicles of 10-

100 μm diameter. The unilamellar vesicles is also very high (95%) as compared to other method discussed in the literature [7]. Owing to their large size these vesicles can be observed under phase contrast or fluorescence microscopy. Therefore, any morphological change of GUV can directly be envisaged using optical microscopy as shown in fig. 2.8,

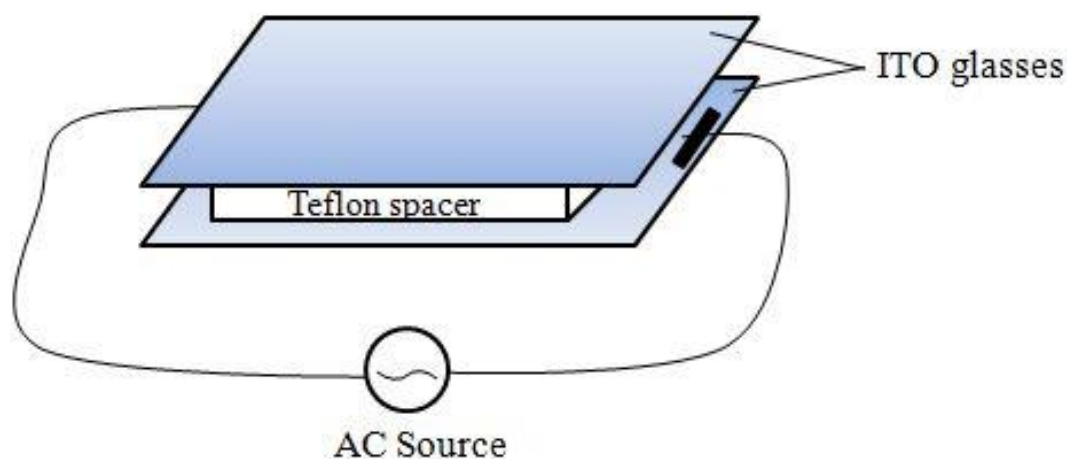


Fig. 2.8 Schematic diagram of electroformation chamber.

sample cell for electroformation consists of two one sided ITO coated glass plates separated by a very thin teflon spacer (1 mm thick). ITO coated side is kept face to face to form electrode. Electric connections for the application of voltage are made from either conducting tape or silver paste. Stock solution of the lipid or lipid mixtures (~ 0.5 mg/ml) has been prepared in chloroform. $\sim 2\text{--}3$ μl from the stock solution was taken out using Hamilton syringe and coated onto both ITO coated side of the electrode. Solvent was then allowed to evaporate which results the formation of a thin lipid film. For this technique to work the lipid film should not be too thick. The optimum thickness is in the range 10-100 bilayers. Both the ITO glass was kept overnight in vacuum desiccator to remove the traces of the solvent. Electroformation chamber was then made using teflon spacer and the chamber was filled with millipore water or buffer with fixed pH. 1-3 volts 10-15 Hz peak to peak frequency alternating voltage was applied across the ITO electrodes for a couple of hour. AC field was slowly switched off so that GUV can detach from the surface. This entire procedure results the formation of GUV of size ranging from 10-100 μm . Aqueous solution of GUV was collected and stored in 5 ml glass bottle for further experiments.

2.9 Phase contrast optical microscopy

A large number of living biological specimens are virtually transparent when observed in the optical microscope under bright field illumination. Earlier these biological structures were made visible by staining. Most of stains or staining procedures will kill the cell. But Phase contrast microscopy technique provides an excellent method of improving contrast in unstained biological specimens without significant loss in resolution. This technique is widely utilized to examine dynamic events in living cells, microorganisms, thin tissue slices, lithographic patterns and sub-cellular particles such as nuclei and other organelles. Phase contrast microscopy invented in 1934 by Dutch physicist Frits Zernike [18]. The phase contrast microscopy is based on the principle that small phase changes in the light rays, induced by differences in the thickness and refractive index of the different parts of an object, can be transformed into differences in brightness or light intensity. Human eyes are not sensitive to detect the phase change in the sample whereas brightness or light intensity can be easily detected by human eyes. Phase contrast microscopy converts invisible phase shift into visible differences of intensities. Unstained living cells absorb practically no light. Poor light absorption results in extremely small differences in the intensity distribution in the image. This makes the cells barely, or not at all, visible in a bright field microscope. When light passes through cells, small phase shifts occur, which are invisible to the human eye. In a phase contrast microscope, these phase shifts are converted into changes in amplitude, which can be observed as differences in image contrast. However, this label-free technique is strongly dependent on the correct alignment of components in the optical pathway. This alignment can be disturbed by the naturally occurring meniscus effect, causing weak phase contrast.

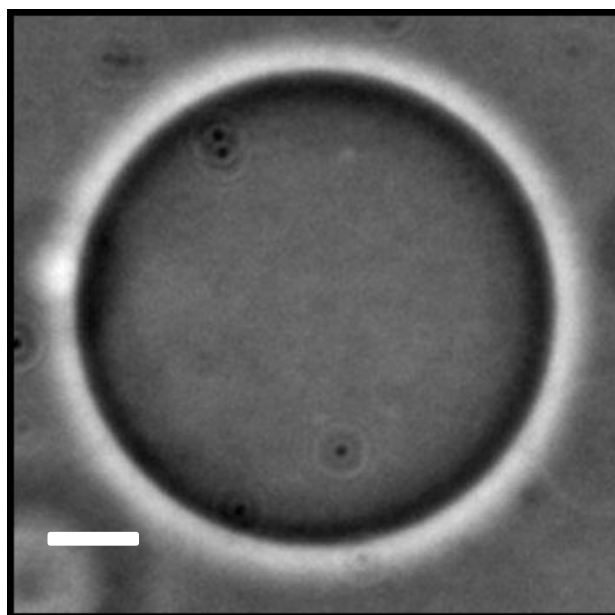


Fig. 2.9 Image of giant unilamellar vesicles obtained from Phase contrast microscopy

Phase contrast microscopy was performed with a DMi8 inverted microscope from Leica (Wetzlar, Germany). Observation chamber consists of a glass slide with rubber spacers. Appropriate amount of salt solution from the 50 μM stock solution in HEPES buffer was added to 200 μl of glucose and uniformly mixed. 10-20 μl of GUV suspension was added to the chamber. The chamber was then closed immediately for observation under phase contrast microscope. Response of individual GUV when exposed to the salt solution was continuously recorded with time using a CCD camera. Images were analysed using image analysis software, ImageJ. A straight line was drawn across the GUV to obtain an intensity profile. Peak to peak intensity (I_{ptp}) across the halo region is calculated. Average (I_{ptp}) is obtained from the several line profiles across the GUV. The time in second versus (I_{ptp}) was plotted in order to observe any significant change in the intensity profile of the GUV.

References:

1. H. H. Hub, U. Zimmermann, H. Ringsdorf, *Febs Letters*, **140**, 254-256 (1982)
2. M. J. Hope, M. B. Bally, G. Webb and P.R. Cullis, *Biochimica et Biophysica Acta*, **812**, 55-65 (1985)
3. N. J. Cho, L. Y. Hwang, J. J. R. Solandt, C. W. Frank, *Materials*, **6**, 3294-3308 (2013).
4. M. I. Angelova, S. Soleau, Ph. Meleard, J. E. Faucon and P. Bothorel, *Progr. Colloid. Polym. Sci.*, **89**, 127 (1992)

5. D. S. Dimitrov, M. I. Angelova, *Mol. Cryst. Liq. Cryst*, **89**, 152 (1987)
6. D. S. Dimitrov, M. I. Angelova, *Faraday Discuss. Chem. Soc*, **81**, 303 (1986)
7. L. A. Bagatolli, T. Parasassi and E. Gratton., *Chem. Phys. Lipids*, **105**, 135 (2000)
8. V. Patravale, P. Dandekar, R. Jain, Nanoparticulate drug delivery: perspectives on the transition from laboratory to market, (*nanoparticle drug delivery*, 87–121, (2012).
9. E. Lau, size and shape fluctuations of Large Unilamellar Vesicles as investigated using light scattering. (1992).
10. R. J. Hunter, *Zeta potential in colloid science principles and applications*, (Academic Press, 1988)
11. A. K. Patri, J. D. Clogston, *Zeta Potential Measurement, Characterization of Nanoparticles Intended for Drug Delivery*, **697**, 63-70, (2010)
12. J Andrä, M Leippe. Candidacidal activity of shortened synthetic analogs of amoebapores and NK-lysin. *Med. Microbiol.Immunol*, 188, 117–124 (1999).
13. J Andrä, M J H Koch, R Bartels, K Brandenburg. Biophysical characterization of Endotoxin inactivation of NK-2, an antimicrobial peptide derived from mammalian NK-Lysin. *Antimicrob. Agents Chemother*, 48, 1593–1599 (2004).
14. M Zhang, M F Li., L Sun. NKLP27: A Teleost NK-Lysin Peptide that Modulates Immune Response, Induces Degradation of Bacterial DNA, and Inhibits Bacterial and Viral Infection. *PLoS One* 2014, 9, No. e106543.
15. M T Lee, W C Hung, F Y Chen, H W Huang. Mechanism and kinetics of pore formation in membranes by watersoluble amphipathic peptides. *Proc. Natl. Acad. Sci. U.S.A.*, 105, 5087–5092 (2008).
16. M. R. Duff, J. Grubbs, E. E. Howell, *Journal of Visualized Experiments*, **55**, 1- 4 (2011).
17. T.M Domingues, B Mattei, J Seelig, K.R Perez, A Miranda, K.A Riske, *Langmuir*, 29, 8609–8618 (2013).
18. A Sannigrahi, P. Maity, S Karmakar, K Chattopadhyay. *J. Phys. Chem. B*, 121, 1824–1834 (2017).
19. T. D. Grant, J. R. Luft, J. R. Wolfley, H. Tsuruta, A. Martel, G. T. Montelione and E. H. Snell, *Biopolymers*, 95, 517–530 (2011).

20. D. K. Wilkins, S. B. Grimshaw, V. Receveur, C. M. Dobson, J. A. Jones and L. J. Smith, *Biochemistry*, 38, 16424–16431 (1999).
21. M. C. Stumpe and H. Grubmuller, *J. Am. Chem. Soc.*, 129, 16126–16131 (2007).
22. L. R. S. Barbosa, F. Spinozzi, P. Mariani and R. Itri, Wiley, ch. 3, 49–72 (2013).
23. T. D. Grant, J. R. Luft, L. G. Carter, T. Matsui, T. M. Weiss, A. Martel and E. H. Snell, *Acta Crystallogr.*, 71(1), 45–56 (2015).
24. A. Guinier and G. Fournet, *Small-Angle Scattering of X-Rays*, Wiley & Sons, New York, (1955).
25. A. Bergmann, G. Fritz and O. Glatter, *J. Appl. Crystallogr.*, 33, 1212–1216 (2000).
26. M. V. Petoukhov, D. Franke, A. V. Shkumatov, G. Tria, A. G. Kikhney, M. Gajda, C. Gorba, H. D. T. Mertens, P. V. Konarev and D. I. Svergun, *J. Appl. Crystallogr.*, 45, 342–350 (2012).
27. D. I. Svergun, *J. Appl. Crystallogr.*, 25, 495–503 (1992).
28. S. Saha and J. Chowdhury, *J. Photochem. Photobiol.*, B, 193, 89–99 (2019).

Chapter 3

Effect of cholesterol on the interaction of ion with unsaturated phospholipid membranes

3.1 Introduction

As discussed in chapter 1, alkali metal ions play an important role in structure and function of cellular membrane [1]. Also, cholesterol in a bio-membrane plays significant role in many cellular events and is known to regulate the functional activity of protein and ion channel. The major component of phospholipids in cell membrane is phosphatidylcholine (PC). Negatively charged phospholipid (DOPG) is mostly found in all bacterial membrane, plants and mammals. Therefore, saturated phospholipids DOPC/DOPG can be used as good model membrane to study the effect of cholesterol on the interaction of ion with lipid membranes.

In this chapter we have discussed, binding of monovalent salt NaCl with unsaturated phospholipid membrane in presence of different cholesterol concentration. The binding constants obtained from zeta potential and dynamic light scattering experiments are compared with that obtained from the fit using hill equation for with and without cholesterol. We have discussed some interesting results related to effect of cholesterol on ion binding to the phospholipid membrane. Related earlier studies are summarized in section 3.2. Detailed experimental results have been discussed in section 3.3. We conclude this chapter in section 3.4.

3.2 Earlier Studies

Cholesterol is a ubiquitous component of all animal cell membranes. It plays a vital role in maintaining structure and regulating functions and properties of membranes (1). Inhomogeneous distribution of cholesterol, so called rafts, has led to large number of studies on lipid-cholesterol membranes (2; 3; 4; 5). Membrane cholesterol and partitioning of cholesterol into the membrane domains are also known to regulate ion channel (6). Activity of the ion channel is highly influenced by the level of membrane cholesterol. For example, increase in the cholesterol level leads to suppression of ion-channel activity (7). Besides ion

transport, ions in the membrane regulate the surface charge which affects liposome stability and interaction with immune cells, ultimately influencing drug delivery efficiency (8; 9). Ions also alters the interaction of peripheral membrane protein (10). Studies on the effect of various ions, especially alkali metal ions on the phospholipid membranes have received a significant attention in view of understanding ion transports and other biological functions (11; 12; 13). Recently we have explored effect of alkali metal ions on the electrostatic and thermodynamic properties of the membranes (14; 15). As cholesterol regulates the ion transports across the membranes, we intend to investigate the effect of cholesterol on the ion-membrane interaction.

A variety of experimental techniques along with computer simulation has been employed in order to gain insights into the ion-membrane interaction (16; 17; 18). Ion-membrane interaction has an important role in restructuring of macromolecules, such as proteins, peptides, etc. at the membrane-solvent interface and in modulating the membrane properties (16; 19). For example, asymmetric binding of Na^+ and Cl^- showed significant influence on the ion transport across the bilayer (20). Among all different monovalent ions, present in the intra-cellular and extra cellular fluid, Na^+ , K^+ are most abundant cations. Recently binding of these cations with different lipids have been studied in details (17). Na^+ has higher binding affinity than among all other alkali metal ions except Li^+ (21). However, the measurement of binding affinity for different ions to the phospholipid membranes is incredibly complex, and there is considerable variation of binding affinities even for a particular ion to a specific lipid bilayer (12). Anions such as Cl^- also plays a significant role in maintaining hydration and balancing cations in the extracellular fluid for maintaining electrical neutrality in the fluid. Effect of counter anions on the Na^+ binding revealed that the presence of Cl^- does not influence significantly compared to others ions, such as I^- and Br^- (15).

Cholesterol in the membrane is known to alter significantly the elastic properties and permeability of the membrane (1; 3; 22). Therefore, cholesterol is expected to change the surface charge and hence the electrostatic behaviour of the membrane. Recent computer simulation study revealed that cholesterol affects the surface charge of the membrane in the presence of ions (23). In particular, the cholesterol in the membrane containing Na^+ ions replaces ions from the membrane-water interface and hence decreases Na^+ ion binding with the lipid head group (24). As a consequence, zeta potential is also found to decrease in

accordance with the decrease in surface charge of neutral phospholipids, such as POPC and DSPC. Doktorova et al have found that cholesterol actually promotes the protein binding by altering the electrostatic and solvation properties of the membrane (25). Earlier simulation and zeta potential measurements have been performed mostly in neutral phospholipids. However, zeta potential measurement is most appropriate for charged membranes. Therefore, it is naïve to compare simulation results of ion-membrane interaction in the presence of cholesterol with zeta potential.

In this chapter, we have studied effect of ions on the phospholipid membranes containing cholesterol, in order to gain insights into the role of cholesterol on the ion-membrane interaction. We have used mixture of negatively charged lipids DOPG and zwitterionic lipid DOPC to prepare large unilamellar vesicles. We have explored Gouy Chapman theory to estimate binding constants and surface charge of the membranes containing ions as well as cholesterol. A dramatic change in the zeta potential of negatively charged membrane in the presence of small amount of cholesterol has been observed. Present study would be useful in understanding many biophysical processes, including the liposomal drug delivery.

3.3 Experimental results and discussion

3.3.1 Size distribution of vesicles containing cholesterol: Effect of NaCl

DLS was performed to determine the size distribution of DOPC-DOPG LUV for different mol% of cholesterol concentration (X_c) ranging from 5 to 20 mol%. Results on DOPC-DOPG LUV without cholesterol have already been discussed in our earlier study (14). For a particular X_c , we have observed decrease in the average size of LUV with increasing NaCl concentration (fig. 1). It is evident from Fig. 1 that for higher cholesterol concentrations typically 15 and 20 mol%, average size eventually saturates to a lower value of vesicle diameter ~ 110 nm for salt concentrations beyond 40 mM. However, for 5 and 10 mol% of X_c , average size continues to decrease till 100 mM concentration of salt (Fig. 1). Interestingly, concentration dependence size reduction is represented using decay constant obtained from single exponential decay curve is also shown in the figure legend of Fig.1. For example, decrease in average size of LUV is faster at higher X_c ($\gtrsim 15$ mol%) than that of lower X_c ($\lesssim 10$ mol%). It is important to mention that the average diameter of the vesicle tends to decrease with increasing cholesterol concentration even in the absence of salt. For

better clarity, we have presented the result in Fig 2 in view of understanding effect of cholesterol for a given salt concentration. As discussed before, average size decreases significantly with X_c at a given salt concentration. Cholesterol seems to have no effect or very little effect on the size distribution for salt concentration above ~ 40 mM. Besides average size, polydispersity is one of the important factors to consider while illustrating the effect of cholesterol on the size distribution. Polydispersity index (PDI) of all measurements, which is an indicative of dispersion of size distributions, was found to be less than 0.1 and does not alter PDI values significantly with NaCl concentration as well as cholesterol concentration (See table 1a). As we use the same buffer for vesicles preparation as well as preparation of salt solution, there will be no net osmotic stress upon addition of salt. Therefore, observed reduction of size is not due to osmotic stress.

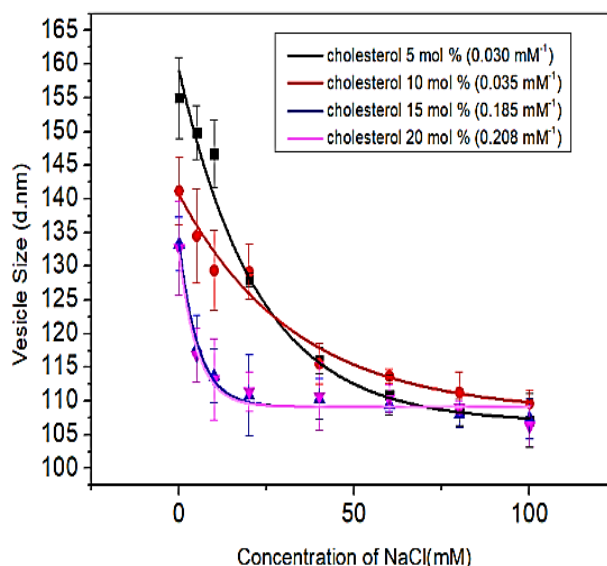


Fig.1 Average size of vesicles prepared from DOPC, DOPG (4:1) and different cholesterol concentrations (indicated in the figure legend) for different salt concentration. Data were obtained from by taking average over three consecutive measurements. Error is determined from the average value of three independent measurements. The number within the bracket in the figure legend is the representative number indicating how vesicle size decreases with increasing salt concentration. This was obtained from the fit using single exponential decay function. This is for comparison on size reduction among different cholesterol concentration.

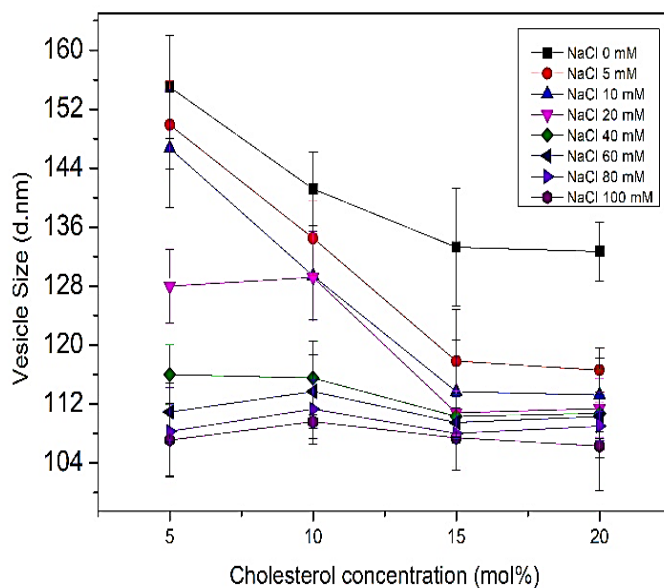


Fig. 2 Variation of average size of the vesicles prepared from DOPC, DOPG (4:1) with cholesterol concentrations for different salt concentration (indicated in the figure legend). This figure is drawn from the result presented in Fig1 for better clarity.

3.3.2 Effect of cholesterol on the ion-membrane interaction: Zeta potential

Zeta potential (ζ) was measured in LUV composed of mixture of DOPC and DOPG (4:1) containing cholesterol. It is clearly evident from fig. 3 that, zeta potential shows high negative value (-60 mV) in the absence of NaCl for all X_c . However, zeta potential becomes less negative on increasing X_c . The zeta potential gradually increases (becomes less and less negative) with increasing salt concentration (Fig. 3). Interestingly, the ζ value saturates close to zero, but never exceeds to zero. The underlying cause of partial charge compensation will be illustrated in the discussion section. The variation of ζ with increasing salt concentration for different cholesterol concentration are very similar. However, we could unambiguously distinguish different curves, corresponding to different cholesterol concentration. For NaCl concentration ~ 100 mM, zeta potential meet at value ~ -2 to -5 mV for all X_c . We have not shown the value of zeta potential at salt concentration > 100 mM. From earlier study on similar system, we found that higher concentration of salt, typically > 100 mM, vesicle solution after zeta potential measurement shows colour change which we interpreted as electrolysis leading to the damage of the electrode of the zeta cuvette (14). The binding curve represented change in zeta potential is very well fitted with the standard Hill equation which was originally designed for binding of ligand with macromolecules, such as proteins. Here, the change in zeta potential can be consequence of binding of Na^+ with the membrane. It is important to mention that counter-anions, Cl^- in the present case, show significant effect on

the Na⁺ binding, as reported in earlier study (15). Interestingly Cl⁻ has similar binding propensity as revealed from the earlier molecular dynamic simulation on POPC bilayers (30). However, controversy on the similar affinity of both anions and cations remains in the literature, as simulation study are constrained by the choice of force field, type of lipids and system size as well (31). We have obtained the association or binding constant from the fit to the Hill equation, as shown in the inset of fig. 3. These values of binding constants underpin the estimated binding constant from electrostatic double layer theory. We have now analysed the data in order to gain insights into the electrostatics of the membranes.

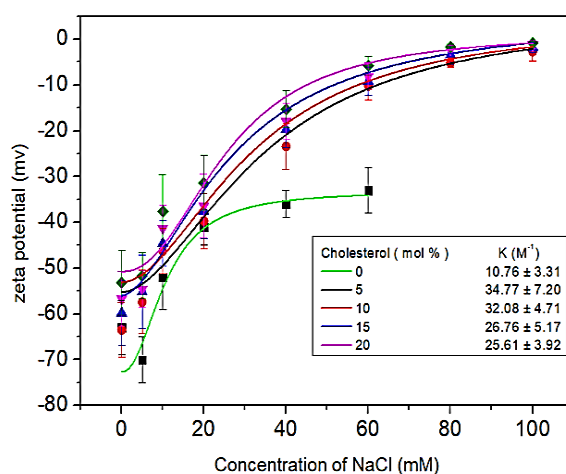


Fig:3 Variation of zeta potential with different NaCl concentration for different cholesterol concentration as indicated in the figure legend. Solid line is obtained from the fit using hill equation. Binding constant (K) obtained from the fit is also shown in figure legend. Zeta potential without cholesterol is taken from the ref. (14) for comparison. Error bar is estimated from three consecutive measurements.

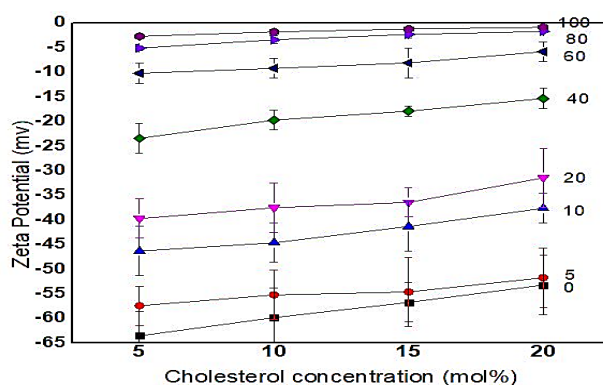


Fig. 4 Zeta potential as a function of different cholesterol concentrations plotted for various salt concentration (mM) indicated by number in the figure. Error bar is obtained from three successive measurement of zeta potential.

3.3.3 Electrostatics of the membrane: Gouy Chapman model

Gouy Chapman model is based on electrostatic double layer theory and is widely used to describe the electrostatic behaviour of charge surface in the presence of ions at moderate electrolyte concentration (32). In the present study, this model is employed to describe the distribution of ions at the vicinity of LUV in the form of electrostatic double layer followed by diffused layers which decays to a distance known as screening length. It is assumed that for anionic membranes, i.e, LUV embedded in an electrolyte solution, form electrostatic diffuse double layer of cations. Electrolyte solution is treated as continuous dielectric medium. Further, ions are located on the surface of the membranes and are smeared uniformly over the entire surface. Detailed procedure to estimate the electrostatic parameters, in case of 1:1 electrolytes, are described in our previous papers (14; 15). Table 1 summarises the results obtained from Gouy Chapman model at NaCl concentration 5 mM. Surface potential (ψ_0) of the membrane in the absence of cholesterol is found to be -77 mV at 5 mM NaCl. The absolute value of ψ_0 decreases gradually with increasing X_c . As a consequence, surface charge density σ of LUV in the absence of cholesterol decreases to a value from -0.025 C/m² to -0.01 C/m² when cholesterol is added. At a particular salt concentration, σ does not change significantly with increasing X_c . However, the absolute value of σ decreases significantly with increasing salt concentration (Table 2). The numbers within the bracket indicate values of electrostatic parameters obtained from the DOPC-DOPG (4:1) membrane without cholesterol. This is to compare results without cholesterol and to understand the effect of cholesterol on the ion-membrane interaction. At a particular salt concentration, intrinsic concentration which is the concentration of ions at the vicinity of the membrane decreases slightly as cholesterol concentration is increased from 0 to 20 mol%. However, increasing salt concentration, intrinsic concentrations decrease one order of magnitude compared to that of without salt. Estimated binding constant K does not change significantly with X_c for NaCl concentration < 40 mM and beyond 40 mM, K increases significantly with X_c (Fig. 5).

Table 1: Electrostatic parameters obtained from the Gouy Chapman theory from the measured zeta potential of LUV for different cholesterol concentration at 5 mM of NaCl concentration. LUVs are prepared from mixture of DOPC and DOPG at 4:1 ratio and cholesterol.

Chol (mol%)	Surface potential (ψ_0) (mV)	Surface Charge (σ) (C/m^2)	Intrinsic concentration (M)	Binding constant (K) (M^{-1})
0	-77 ± 4	-0.025 ± 0.003	0.050 ± 0.03	4 ± 3
5	-60 ± 2	-0.012 ± 0.003	0.053 ± 0.02	50 ± 8
10	-58 ± 3	-0.011 ± 0.004	0.048 ± 0.04	59 ± 7
15	-57 ± 4	-0.011 ± 0.003	0.047 ± 0.03	62 ± 9
20	-54 ± 4	-0.010 ± 0.002	0.042 ± 0.01	78 ± 9

Table1a: Polydispersity index of vesicle solution as measured from DLS. Small value of PDI (<0.1) indicates that vesicles are highly monodisperse. This is to show that vesicles remain monodispersed with increasing NaCl concentration. This result is for 10 mol% of cholesterol concentration.

NaCl	0	1	2	5	7	10	20	40	60	80	100	150
PDI	0.06	0.07	0.09	0.09	0.08	0.12	0.08	0.06	0.07	0.08	0.06	0.06

Table 2: Electrostatic parameters obtained at 10 mol% of cholesterol for different salt concentration. Numbers in the bracket indicate the corresponding values without cholesterol. The number presented within bracket are taken from ref (14) for comparison.

NaCl (mM)	Surface potential (mV)	Surface charge C/m^2	Intrinsic concentration (M)	Binding constant (M^{-1})
10 (10)	-48 (-77)	-0.0126 (-0.025)	0.065 (0.20)	39.5 (4)
20 (30)	-41 (-60)	-0.015 (-0.029)	0.100 (0.30)	20.0 (1.8)
40 (50)	-23 (-48)	-0.010 (-0.029)	0.096 (0.30)	33.7 (1.7)
60 (70)	-10 (-44)	-0.0061 (-0.030)	0.091 (0.39)	70 (1.3)
80 (90)	-4 (-41)	-0.0026 (-0.300)	0.094 (0.44)	171 (1)

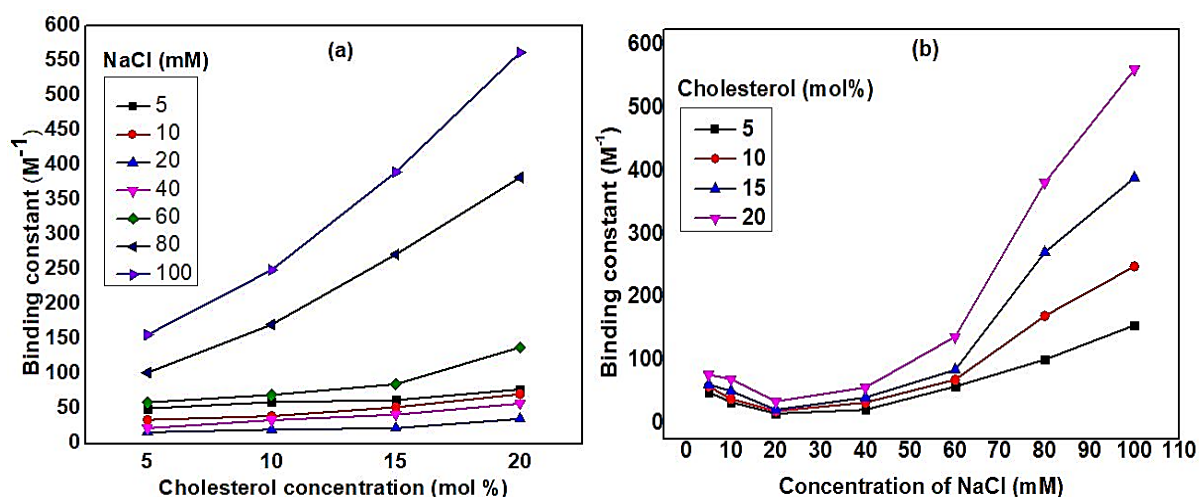


Fig. 5: (a) Intrinsic binding constant as a function of cholesterol concentration for different NaCl concentrations indicated in the figure legend. (b) Binding constant was plotted with NaCl concentration for different cholesterol concentration.

3.3.4 Binding of ions as evidenced from fluorescence spectroscopy

Fluorescence spectra of lyophilic dye Nile red in the presence of anionic LUV containing cholesterol dispersed in NaI salt are shown in Fig. 6. Among all halide ions, I^- is known to act as quencher (33). Therefore, binding of Na^+ can be best envisaged by NaI using fluorescence technique, as already implemented in our previous study on cationic vesicles (34). As shown in Fig. 6, it is clearly evident that intensity of Nile red spectrum gradually decreases with increasing NaI concentration. This indicates the quenching of Nile red suggesting the penetration of I^- into the core of the membrane and binding of Na^+ ion to the membrane surface. This is supported by the fact that both cations and anions have similar affinity towards the membranes, as reported by Klasczyk et al. (21). Plot of relative intensity ($\frac{I_0}{I}$) vs concentration of salt shows nonlinear nature of quenching. This curve was best fitted with modified Stern Volmer equation, originally derived for purely collisional (Dynamic) quenching. The quenching of fluorescence intensity in the presence of 15 mol% cholesterol is insignificant compared to one with very low (~ 1 mol%) X_c . This result reveals that cholesterol prevents from penetration of I^- leading to the reduction of accessible part of the fluorophore.

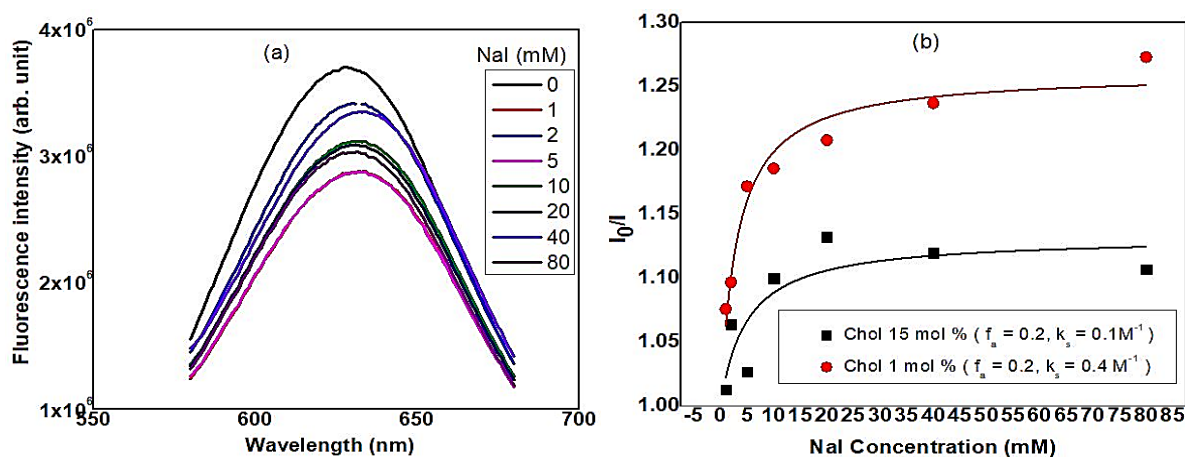


Fig. 6 (a) Fluorescence spectra of LUV containing 1 mol% of cholesterol and Nile red in the presence of NaI. The resultant spectra were obtained after subtracting the dilution (Nile red in buffer). (b) Relative intensity of Nile red in the presence of different NaI concentration. Solid line is obtained from the fit using modified Stern Volmer equation. LUV composition: DOPC–DOPG (4:1). Quenching constant and fraction of accessible fluorophore are indicated in the figure.

3.3.5 Discussion

Results on the size distribution of LUV using DLS clearly shows significant and rapid decrease in average size of the LUV containing cholesterol with increasing salt concentration. It is known from our previous study that adsorption of ions leads to compression of electrostatic double layer, resulting in a decrease in the hydrodynamic radius of the vesicle (15). Average size of the LUV decreases even in the absence of ions (Fig. 2). This could be due to distribution of water molecules resulting in a decrease of dipole relaxation of the lipid interphase leading to reduction of water molecule i.e., the hydration layer as found in recent molecular dynamic simulation (35). Interestingly, in the presence of cholesterol, the decrease in average vesicle size occurs very fast at low concentration of NaCl. Such decrease is not very significant at higher X_c . Recent study on the size distribution of GUV containing cholesterol have shown increase in the average size due to increase in the bending modulus (36). Further, increase in size of sonicated small vesicles was described in terms of increase in area per molecule and decrease in thickness (37). The decrease in average size with increasing cholesterol concentration (fig. 1 and 2) is thus intriguing. Although, many earlier literatures did not report any significant increase in bending rigidity (38; 39) of membrane made from unsaturated lipids, recent combining techniques like neutron spin-echo spectroscopy, solid-state deuterium NMR spectroscopy, and molecular dynamics simulations showed locally increase bending rigidity of unsaturated lipids (40). The increase in the

membrane rigidity and decrease in the permeability in the presence of cholesterol reduces hydration layer at the vicinity of the membrane (35). Further addition of NaCl tends to decrease the bending modulus very rapidly, leading to large Brownian fluctuations (39). This will decrease the effective size of the vesicles, as measured from DLS. Therefore, rigid and impermeable membrane along with significant reduction of Brownian fluctuations (41) might lead to significant decrease in the average hydrodynamic radius of the vesicles. However, actual size of the vesicles may increase. It is important to mention that unlike miscibility of the phase diagram seen in the ternary phospholipid mixtures consisting of one saturated lipid, we have only single fluid phase. Further, the presence of salt has a minimal effect in the phase behaviour of the ternary mixture (42). Therefore, issue of miscibility of the ternary system studied here is irrelevant.

We have explored systematically the effect of cholesterol on the electrostatic behaviour of ion-membrane interaction. The decrease in zeta potential from its negative value without the presence of alkali metal ions is attributed to the fact that cholesterol increases surface charge density of the membrane. Cholesterol is intercalated between the phospholipids leading to increase in surface charge density. We have indeed obtained the decrease in surface charge density with increasing cholesterol content (Table 1). As expected, at a particular cholesterol concentration zeta increases significantly with increasing salt ion concentration (Fig. 3 and 4). For example, LUV without cholesterol exposed to 50 mM NaCl concentration exhibit zeta potential value -41 mV (14). Interestingly, LUV containing 5 to 20 mol% cholesterol shows much lower zeta potential (~ -5 mV) at similar salt concentration. This difference in zeta potential is due to modification of surface charge of the membranes due to cholesterol. Increasing surface charge density is also consistent with the fact that cholesterol increases the bending rigidity (39). Magarkar et al. has reported similar work in which the cholesterol level affects surface charge of lipid membrane in saline water (24). However, they have used zwitterionic saturated phospholipids DSPC and unsaturated phospholipid POPC. Although Na^+ ions bind to neutral phospholipids (21; 43), it is unlikely that zeta potential show positive value at low cholesterol concentration and decreases to negative value at higher cholesterol concentration. Our repeated and systematic study reveals completely opposite trend for anionic vesicles. Binding of ions onto the membrane strongly depends on type of head groups of phospholipids as well as the structure and dynamic at the bilayer-water interface (44). For example, Na^+ binds to PC carbonyl oxygen as also with phosphate oxygen group (45), whereas, PG binds Na^+ primarily through ester carbonyl and

glycerol groups (46). As cholesterol resides next to phospholipid head group and tend to alter the structure of hydrogen bonding network at the interface, it is expected to change the surface property of the membrane (47; 48). Therefore, reduction in negative zeta potential even in the absence of salt (fig. 4) is not surprising.

It is important to note that zeta potential can be realised only for charged surface. The charge screening effect prevents cations for further adsorption to the membranes. Here electrostatic double layer repulsion dominates over van der Waal attraction and hence charge neutralisation as well as overcharge compensation is not possible in this system (14). Knetch et al also found ion adsorption to the membrane, but no charge neutralization (21). Therefore, complete charge compensation reported by Magarkar et al. is indeed controversial. It has been reported that cholesterol does not affect the transient adsorption of Na⁺. However, binding of cations depends on the PC head group (49). Significant effect of cholesterol obtained in the present study is due to anionic head group of the membrane. Kucerka et al. have shown that cholesterol in polyunsaturated fatty acid (PUFA) membrane exhibits different orientation and location in different membranes composition (50). Such orientation or location might also alter the interface and hence it affects ion adsorption. However, to validate this hypothesis detailed structural study of the ternary system are necessary to accomplish.

The effect of cholesterol on the binding thermodynamics of ion-membrane binding has been systematically explored using electrostatic double layer theory. In the absence of cholesterol, surface charge density (σ) and intrinsic binding constant (K) do not seem to alter significantly with increasing ion concentration (34). However, in case of anionic vesicles containing cholesterol, both σ and K increase significantly with increasing cholesterol concentration. Magarkar et al. reported that mass density of Na⁺ ions seem to decrease with cholesterol concentration which was interpreted as decrease in Na⁺ binding to the membrane (24). Interestingly, we have found higher binding affinity of Na⁺ with increasing cholesterol concentration (Table 1) as estimated from the electrostatic double layer theory. This result also substantiates from the decrease in the negative value of surface charge density. This underpins the fact that cholesterol tend to increase the Na⁺ binding to the membrane and hence the binding constant. Binding constant estimated from the electrostatic double layer theory is in agreement with the value obtained from Hill equation (Fig. 3). This value of binding constant is higher than that of without cholesterol (14). Interesting the binding constant initially decreases till 50 mM ion concentration and thereafter it increases 50 mM for

all X_c . Such a concentration dependence binding constant is very much intriguing. However, we believe that binding of ions is not purely electrostatic. There is an entropic contribution due to release of water molecules in the hydration layer of the membrane upon adsorption of ions. Here we have estimated intrinsic binding constant and not the apparent binding constant which may not alter significantly with concentration. Intrinsic binding occurs as result of competition between screening effect and binding phenomenon. Therefore, at higher concentration of salts it is expected to dominant screening effect over binding. Further, the cholesterol in the membrane also alters the intrinsic concentration and hence we observe the concentration dependence binding constant. As the negative surface charge decreases with cholesterol, it is expected that charge screening would be much faster than that of without cholesterol. We do find that much lower zeta potential (- 4 mV) for 80 mM salt concentration and at $X_c = 10$, whereas zeta potential of LUV without cholesterol becomes -41 mV at similar salt concentration (Table 1). It has been reported in earlier monolayer study on the interaction of cholesterol on NaCl that Na^+ ions interacts with the -OH group of the cholesterol located at the interface (51). Further Na^+ cations has the strongest affinity with cholesterol as found from radial distribution function obtained from the molecular dynamics (51). This might be the reason for increasing binding constant for higher salt concentration. It is important to mention that, in spite of assuming uniform charge distribution over the membrane, the Gouy Chapman theory captures many features of binding phenomenon. However, in a realistic situation discreteness of surface charge density may be required in order to get more insights into the ion-membrane interaction.

It is important to note that intrinsic concentration of ions found in LUV containing cholesterol is almost one order of magnitude less than that of without cholesterol (see table 2 for comparison). Cholesterol has higher affinity to be associated with PC group in the membrane (52). This might decrease the binding site for cations. Apparently, this would lead the decrease in the binding constant. However, the fact that surface charge density of vesicle containing cholesterol is less negative (-0.01C/m^2) than that of without cholesterol (-0.025C/m^2). Therefore, cholesterol reduces charge density which is consistent with the results obtained by Magarkar et al. Earlier simulation studies on the interaction of NaCl with phospholipid membranes have reported the evidence of weaker binding of Cl^- compared to Na^+ binding and Cl^- ions mostly stay in water phase (53; 54; 55). However, earlier simulation study by Benjamin et al. suggested that both Na^+ and Cl^- have similar affinity to the membrane (30). Recent experimental study along with computer simulation showed that

the distribution of the Cl^- over the membrane surface is the effect of cation binding to the membrane and not due to direct interaction with the choline groups (56). In order to validate this hypothesis, we have performed fluorescence spectroscopy of LUV containing cholesterol and found that anions are indeed present in the membrane. This was done from the Nile red emission spectra, at a given excitation, as emission of Nile red is extremely sensitive to the environment. The discrepancies of ion binding obtained in the previous study might arise from the use of different force field in the simulation.

Fluorescence spectroscopy study was employed in order to obtain complementary information about effect of cholesterol on the ion-membrane interaction. Nile red, used for fluorescence study, is known to reside within the core of the hydrocarbon chain for its efficient emission (57). Therefore, cholesterol which increases the rigidity of the hydrocarbon part in the fluid phase, is expected to show quenching behaviour if Γ is accessible to the Nile red. The non-linear Stern Volmer fit to the quenching curve shown in fig. 6 essentially suggest that a fraction of Nile red is accessible to the quencher. In the presence of cholesterol, quenching is much less significant, indicating that cholesterol prevents Γ ions to penetrate into the core of the membrane. This is expected as cholesterol is known to decrease the permeability of the membrane (1). However, this does not rule out the possibilities that Na^+ binding is also less efficient. This is supported by the fact that both cations and anions have similar affinity towards the membrane (30). As the quenching based on the Γ accessibility of Nile red, the very low emission intensity in the presence of cholesterol can be analysed as binding assay. However, fluorescence study provides an insight into the effect of cholesterol on ion-membrane interaction.

3.4 Conclusion

This study has shown that cholesterol significantly affects the charge state and hence binding affinity of the membrane. Negative zeta potential and hence surface potential of the membrane containing cholesterol decreases significantly and becomes close to zero for higher salt concentration compared to that without cholesterol. Although intrinsic concentration of the ions which is the concentration at the vicinity of the membrane-water interface increases significantly with cholesterol content, it is one of magnitude less than that of without cholesterol. This is due to stronger affinity of the phosphate group with the cholesterol. Electrostatic double layer theory was employed in order to estimate binding parameters of the ion-membrane interaction in the presence of cholesterol. Our results will

have great implications in the context of ion-channel activity and protein-membrane interaction and other biophysical process where cholesterol and ions are involved.

References

1. Finegold, L. Cholesterol in Membrane Models, edited by L. Finegold. s.l. : CRC Press, Boca Raton, FL (1993).
2. Witold K. Subczynski, 1 Marta Pasenkiewicz-Gierula, Justyna Widomska, Laxman Mainali, and Marija Raguz, *Cell Biochem. Biophys*, 75(3-4), 369–385 (2017).
3. Smit, Frédérick de Meyer and Berend, *Proc. Natl. Acad. Sc, USA*, 106 (10) ,3654-3658 (2009).
4. Timothée Rivel, Christophe Ramseyer Semen Yesylevskyy, *Scientific Report*, 9, 5627 (2019).
5. K Simons, E Ikonen, Functional rafts in cell membranes, *Nature*, 387(6633), 569-72 (1997).
6. Irena Levitan, Dev K. Singh and Avia Rosenhouse-Dantsker, *Front. Physiol*, 5, 1-14(2014).
7. Irena Levitan, Yun Fang, Avia Rosenhouse-Dantsker, Victor Romanenko. Cholesterol and Ion ChannelsIn: Harris J. (eds), 51, 509-549 (2010).
8. Lasse Hyldgaard Klausen, Thomas Fuhs, Mingdong Dong, *Nat. Commun*, 7, 12447 (2016).
9. Adéla Melcrová, Sarka Pokorna, Saranya Pullanchery, Miriam Kohagen, Piotr Jurkiewicz, Martin Hof, Pavel Jungwirth, Paul S. Cremer & Lukasz Cwiklik, *Sci Rep* , 6, 38035(2016).
10. Deborah M. Boes, Albert Godoy-Hernandez, Duncan G. G. McMillan., *Membranes*,11, 346 (2021).
11. Role of Ion–Phospholipid Interactions in Zwitterionic Phospholipid Bilayer Ion Permeation, *J. Phys. Chem. Lett*, 15, 6353–6358 (2020).

12. Andrea Catte, Mykhailo Grych, Matti Javanainen, Claire Loison, Josef Melcr, Markus S Miettinen, Luca Monticelli, Jukka Määttä, Vasily S Oganessian, O H Samuli Ollila, Joonas Tynkkynen, Sergey Vilov, *Phys Chem Chem Phys*, 18(47), 32560-32569 (2016).
13. Zschörnig, Hans Binder and Olaf., *Chem. Phys. Lipids*, 115, 39-61 (2002).
14. Pabitra Maity, Baishakhi Saha , Gopinatha Suresh Kumar, Sanat Karmakar, *Biochim. Biophys. Acta*, 1858 , 706–714 (2016).
15. Pabitra Maity, Baishakhi Saha, Gopinatha Suresh Kumar and Sanat Karmakar, 6, 83916. (2016).
16. Membrane-ion interactions. Friedman, Ran., *J Membr Biol.* , 251(3) ,453–460 (2018).
17. Josef Melcr, Hector Martinez-Seara, Ricky Nencini, Jiří Kolafa, Pavel Jungwirth, and O. H. Samuli Ollila, *J. Phys. Chem. B* , 122,4546–4557 (2018).
18. Evelyne Deplazes, Jacqueline White, Christopher Murphy, Charles G Cranfield & Alvaro Garcia., *Biophys. Rev.*, 11, 483-490 (2019).
19. Zur Lehre von der Wirkung der Salze (About the (About the Science of the effect of salts): Franz Hofmeister's historical papers. Kunz, W., Henle, J. and Ninham, B. W. *Curr. Opin. Colloid. Interface Sci*, 9,19–37 (2014).
20. S---J. Lee, Y. Song, N.A. Baker., *Biophys. J.* 94, 3565–3576 (2008).
21. B. Klasczyk, B. V. Knecht, R. Lipowsky and R. Dimova., *Langmuir*, 26, 18951–18958 (2010).
22. Fathima T. Doole, Teshani Kumarage, Rana Ashkar & Michael F. Brown. 255, 385–405(2022).
23. Lingxue Mao, Linlin Yang, Qiansen Zhang, Hualiang Jianga, Huaiyu Yang. 2015, *Biochim. Biophys. Res. Comm*, 468,125-129 (2015).
24. Aniket Magarkar, Vivek Dhawan, Paraskevi Kallinteri, Tapani Viitala, Mohammed Elmowafy., *Scientific reports*, 4, 5005 (2014).
25. Milka Doktorova, 1 Frederick A. Heberle, Richard L. Kingston, George Khelashvili, Michel A. Cuendet, Yi Wen,7 John Katsaras, Gerald W. Feigenson, Volker M. Vogt, and Robert A. Dick. 2017, *Biophys. J*, 113, 2004–2015 (2017).
26. Klasczyk, VolkerKnecht and Benjamin. , *Biophys. J*, 104, 818-824 (2013).

27. Woolf, Thomas B. , Biophys. J, Vol. 104, 746-747 (2013).
28. Israelachvili, J N. Intermolecular and surface forces. [ed.] 3rd Ed. s.l. : Academic press, 2011.
29. Carrigan, S., et al., et al., J. Photochem. Photobiol, 99, 29-35(1996).
30. Pabitra Maity, Baishakhi Saha, Gopinatha Suresh Kumar and Sanat Karmakar., Langmuir, Vol. 34, 9810–9817(2018).
31. Lyubartsev, Inna Ermilova and Alexander P. , Soft Matter, 15, 78(2019).
32. Animesh Halder, Baishakhi Saha, Pabitra Maity, G. Suresh Kumar, Dipak K Sinha and S. Karmakar., Spectrochimica Acta Part A: Molecular and Biomolecular Spectroscopy, 191, 104-110 (2018).
33. P. Maity, B. Saha, G. Suresh Kumar S. Karmakar. 2016, Biophys. Biochim. Acta, 1858, 607-617(2016).
34. Membrane-Ion interactions. Friedman, Ran., 251, 453-460 (2018).
35. Igor Vorobyov ¶, Timothy E. Olson Jung H. Kim , Roger E. Koeppe, Olaf S. Andersen, Toby W. Allen., Biophys. J, 106, 586-597(2014).
36. Benjamin Klasczyk, Volker Knecht, Reinhard Lipowsky, and Rumiana Dimova. 2010, Langmuir, Vol. 26, pp. 18951–18958.
37. Ronald J. Clarke, Christian Lüpfer. , Biophys. J, 76, 2614-2624(1999).
38. Lorena Redondo-Morata, Marina I. Giannotti, Fausto Sanz.Mol. Membr. Biol, Vol. 31,17-28 (2014).
39. Jonathan N. Sachs, Hirsh Nanda, Horia I. Petrache, Thomas B. Woolf., Biophys. J, 86, 3772-3782 (2004).
40. Dynamics of Water Interacting with Interfaces, Molecules, and Ions,. Fayer, M. D., Acc. Chem. Res., 45, 3-14 (2011).
41. Erdinc Sezgin, Ilya Levental, Satyajit Mayor & Christian Eggeling., Nat Rev Mol Cell Biol , 18, 361–374 (2017).
42. SIMONS, DANIEL LINGWOOD AND KAI., Science, Vol. 327, 46-50(2010).
43. Oskar Engberg, Victor Hautala, Tomokazu Yasuda, Henrike Dehio, Michio Murata, J. Peter Slotte, and Thomas K. M. Nyholm., Biophys. J, 111,546–556(2016).

44. Singer SJ, Nicolson GL., *Science*, 175, 720-731(1972).
45. Matti Javanainen, Ade'la Melcrova, Aniket Magarkar, de Piotr Jurkiewicz, Martin Hof, Pavel Jungwirth and Hector Martinez-Seara., *Chem. Commun.* ,53, 5380(2017).
46. Aniket Magarkar, Vivek Dhawan, Paraskevi Kallinteri, Tapani Viitala, Mohammed Elmowafy, Tomasz RoTomasz Rog, Alex Bunker., *Scientific Report*, 5005, 1-4(2014).
47. Kalyan Kumar Banerjee, Pabitra Maity, Surajit Das and Sanat Karmakar., *Chem. Phys. Lipids*, 254, 105307(2023).
48. Pabitra Maity, Baishakhi Saha, Gopinatha Suresh Kumar and Sanat Karmakar. 2018, *Langmuir*, 34,9810–9817(2018).
49. Fre'de'rick de Meyera, b and Berend Smit. ,106, 3654-3658 (2009).
50. Sezgin, E., Levental, I., Mayor, S. Christian Eggeling., *Nat Rev Mol Cell Biol*, 18, 361–374 (2017).
51. Kai Simons, Winchil L.C. Vaz., *Annu. Rev. Biophys. Biomol. Struct.*, 33, 269–95(2004).
52. Keller, Sarah L. Veatch and Sarah L., *Phys. Rev. Lett.*, 89, 268101(2002).
53. Tobias Baumgart, Samuel T. Hess & Watt W. Webb., *Nature*, 425, 821–824 (2003).
54. An Ghysels, Andreas Krämer, Richard M. Venable, Walter E. Teague Jr, Edward Lyman, Klaus Gawrisch & Richard W. Pastor., *Nat. Comm.* , 10, 5616(2019).
55. Effects of the Lipid Bilayer Phase State on the Water Membrane Interface. 2010, *J. Phys. Chem B*, Vol. 114, pp. 11784–11792.
56. Bidisha Das, Sumangal Roychowdhury, Priyesh Mohanty, Azamat Rizuanoy, Joy Chakraborty, Jeetain Mittal, K. Chattopadhyay. , *EMBO J*, 42, 11185(2022)
57. P. Maity, B. Saha, G.S Kumar, S. Karmakar., *RSC Adv.*, Vol. 6, 83916 (2016).
58. M. M. AE. Claessens, B. F. van Oort, F. A. M. Leermakers, F. A. Hoekstra, M. A. C. Stuart., *Biophys. J*, 87, 3882-3893(2004).
59. M. Doktorova, F. A. Heberle, R. L. Kingston, G. Khelashvili, M. A. Cuendet, Y. Wen, J. Katsaras, G. W. Feigenson, V. M. Vogt, R. A. Dick., *Biophys. J*, 113, 2004-2015(2017).

Chapter 4

Interaction of sodium salt with DMPC/DMPG membrane: Effect of cholesterol

4.1 Introduction

In the previous chapter, we have discussed how cholesterol affects the interaction of alkali metal salt NaCl with unsaturated phospholipid membrane DOPC: DOPG. We observed that cholesterol strongly affects the binding of ion into the bio-membrane. It would be interesting to see, how chain saturation affects ion-membrane interaction in the presence of cholesterol. Therefore, we have used two saturated phospholipid DMPC and DMPG at 4:1 ratio and investigated the interaction of ion with membrane.

In this chapter, we present a systematic study on how alkali metal salts, like NaCl and NaI, affect anionic vesicles made from saturated phospholipids. An isothermal titration calorimetry study on large unilamellar vesicles made from dimyristoyl phosphatidylcholine (DMPC) revealed that Na^+ shows higher binding affinity to the DMPC membrane phase at 15 °C compared to the fluid phase at 30 °C. Further, cations also show stronger affinity to the membrane in the fluid composed of saturated lipids than that of unsaturated lipids. The binding affinity of Na^+ with anionic vesicles prepared from a mixture of DMPC and DMPG was found to decrease significantly with increasing cholesterol as well as salt concentrations, as revealed by the zeta potential study. Besides the binding constant, the Gouy-Chapman theory based on the electrostatic double layer shows that cholesterol reduces the surface charge density without altering the significant area per molecule. Further, the effect of counter-ions was investigated using fluorescence spectroscopy of an environment-sensitive lipophilic dye, Nile red. Although cholesterol alters the emission properties of Nile red significantly, there is no significant change in the presence of ions. This result suggests that anions do not bind significantly to anionic vesicles. The main striking feature of the ion-membrane interaction in the presence of cholesterol is that membranes with saturated lipids exhibit a completely opposite trend from membranes with unsaturated lipids. Earlier studies related to work has discussed in section 4.2. Detailed experimental results are discussed in section 4.3. We have concluded the chapter in section 4.4.

4.2 Earlier studies

Lipids are fatty acid and their derivatives are component of all biological membrane. It also acts as energy storage molecule in both animal and plants. In saturated lipid, the fatty acid chains have all single bonds between the carbon atoms. Along the chain, some carbon atoms are linked by single bonds and others are linked by double bonds. A double bond along the carbon chain can react with a pair of hydrogen atoms to change into a single bond, where each hydrogen atom is bonded to one of the two C atoms. Unilamellar vesicles, which are single bilayer shell, serve as an excellent model system to study the structure and function of biological membranes. Studies on ion-membrane interaction, for example, yield significant insights into the effect of ions on the membrane's transport properties. The presence of ions, especially alkali metal ions, leads to a significant alteration of the electrostatic properties of the membrane (31; 32). For example, the rate of lipid flip-flop dynamics is greatly influenced by ions in the membranes. The asymmetric binding of Na^+ and K^+ causes the transmembrane potential. Ion-induced defects are known to regulate permeation processes, diffusion mechanisms, and the free energy barrier (3; 4). Anions and cations in the membranes are capable of modifying the membrane surface potential (5) and dipole potential (6). The distribution of ions at the membrane-water interface plays an important role in substantially modifying the structure and dynamics of the membranes (7). For instance, head group conformational fluctuations, such as changes in tilt angle, are a determining factor in structural rearrangements upon adsorption of ions onto the membrane (8).

It has been shown that the water layer, i.e., the hydration layer, plays an important role in the ion-membrane interaction. Therefore, low hydration or partial hydration in the gel phase prevents ion penetration into the core of the bilayer as compared with the bilayer in the liquid-crystalline phase. Weak binding of Na^+ ions in the gel phase was explained by low hydration and less penetration or exchange of ions due to the more compact structure of the bilayers in this phase. Besides the anionic membrane, neutral vesicles made from phosphatidylcholine (PC) can also interact significantly (5). Entropic contribution and water dynamics at the membrane interface may play an important role in determining the interaction of ions with the zwitterionic membrane (9). However, the question remains: does chain saturation play any role in the ion-binding process? There are many earlier reports that showed the binding affinity of Na^+ ions with DOPC and DOPG membranes. It was generally overlooked to study saturated lipids due to their higher chain melting transition. In this study,

we have investigated the effect of chain saturation and compared it with that of unsaturated lipids.

Cholesterol is an essential and ubiquitous component of all plasma membranes (10). It is believed that the surface of the membrane is heterogeneous in nature, and non-uniform cholesterol distribution leads to the proposition of the raft hypothesis (11; 12). Engberg et al. have shown the relative affinity of cholesterol in saturated and unsaturated phospholipid bilayers and determined the degree to which cholesterol facilitates lateral segregation (13). Cholesterol also maintains membrane fluidity and provides rigidity and integrity to the plasma membrane (14). As ions modulate the bilayer properties, it would be interesting to investigate how cholesterol modifies the ion-membrane interaction. Javanainen et al. have employed fluorescence techniques and computer simulations to determine the effect of cholesterol on the adsorption of sodium and calcium ions onto zwitterionic phosphatidylcholine POPC (15). They have shown that the binding of monovalent Na^+ ions and divalent Ca^{+2} ions with zwitterionic phospholipid is greatly influenced by cholesterol. It has been suggested from their study that transient adsorption of Na^+ depends on the number of head groups present in the membrane and does not alter significantly in the presence of cholesterol.

Recent simulations as well as experimental studies have shown that Na^+ binding decreases with increasing cholesterol concentrations in the phospholipid membranes (44). This result was supported by the fact that zeta potential decreases with increasing cholesterol content, indicating reduced surface charge and hence less Na^+ binding. It has been shown that Na^+ ions preferentially bind to the phosphate oxygen of the phospholipids and weakly bind to cholesterol oxygen. Therefore, such favoured binding of Na^+ with the phosphate group of lipids is the cause of decreasing Na^+ binding with increasing cholesterol content. Recently, we have explored the effect of cholesterol on the DOPC-DOPG membrane (17). It has been found that cholesterol increases the binding affinity of Na^+ ions in negatively charged membranes. Since binding affinity and other electrostatic parameters were determined from the zeta potential of the anionic membrane, it is not useful to compare this simulation study with the zwitterionic membrane. Further, in accordance with the raft hypothesis, the cholesterol affinity of saturated lipids is higher than that of unsaturated lipids. Therefore, in the present study, we have systematically investigated the effect of Na^+ ions on the anionic saturated membrane composed of DMPC and DMPG. We also compared the results of the

present work with previously reported systems consisting of unsaturated membranes (DOPC/DOPG).

4.3 Results

4.3.1 Interaction of NaCl with membranes composed of saturated lipids DMPC: ITC study

We have used saturated phospholipid DMPC in order to gain insights into the ion-membrane interaction at two different temperatures (15 °C and 30 °C). DMPC vesicles exhibit fluid (L_α) phase above 23 °C (T_m). At 15 °C, DMPC membrane may not transform to the gel phase, rather it is the onset of ripple (P_β') to gel (L'_β) phase transition. We performed ITC to estimate the binding constant and other thermodynamic parameters of the binding kinetics of NaCl with DMPC vesicles at two different temperatures (15 °C and 30 °C). Fig.1 shows the binding isotherm at two different temperatures. The binding constant obtained from the fit using the partition model is found to be much higher at 15 °C which than in the fluid phase of DMPC vesicles. The binding constant, entropy, and enthalpy change obtained from the partition model are summarised in table 1.

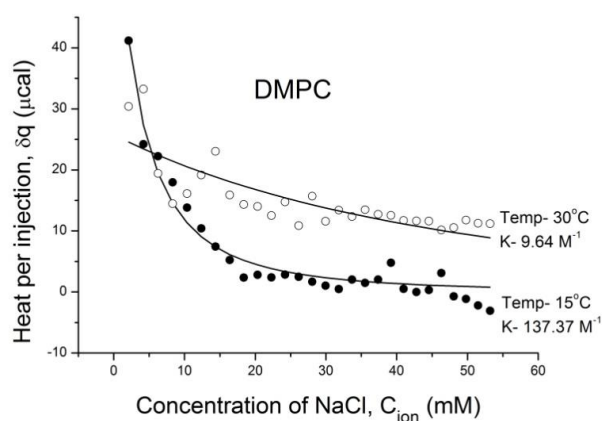


Fig.1. ITC isotherms were obtained for DMPC vesicles at two different temperatures. Partition model was used to fit these isotherms from which we have obtained binding constant and other thermodynamic parameters. (See table 1).

Table 1 Binding constant (K) and molar enthalpy (ΔH), Gibbs free energy (ΔG) and entropic contribution ($T\Delta S$), were obtained from the fit using partition model for two different temperatures.

Temperature ($^{\circ}\text{C}$)	Binding constant (k) (M^{-1})	Enthalpy (ΔH) (kcal / mol)	Gibbs free energy (ΔG) (kcal/mole)	Entropic contribution ($T\Delta S$) (kcal/mole)
15	137.4	0.14	-5.27	5.41
30	9.60	0.74	-3.70	4.44

4.3.2 Effect of cholesterol on the ion-membrane interaction

4.3.2.1 Interaction of NaCl with binary mixture of DMPC and cholesterol

We have already discussed the influence of ions on the phase state of DMPC membranes. As cholesterol modulates the bilayer elastic properties as well as the permeability of the membrane, it would be interesting to investigate how cholesterol alters the thermodynamics of the cationic adsorption (Na^+ binding) onto the DMPC membrane. An ITC experiment has been performed to determine the interaction of NaCl with DMPC-cholesterol membranes. ITC heat flow at 15°C shows an endothermic response, whereas, the heat flow at 30°C exhibits an exothermic response. The heat of dilution also shows a similar heat flow. Therefore, it is conceivable that both electrostatic (exothermic) and entropic contributions (endothermic) are present simultaneously, resulting in a very low net heat contribution due to ion-membrane interaction. As both heat flows are comparable, it was not possible to obtain a good fit for the isotherm or extract the binding constant and other thermodynamic parameters.

4.3.2.2 Effect of Na^+ ions on the ternary mixture of DMPC, DMPG and cholesterol:

- **Size distribution of LUV as observed from dynamic light scattering**

To understand the electrostatics of ion-membrane interaction, we have employed dynamic light scattering and zeta potential studies. As the surface charge plays an important role in determining the cationic adsorption, zeta potential would be an appropriate technique to elucidate the electrostatics of the ion-membrane interaction. It is important to mention that zeta potential can be envisaged only from charged membranes. Therefore, we have taken the mixture of DMPC and DMPG in a 4:1 ratio to prepare SUVs. In a ternary system composed of saturated phospholipids DMPC, DMPG and cholesterol, the phospholipid ratio (DMPC: DMPG = 4:1) was kept fixed, and cholesterol concentrations were varied (0, 10, 20 mol%).

So samples with varying cholesterol concentrations will not change the relative amounts of DMPC and DMPG. This will ensure a constant membrane charge, as DMPG drives the surface charge. Before measuring zeta potential, we performed a dynamic light scattering experiment to determine the size distribution of SUVs for different cholesterol concentrations.

The average size (hydrodynamic diameter) of SUVs prepared from a pure DMPC-DMPG mixture was found to be ~ 44 nm. In the absence of cholesterol, vesicle size increases from 45 nm to 134 nm with increasing NaI concentrations from 0 mM to 150 mM. A similar trend was found at 10 mol% of cholesterol. However, the behaviour of size distributions at 20 mol% of cholesterol shows the opposite trend. Although initially, average size increased to 160 nm until the NaI concentration reached 20 mM, a sudden decrease in size was observed. The decrease in the average size is not very significant above the NaI concentration of 40 mM. The increase in vesicle size is much faster at 20 mol% of cholesterol than at lower cholesterol concentrations. It is clearly evident from fig. 2 that the vesicle size increases with increasing cholesterol concentration, even in the absence of salt ions. In order to avoid any resultant osmotic stress due to the mismatch of the buffer concentration, the same buffer solution with physiological pH was used to prepare SUVs as well as salt solutions. This confirms that any change in the size distribution of SUVs is not due to osmotic stress.

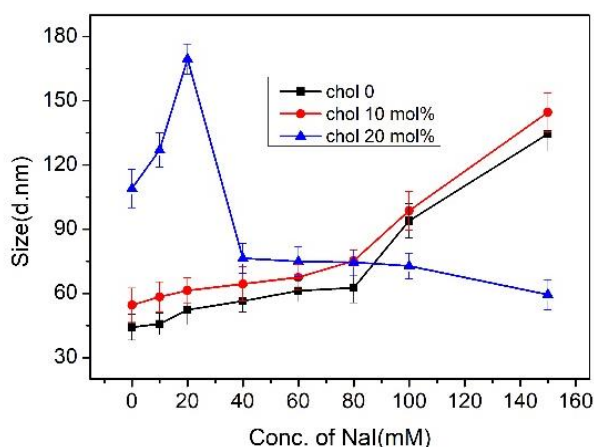


Fig. 2 Variation of average size of SUVs prepared from DMPC-DMPG (4:1) with salt concentration at two different cholesterol concentrations (10, 20 mol%) indicated in the figure legend. Error is determined from the average value of three different measurements.

- **Binding of cations with the anionic membrane containing cholesterol: Zeta potential study**

Zeta potential (ζ) was measured for small unilamellar vesicles (SUVs), composed of a mixture of saturated lipid DMPC-DMPG (4:1) and cholesterol. It is clearly evident from the results (Fig 3) that the ζ shows a high negative value (-48 mV) in the absence of NaI for all cholesterol concentrations. Further, ζ decreases slightly with increasing cholesterol concentrations for a particular ion concentration (Fig 3b). Now, if we increase the ion concentration gradually, zeta potential becomes less negative (the negative value decreases), which means zeta potential increases with the increase in ion concentration. For lower salt concentrations (< 20 mM), the increase in zeta potential is very similar for all cholesterol concentrations. However, variations in zeta potential can be distinguished at intermediate salt concentrations. For example, zeta potential at 60 mM shows a much lower value (-22 mV) for a cholesterol concentration of 20 mol% than that without cholesterol (~ -13 mV). Finally, zeta potential shows saturation at a similar zeta potential for all cholesterol concentrations. Interestingly, the zeta potential value saturates close to zero but never exceeds zero. The underlying cause of partial charge compensation will be discussed later. A quantitative description of the cation binding process was done using the Gouy Chapman theory based on the concept of the electrostatic double layer described in our previous papers (1; 17). Table 2 summarises the electrostatic parameters estimated from the Gouy Chapman theory.

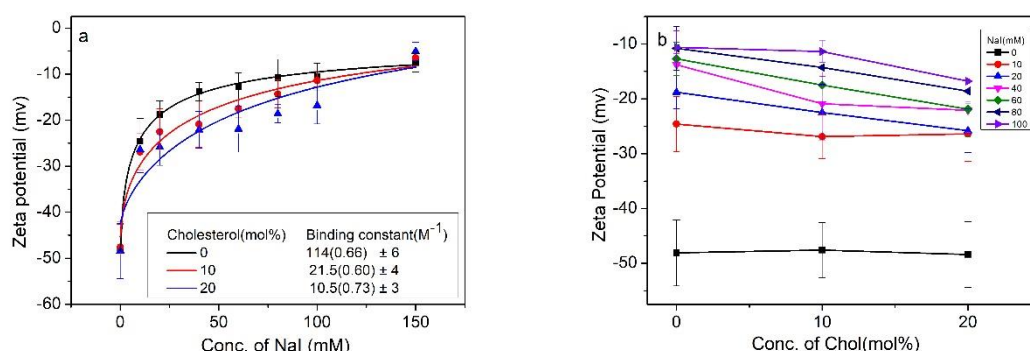


Fig.3 (a) Variation of zeta potential of DMPC-DMPG vesicles with NaI concentrations at two different cholesterol concentration. Solid lines in (a) are obtained from fit using Hill equation, describing the binding phenomenon. The binding constant obtained from the fit are presented in the inset of the fig a. The number within the bracket represent the cooperativity index. Fig. (b) is derived from the fig (a) to show the effect of cholesterol concentration at a fixed salt concentration.

Table 2: Electrostatics of the membranes obtained using the Gouy Chapman theory from the measured zeta potential of SUVs for different cholesterol concentration at 20 mM NaI concentration.

SUVs are prepared from binary mixture of saturated phospholipid DMPC-DMPG(4:1) and cholesterol (1; 17).

Chol (mol%)	Surface potential (ψ_0) (mV)	Surface Charge (σ) (C/m^2)	Intrinsic concentration C_0 (M)	Binding constant (K) (M^{-1})	ΔG (KJ/mol)
0	-21 ± 4	-0.0068 ± 0.0008	0.045 ± 0.007	124 ± 8	-22 ± 6
10	-25 ± 5	-0.0083 ± 0.0009	0.053 ± 0.008	84 ± 6	-21 ± 5
20	-26 ± 3	-0.0096 ± 0.0007	0.060 ± 0.006	60 ± 7	-20 ± 7

As shown in table 2, the surface charge density decreases with cholesterol concentration at a particular salt concentration. As a consequence, the intrinsic binding constant of cation decreases with increasing cholesterol concentrations as shown in fig. 4. This result suggests that cholesterol reduces the binding affinity of the cations. We have not measured the value of the zeta potential for salt concentrations above 150 mM. This is due to the fact that measurement of zeta potential at very high salt concentrations causes electrolysis, leading to damage to the gold electrodes in the zeta cuvette. This is evident from the colour change of the solution at concentrations of electrolytes greater than 150 mM. For comparison, zeta potential as a function of salt concentration was also fitted to a Hill equation, originally developed for the binding of ligands to macromolecules. The values of the binding constant for different cholesterol concentrations are consistent with those obtained from the Gouy Chapman theory (Fig 3a). The difference in the numerical values may be due to simplified underlying assumptions in the Gouy Chapman theory. Further zeta potential is realised only for the charged component. Therefore, the change in zeta potential is only due to the electrostatic contribution. However, the entropic contribution plays a vital role in the binding process. This could also lead to a difference in the binding constant obtained from Hill fit and Gouy Chapman theory. It is important to mention that binding parameters, such as binding constant and surface charge density obtained from DMPC/DMPG membranes containing cholesterol show an opposite trend with the previously published results on DOPC-DOPG-cholesterol membranes (fig. 4) (17). However, membranes without cholesterol exhibit similar behaviour.

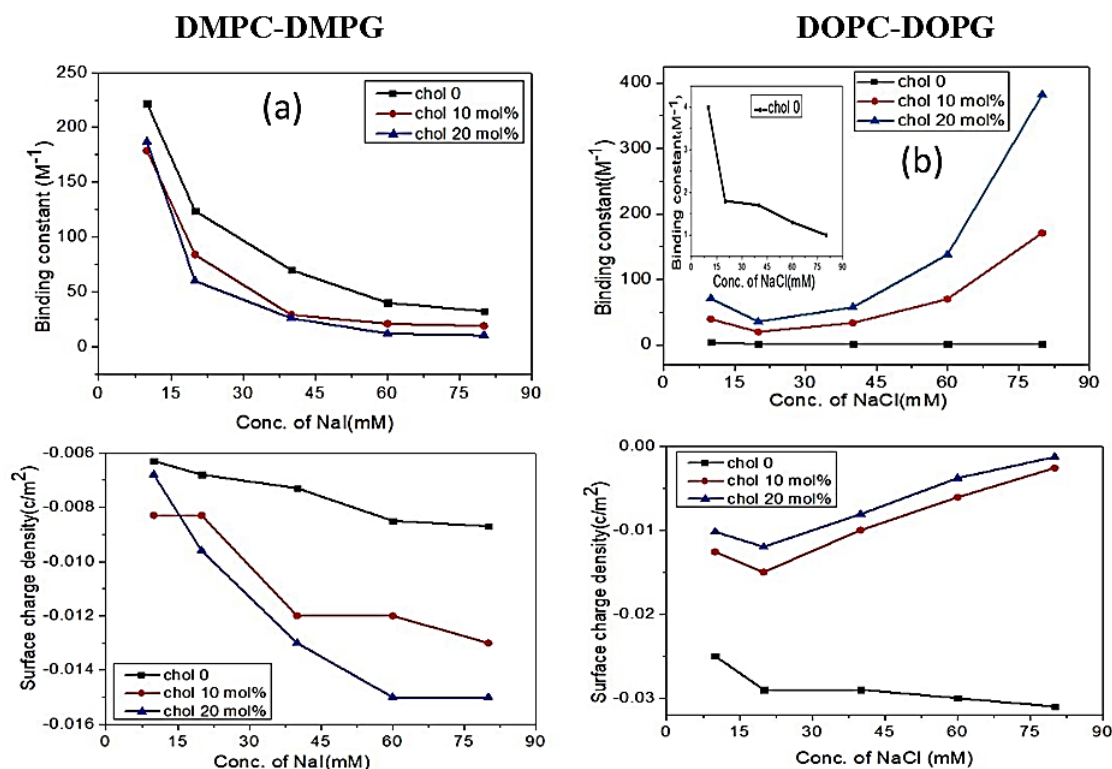


Fig.4: Comparison of the variation of the binding constant of Na^+ and the surface charge density of the membrane with the NaI concentration for two different cholesterol concentrations in DMPC/DMPG and DOPC/DOPG membranes. Data for DOPC-DOPG membrane with and without cholesterol were taken from the ref. (17) and ref. (1), respectively. In the absence of cholesterol, the variation of binding constant with NaI is shown in the inset of the fig (b) for clarity. Solid lines are guide to the points and not obtained from fit.

4.3.3 Effect of cholesterol on the ion-membrane interaction: Fluorescence spectroscopy study.

We have measured the fluorescence emission intensity of Nile red labeled SUVs in the presence of NaI solution at different concentrations ranging from 0 mM to 100 mM. Γ is known to be a good quencher (25). As other counterions, such as, Cl^- and Br^- do not seem to act as quenchers, we have used NaI only. However, this does not rule out the possibility that Cl^- and Br^- do not interact with the membrane. Nile red is an environment sensitive probe, and when in contact with membranes, it is capable of fluorescence emission. In particular, Nile red emits fluorescence when it penetrates into the membrane core and resides in the hydrocarbon core of the bilayer. It has been known that the fluorescence properties of Nile red

are known to alter due to a change in the polarity of its immediate environment as a result of a large change in dipole moment upon excitation (26). Further, Nile red emission also affects the hydration at the interface of the membrane. Therefore, it would be an appropriate probe to look at how ions in the membrane alter the membrane properties. As, the fluorescence emission of Nile red quenches in the presence of I^- , the effect of anions can also be studied. We have studied the fluorescence emission of Nile red labeled vesicles made from DMPC, DOPC and a mixture of DMPC-DMPG with cholesterol (fig 5) for NaI concentration ranging from 0 to 100 mM (comparison has been done at a certain concentration 20 mM as done in previous DLS results). However, in the case of DMPC, a significant shift in the emission maximum (λ_{max}) was observed with cholesterol concentration when the membrane was at 15 °C (Fig 5a). No significant shift was seen for DMPC at 30 °C (Fig. 5b) and DOPC vesicles (fig 5c). The shift in λ_{max} was also obtained for vesicles made from DMPC-DMPG mixtures with varying cholesterol concentrations (fig. 5 d). The emission spectra of different lipids without ion is given in fig. 6. As Nile red is known to show REES, we have fixed the excitation wavelength to monitor the emission. Therefore, any shift in λ_{max} is due to the presence of cholesterol only. The variation of λ_{max} with cholesterol concentration for different compositions is shown in Fig 7. It is clearly evident from these results that NaI has no significant effect on the Nile red emission spectra. Halder et al. have studied how the emission properties of Nile red alter with composition as well as the phase state of the membrane (26). Our results are in agreement with those of earlier results without the presence of ions. The fluorescence intensity of Nile red decreases with increasing NaI concentration due to the presence of I^- as a quencher. It is clearly evident from Fig. 8 that fluorescence quenching decreases with increasing cholesterol concentrations. The quenching curve, as shown in Fig. 8, shows non-linear behaviour, indicating dynamic quenching. However, we could not rule out the contributions to static quenching in the quenching process. In order to check vesicle diffusion labeled with Nile red, we have performed preliminary fluorescence correlation spectroscopy (FCS) of SUVs made from DMPC-DMPG. FCS shows a decrease in the diffusion constant with increasing cholesterol content. Therefore, the complex formation of Nile red with the quencher is less probable. The quenching curves were fitted to a non-linear Stern Volmer equation to estimate the quenching constant (K_s) and fraction of initial fluorescence accessible to the quencher (f_a). The K_s and f_a obtained with cholesterol concentration are low, indicating the restriction of I^- to penetrate into the membrane core. This result does not conclusively rule out the possibility of

Na^+ absorption onto the membrane. It is rather supporting evidence that, due to the presence of Na^+ , membrane is still negatively charged and hence I^- is prevented from entering the membrane core due to electrostatic repulsion.

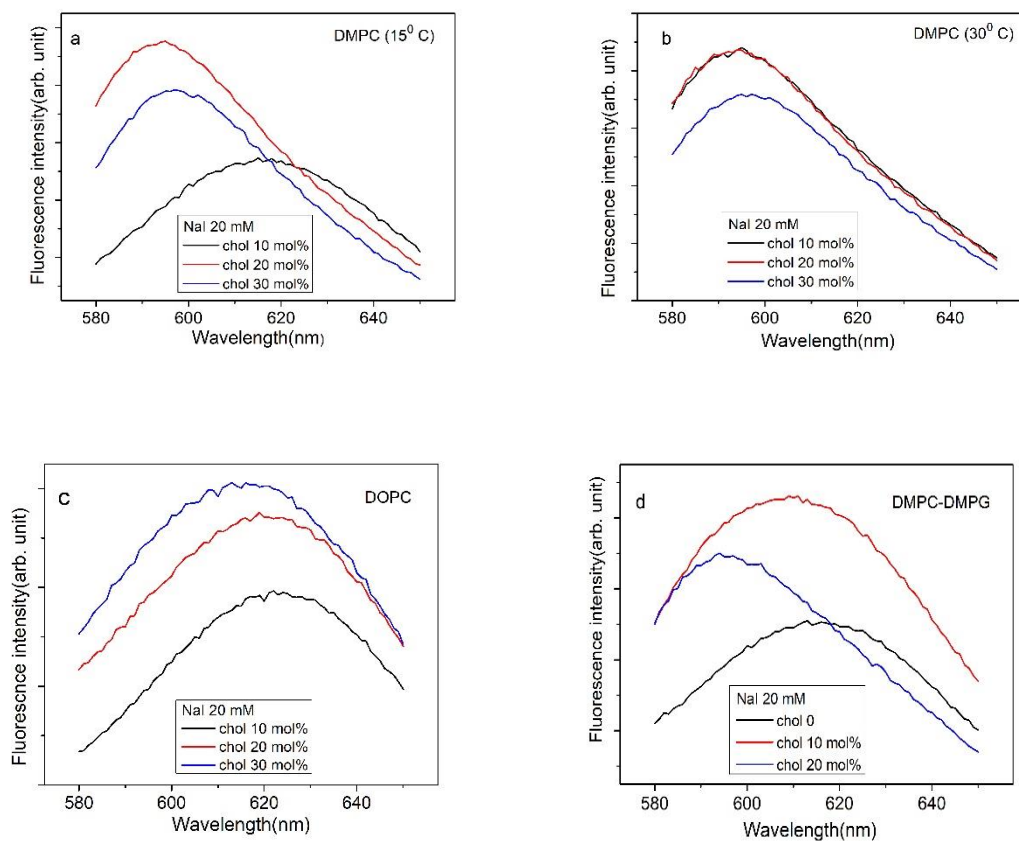
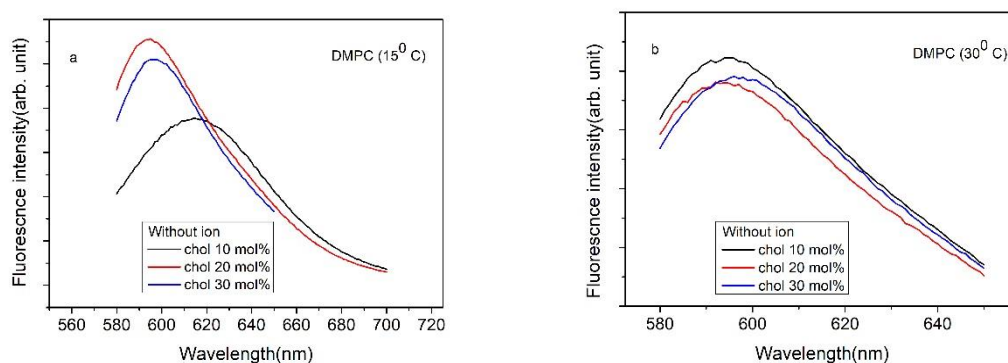


Fig. 5. The emission spectra of Nile red labeled SUVs containing cholesterol for various lipid compositions indicated in the figure legend. (a) DMPC at 15 °C (b) DMPC 30 °C (c) DOPC at 25 °C (d) DMPC-DMPG (4:1) at 25 °C.



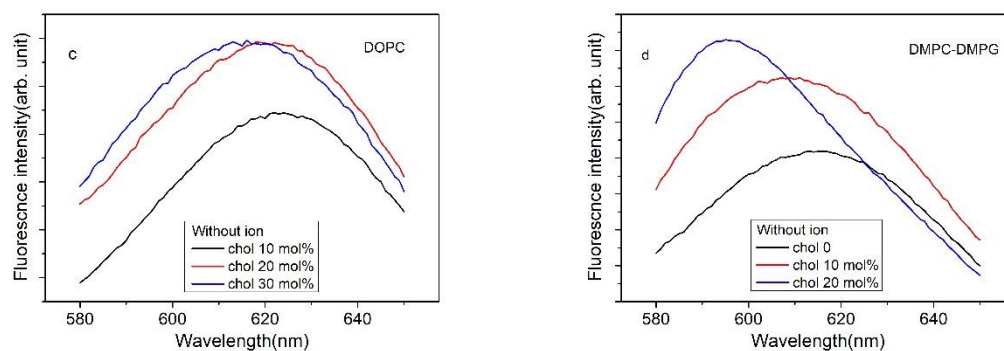


Fig. 6. The emission spectra of Nile red labeled SUVs containing cholesterol for various lipid compositions indicated in the figure legend. (a) DMPC at 15 °C (b) DMPC 30 °C (c) DOPC at 25 °C (d) DMPC-DMPG(4:1) at 25 °C. Spectra were taken in the absence of ions.

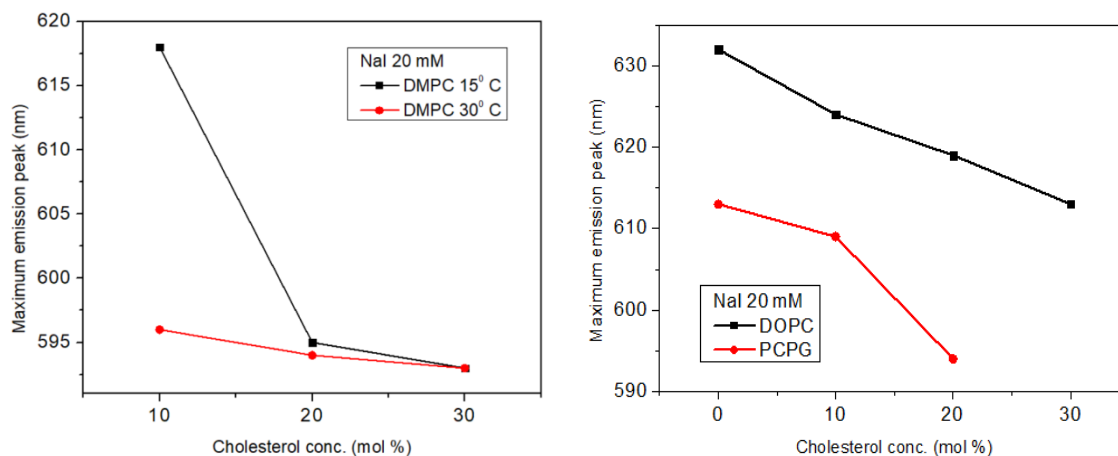


Fig7: Variation of maximum emission peak of Nile red with cholesterol concentration for various lipid compositions indicated in figure legend.

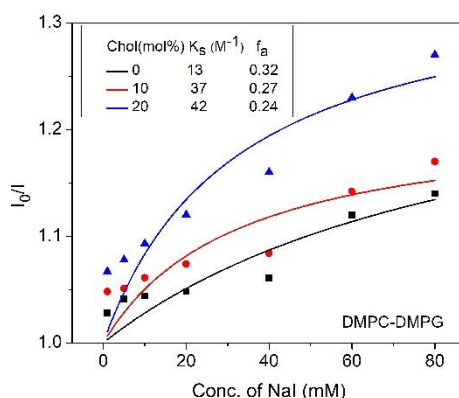


Fig. 8: Quenching of fluorescence intensity of Nile red with increasing NaI concentration for different cholesterol concentrations. K_s is the quenching constant and f_a is the fraction initial fluorescence that is accessible to the quencher.

4.3.4 Fluorescence Correlation Spectroscopy (FCS)

Fluorescence correlation spectroscopy (FCS) is commonly used to study the conformational and diffusional fluctuations of labeled molecules at the single molecule level. FCS detects fluorescence signals and analyzes the intensity fluctuations of fluorescent molecules in a small observation volume. Fluorescence intensity fluctuations can occur due to molecular diffusion in and out of the observation volume or due to any conformational changes in fluorescence profiles. Analysis of fluorescence intensity fluctuation because of molecular diffusion using a suitable correlation function provides an estimate of diffusion time (τ_D) which is used to estimate the diffusion constant. In the present study, we have studied how the diffusion of vesicles is affected in the presence of ions.

The FCS measurements were carried out using an ISS alba FFS/FLIM confocal system (Champaign, IL, USA), coupled to a Nikon Ti2U microscope equipped with the Nikon CFI PlanApo 60X/1.2 NA water immersion objective. The 48-nm picosecond pulsed diode laser was used for the excitation of the FCS measurements. The fluorescence emission was collected using a pair of SPAD (single photon avalanche detector) detectors with the 50/50 beam splitter and the 530/43 nm band pass filter. Details of the fitting procedure for the correlation curve were described in reference (37).

The FCS correlation curves were fit to the 3D Gaussian diffusion model. In the 3D Gaussian diffusion model involving a single type of diffusing molecules, the correlation function $G(\tau)$ can be defined as

$$G(\tau) = 1 + \frac{1}{N} \left(\frac{1}{1 + \left(\frac{\tau}{\tau_D}\right)} \right) \left(\frac{1}{\sqrt{1 + S^2 \left(\frac{\tau}{\tau_D}\right)}} \right)$$

Where τ_D denotes the diffusion time of the diffusing molecules, N is the average number of molecules within the observation volume, and S is the structural parameter that defines the ratio between the radius and the height. The value of τ_D obtained by fitting the correlation function $G(\tau)$ is related to the diffusion coefficient (D) by the following equation:

$$\tau_D = \frac{w^2}{4D}$$

Where w is the volume of the observation volume.

If we analyze the value of diffusion coefficients (D) and diffusion time (τ_D), we can observe that for a particular ion concentration (NaI 20 mM), the value of diffusion coefficients is increasing with increasing cholesterol concentrations.

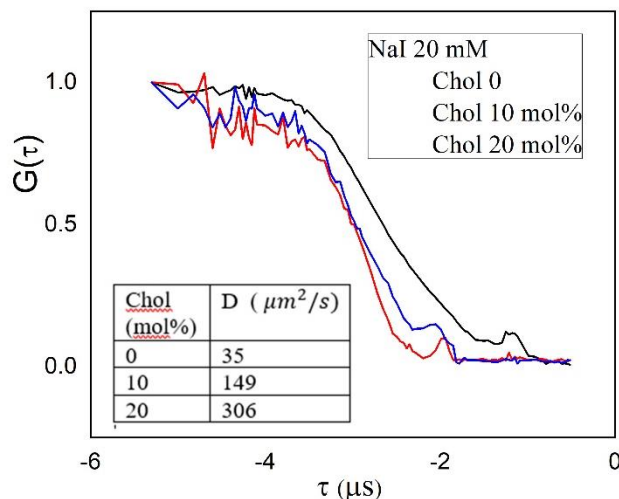


Fig 4.9 Autocorrelation curves drawn at different cholesterol concentration for DMPC-DMPG(4:1) lipid composition. The diffusion coefficients (D) obtained at 20 mM NaCl and NaI concentration are given in the figure legend.

4.3.5 Discussion

An isothermal titration calorimetry study on DMPC vesicles for both gel phase and fluid phase suggest that the fluid phase has a lower binding affinity (9.64 M^{-1}) compared to gel phase (137 M^{-1}). Large binding constant in the gel phase of DMPC compared to the fluid phase obtained from the partition model is very surprising. It is expected that water as well as ion penetration must be restricted due to the more compact structure in the gel phase. Therefore, an increase in the Na^+ binding in the gel phase of DMPC is very intriguing. The net endothermic heat signals (data not shown) obtained from ITC indicate the entropic contribution to the ion-membrane interaction. An earlier simulation study has shown that the membrane phase determines the behaviour of water, ions, and PC head groups (9). Therefore, ion binding onto the membranes is governed by the water dynamics and hydrogen bonding between the head group and water. In the gel phase, partial dehydration (fewer PC-water interactions), particularly in the carbonyl group region, has been found. The rigid structure in the gel phase, almost prevents water as well as ion penetration into this region as compared with the bilayer in the fluid phase. Further, the liquid crystalline phase or the fluid phase

facilitates the exchange of Na^+ ions between the water layer and the interfacial region. The simulation study also revealed that the lack of Na^+ in the carbonyl group of the gel phase is due to the more compact structure of the bilayer. Therefore, it is conceivable that most of the Na^+ ions are adsorbed into the phosphate group of the membrane. As experiments were performed at 15°C , it may be the onset of a transition from the ripple phase to the gel phase, and hence higher thermal fluctuations as well as undulating bilayers might be the cause of higher binding constant at 15°C . As DMPC is a neutral phospholipid, it is not appropriate to study zeta potential to investigate ion binding. Therefore, it is not possible to cross-check the binding phenomenon using zeta potential. We have studied mixtures of DMPC and DMPG in order to understand the electrostatic contribution to the ion binding interaction.

In the presence of NaI, the behaviour of the average size of SUVs containing 0 and 10 mol% of cholesterol shows an opposite trend compared to 20 mol% of cholesterol (Fig. 2). The increase in the average size (diameter) of the vesicles observed in cases of 0 and 10 mol% of cholesterol could be due to an increase in ion hydration at higher salt concentration (30). However, we cannot rule out the possibility of mild aggregation in the presence of ions. At 20 mol% of cholesterol, size decreases for higher salt concentrations. This could be due to the reduction of hydration layer in the presence of cholesterol. Further, the compression of electrostatic double layer as a result of adsorption of ions may also lead to a decrease in the average diameter of the vesicles. The decrease in the average size is not significant, indicating a charge screening effect at higher salt concentrations.

The binding constant in the fluid phase of DMPC (9.64 M^{-1}) was found to be greater than the fluid phase of DOPC (0.44 M^{-1}) (5; 22). This result suggests that chain saturation affects the Na^+ binding to the membrane. Such differences of binding constant might be the consequence of all *trans* conformation of hydrocarbon chains in DMPC and the *cis* configuration in DOPC. This results in a higher flexibility in the fluid phase of DOPC, which in turn affects the hydration dynamics at the interface. Zeta potential was used to obtain the binding affinity of cations, and Gouy Chapman theory was employed to estimate the binding constant. As zeta potential can be envisaged from a charged surface, we have prepared vesicles with a mixture of DMPC and an anionic phospholipid, DMPG, at a ratio of 4:1. The binding constant obtained from the Hill equation (see the inset of fig. 3a) is consistent with that estimated from the Gouy Chapman theory.

The incorporation of cholesterol into the anionic membrane reduces the binding constant of Na^+ ions (Fig 5). This is due to the fact that cholesterol decreases (becomes more negative) the surface charge density (31). Magarkar et al have reported through molecular dynamic simulation and zeta potential experiments that increasing the level of cholesterol in DSPC and POPC membranes decreases surface charge in the physiological environment (20). Therefore, the decrease in the binding constant of Na^+ ions found in the present study is in agreement with that obtained from DSPC and POPC vesicles. It has been reported from molecular dynamic simulation that Na^+ ions tend to bind with the phosphate oxygen of the PC head group and are less prone to bind cholesterol $-\text{OH}$ groups. On the other hand, cholesterol $-\text{OH}$ associates with phosphate oxygen (20; 32). Therefore, increasing cholesterol concentration replaces Na^+ ions with cholesterol $-\text{OH}$ groups which eventually decrease the binding affinity of the cations with the membrane. As there is no intrinsic surface charge in PC vesicles, it is not useful to compare the zeta potential results with our findings.

It is important to mention that cholesterol is known to reduce the effective surface area per lipid (33). This can also lead to a decrease in surface charge density. However, it has been shown from our previous study that cholesterol does not change the area per lipid significantly in the DOPC-DOPG mixture (17). This is primarily due to the stronger affinity of cholesterol for the zwitterionic lipid DOPC than DOPG. We might encounter a similar situation in the case of DMPC-DMPG mixture. It was also found from the hypothesis that the liquid ordered (l_o) phase is the cholesterol rich phase containing saturated lipid only (34; 35). Therefore, like in the case of DOPC-DOPG membrane, an increase in the cholesterol content in the DMPC-DMPG membrane does not change the area per lipid significantly, and hence the change in surface charge density in the presence of cholesterol is due to the alteration of the binding affinity of cations only. It is interesting to observe that although the negative value of zeta potential decreases as a result of cation adsorption, it never exceeds zero. In other words, there is no complete charge compensation of the membrane. The charge screening as well as the binding of cations occur simultaneously. At sufficiently high salt concentration the charge screening effect overrules the binding phenomena and prevents further adsorption of cations. Hence zeta potential gets saturated before it fully neutralises the membrane.

The main striking feature of the ion-membrane interaction in the case of DMPC-DMPG membrane is that it exhibits a completely opposite trend from DOPC-DOPG membrane (17). Such differences between saturated and unsaturated lipid compositions were

not elucidated in any of the earlier studies. The binding constant, surface charge density, and intrinsic concentration obtained from zeta potential in the present study show opposite behaviour from DOPC-DOPG vesicles. Such an opposite trend in the ion-membrane interaction of saturated lipids and unsaturated lipids could be due to the much higher affinity of cholesterol molecules towards saturated phospholipids compared to unsaturated lipids. This result is consistent with the rafts hypothesis, which resembles the cholesterol rich liquid ordered (l_o) phase containing saturated lipids.

In order to obtain insights into the interaction of counter ions (anion Γ^- in this case), an environment sensitive fluorescence probe, Nile red was used. It is known to exhibit fluorescence in a hydrophobic environment and increases its efficiency with increasing hydrophobicity or decreasing solvent polarity, resulting in a progressive blue shifted emission maximum (29). Therefore, the location of quencher may significantly alter the fluorescence emission of Nile red. The lower emission maxima (580 nm) of the gel phase of DMPC (15 °C) compared to the fluid phase (630 nm) is due to motionally restricted phospholipids, which in turn change the rotational diffusion of the molecule (36). In the presence of cholesterol, the emission also shifted to lower wavelengths with increasing cholesterol. This is expected, as cholesterol is known to reduce the rotational diffusion of the hydrocarbon chain, which will affect the emission spectra of Nile red (29). The presence of 20 mM NaI does not shift or alter the emission spectra further, indicating Γ^- ions do not restrict the motion of hydrocarbon core of the bilayer (Fig. 4.6 and 4.7 for comparison). This is also supported by the fact that the quenching of Nile red is also small, as indicated in low quenching constant (13 M^{-1} for zero cholesterol concentration) due to the small fraction (~ 0.2) of Nile red accessible to the quencher Γ^- (See the inset of Fig 6). Magarakar et al. have shown from the mass density of Cl^- at the interface that there is no significant binding of Cl^- in the membrane (20). Therefore, our result is in agreement with the previous report.

4.4 Conclusion

We have studied the effect of chain saturation, lipid phase state, and cholesterol on the Na^+ binding to the phospholipid membranes. Beside the electrostatic contribution, the significant entropic contribution due to the release of water molecules at the membrane water interface upon Na^+ binding leads to low net heat flow in the isothermal titration calorimetry experiments. The thermodynamic parameters of binding kinetics were estimated from the partition model. The gel phase shows a higher binding constant relative to the fluid phase of

DMPC vesicles. On the other hand, the binding constant of saturated lipid DMPC in the fluid phase was found to be higher than that of unsaturated lipid DOPC. We were not able to analyse the binding isotherm of the DMPC-cholesterol membrane due to the low net heat flow. A systematic investigation of the effect of cholesterol on the ion-membrane interaction shows a decrease in the binding constant for both increases in cholesterol and ion concentrations due to a decrease in the surface charge density of the membrane. Interestingly, the ion-membrane interaction of saturated lipids exhibits a completely reverse trend with unsaturated lipids. Therefore, cholesterol modulates the surface charge density of the membrane and alters the binding affinity of ions. However, there is no significant counter-ion effect on the anionic membrane containing cholesterol. The membrane surface charge plays a significant role in the interactions of bio-membrane with membrane proteins. Further, this study provides useful insights about how liposomes, used as drug delivery vehicles, interact with and are affected by immune system. The binding affinity and arrangement of ions at membrane-water interfaces are of great importance in the formation of electrical double layers and provide insights into the ion-transport process in the cellular membrane.

References

1. P. Maity, B. Saha, G. Suresh Kumar, S. Karmakar, *Biophys. Biochim. Acta* 1858, 607-617(2016).
2. R. Friedman, Membrane-Ion interactions, *J. Membr. Biol.* 251, 453-460(2018).
3. I. Vorobyov , T. E. Olson J. H. Kim , R. E. Koeppe, O. S. Andersen, T. W. Allen, *Biophys. J* 106, 586-597(2014).
4. E. Deplazes, J. White, C. Murphy, C. G. Cranfield, A. Garcia, *Biophys. Rev.* 11, 483-490(2019).
5. B. Klasczyk, V. Knecht, R. Lipowsky, R. Dimova, *Langmuir* 26, 18951–18958(2010).
6. R. J. Clarke, C. Lüpfer, *Biophys. J* 76, 2614-2624(1999).
7. L. Redondo-Morata, M. I. Giannotti, F. Sanz, *Mol. Membr. Biol.* 31, 17-28(2014).
8. J. N. Sachs, H. Nanda, H. I. Petrache, T. B. Woolf, *Biophys. J* 86, 3772-3782(2004).
9. M. D. Fayer, *Acc. Chem. Res.* 45, 3-14(2011).

10. L. Finegold, *Cholesterol in Membrane Models*, CRC Press, Boca Raton, 1993.
11. E. Sezgin, I. Levental, S. Mayor & C. Eggeling, *Nat. Rev. Mol. Cell. Biol.* 18, 361–374 (2017).
12. D. Lingwood, K. Simons, *Science* 327, 46-50(2010).
13. S. L. Veatch, S. L. Keller, *Phys. Rev. Lett.* 89, 268101(2002).
14. T. Baumgart, S. T. Hess, W. W. Webb, *Nature*, 425, 821–824(2003).
15. A. Ghysels, A. Krämer, R. M. Venable, W. E. Teague Jr, E. Lyman, K. Gawrisch, R. W. Pastor, *Nat. Comm.* 10, 5616(2019).
16. S. J. Singer, G. L. Nicolson, *Science* 175, 20-731(1972).
17. K. K. Banerjee, P. Maity, S. Das, S. Karmakar, *Chem. Phys. Lipids* 254, 105307(2023).
18. M. Stepniewski, A. Bunker, M. Pasenkiewicz-Gierula, M. Karttunen, T. Rog, *J. Phys. Chem. B* 114, 11784–11792(2010).
19. M. Javanainen, A. Melcrova, A. Magarkar, P. Jurkiewicz, M. Hof, P. Jungwirth, H. Martinez-Seara, *Chem. Commun.* 53, 5380(2017).
20. A. Magarkar, V. Dhawan, P. Kallinteri, T. Viitala, M. Elmowafy, T. R. Rog, A. Bunker, *Sci. rep.* 4, 5005(2014).
21. M. J. Hope, M. B. Bally, G. Webb, P. R. Cullis, *Biophys. Biochim. Acta* 812, 55-65(1985).
22. R. Hunter, *Zeta Potential in Colloids Science*, Academic Press, New York, 1981.
23. S. Karmakar, U. K. Sur (Ed.) , *Recent Trends in Materials Physics and Chemistry*, Studium Press (India) Pvt Ltd, ISBN: 978-93-85046-32-2, 117-159(2019).
24. A. Sannigrahi, P. Maity, S. Karmakar, K. Chattopadhyay, *J. Phys. Chem. B* 121, 1824-1834(2017).
25. H. Heerklotz, J. Seelig, *Biophys. Biochim. Acta* 1508, 69-85(2000).
26. P. Maity, B. Saha, G. S. Kumar, S. Karmakar, *RSC Adv.* 6, 83916(2016).
27. J. R. Lakowicz, *Principles of Fluorescence Spectroscopy*, Plenum Press, New York, 1983.

28. P. Maity, B. Saha, G. S. Kumar, S. Karmakar, *Langmuir* 34, 9810-9817(2018).
29. A. Halder, B. Saha, P. Maity, G. S. Kumar, D. K. Sinha, S. Karmakar, *Spectrochim Acta A Mol Biomol Spectrosc.* 191, 104-110(2018).
30. M. M. A. E. Claessens, B. F. van Oort, F. A. M. Leermakers, F. A. Hoekstra, M. A. C. Stuart, *Biophys. J* 87, 3882–3893 (2004).
31. M. Doktorova, F. A. Heberle, R. L. Kingston, G. Khelashvili, M. A. Cuendet, Y. Wen, J. Katsaras, G. W. Feigenson, V. M. Vogt, R. A. Dick, *Biophys. J* 113, 2004-2015(2017)
32. I. Ermilova, A. P. Lyubartsev, *Soft Matter* 15, 8-93(2019).
33. F. de Meyer, B. Smit, *Proc. Natl. Acad. Sci: USA* 106, 654-3658(2009).
34. E. Sezgin, I. Levental, S. Mayor, C. Eggeling, *Nat. Rev. Mol. Cell Biol.* 18, 361–374(2017).
35. K. Simons, W.L.C. Vaz, *Annu. Rev. Biophys. Biomol. Struct.* 33, 269–95(2004).
36. S. Mukherjee, H Raghuraman, A. Chattopadhyay, *Biochim Biophys Acta* 1768, 59-66(2006).

Chapter 5

Interaction of alkali metal salts with membrane made up of lecithin-cholesterol

5.1 Introduction

In the preceding chapters, we have examined the influence of cholesterol on the interaction between alkali metal salts, such as NaCl and NaI, and unsaturated phospholipid membranes composed of a DOPC: DOPG mixture, as well as saturated membranes made from DMPC: DMPG. In both studies, we noted that cholesterol significantly impacts ion binding. Although both lipids, DOPG and DMPG, possess anionic characteristics, the influence of cholesterol on ion binding for unsaturated lipids is entirely contrary to that observed in saturated phospholipids. At this point, we aim to investigate the comparative effects of the alkali metal salts NaCl and NaI on ion-membrane binding in the presence of cholesterol.

In this chapter, we have reported detailed dynamic light scattering and zeta potential studies of effect of cholesterol on the interaction of egg lecithin with monovalent sodium salts. We have explored Gouy-Chapman theory to estimate binding constant, surface charge density, surface potential etc. of the membranes containing ion and cholesterol. A significant change in the negative zeta potential of egg PC in presence of small amount of cholesterol has been detected. There is also a significant decrease in intrinsic binding of ions with the increase in cholesterol concentrations. Earlier studies related to this work have discussed in section 5.2. Detailed experimental results are discussed in section 5.3. We have concluded the chapter in section 5.4.

5.2 Earlier studies

Complex structure and functions of membrane has led us to study the model system to get some insight into physical mechanism of membrane functions. Hydrocarbon based surfactants, lipids are an example of group of amphiphilic compounds (36). These vesicles are formed by self-assembly of amphiphilic molecules. The phospholipids and vesicle forming material when suitably mixed with water and similar solvent forms multilamellar vesicles (MLV). But MLV do not serve as good model system of bio membranes as cellular

membranes has single bilayer of lipid molecules. Hence, we have to prepare single bilayer model membrane i.e unilamellar vesicles. SUV or small unilamellar vesicles are used as model system for studying structural and dynamic features of many cellular processes such as infection, exocytosis, endocytosis, cell fusion etc. The interaction of ions with egg lecithin (phosphatidylcholine) in the presence of cholesterol is a subject of considerable interest in biophysical and biochemical studies. This interplay is relevant to understanding biological membranes' structure and function. Lecithin is generally the major fraction of total phospholipid occurring in biological membranes (25). Since the lecithin molecule possesses a phosphate and tri-methylammonium group separated by two methylene groups, its structure allows two ionic forms: one in which the separation of charges is maximal and the other in which a reduced separation of charges results from an internal salt linkage between the phosphate and tri-methylammonium groups in the same molecule (25). In cellular membranes, lecithin provides structural integrity and serves as a medium for protein interactions and signalling events. Widespread occurrence of cholesterol in association with lecithin and other phospholipids in biological membranes has motivated us to study their interactions in relatively simple model system. In the last few decades, cholesterol-lecithin and protein-lipid interactions have been studied using differential scanning calorimetry (DSC) (4-8), SAXS (9-12), nuclear magnetic resonance (10, 11) etc. Most of these studies suggest that due to interaction of cholesterol with lecithin monolayers, gel to liquid phase transition temperature becomes lowered and there is a condensing effect on lecithin molecules in the system. The cholesterol-lecithin interaction has been interpreted in terms of different arrangements of cholesterol and lecithin molecules such as association (9), cholesterol-lecithin complex (11-14), homogeneous mixed bilayer structure or otherwise (12,15,16). In most of these studies cholesterol and lecithin were mixed by dissolving them in organic solvents and aqueous dispersions were heated above the phase transition temperature of the phospholipid in order to have fatty acid chains in melted state. There have been no reports of phase transition behaviour of physically mixed cholesterol lecithin complex either in anhydrous form or in the presence of water. The use of lecithin (19, 20) and cholesterol (17, 18) separately and its combination as drug carriers make it important to study physiochemical properties of cholesterol and lecithin and their interactions. The lability of lecithin largely depends on the degree of unsaturation (21), hence hydrogenated lecithin offers an advantage in preparation of pharmaceutical dosage forms (19, 20, 22, 23, 24). Though the qualitative aspects of effect of cholesterol on lecithin bilayers have generally been agreed upon but the quantitative aspects like surface potential, surface charge density, intrinsic binding etc. are not looked

upon previously with care. In this work we have taken negatively charged egg lecithin as model membrane to prepare small unilamellar vesicles.

5.3 Experimental Results

5.3.1 Effect of various alkali metal ions on the size distribution of small unilamellar vesicles: Dynamic light scattering experiment

In this work we intend to discuss the experimental results of size distribution of SUV obtained from the dynamic light scattering experiment and also the effect of various alkali (NaCl, NaI) metal ions on size distribution for different ion concentration. Typical size distribution of SUV which is obtained from DLS experiment, indicates that the ultrasonic homogenizer (probe sonicator) produces fairly monodisperse small unilamellar vesicles (SUV). As shown in fig. 5.1, the average size of vesicles (d-nm) is ~55 nm at 25°C. The size distribution also depends on the temperature. The average size increases with increasing temperature. Before starting the DLS experiment the sample was degassed to eliminate the air bubble in the sample. We have systematically studied the effect of alkali metal ions on the size distribution of egg lecithin. SUV without salt exhibits average size 65.3 nm and as we increase the ion concentration, vesicle size decreases. At very high concentration of NaCl i.e at 150 mM, vesicle size is 47.23 nm. But ambiguity appears in case NaI i.e I^- counterion, where for very low concentration of ion i.e 2, 5, 10 mM there is an initial increase in vesicle size but after a certain concentration i.e 20 mM vesicle size decreases to 51.6 nm. For 20 mM average vesicle size is 67.6 nm, which is interestingly larger than for any concentration of NaCl. From size distribution we can clearly observe that for NaCl, particle size decreases with increasing ion concentration, but for I^- (NaI) counterion, up to a certain concentration i.e 20 mM particle size increases but after that particle size decreases with increasing ion concentration. These effects arise from changes in the packing of phospholipids, ion-mediated cross-linking, and cholesterol's impact on membrane rigidity and fluidity. The presence of monovalent ions generally does not significantly alter vesicle size, although high concentrations induced slight changes by screening repulsive forces between lecithin molecules. Now if we study the three curves comparatively, we can imply that here the effect on counterions (I^- , Cl^-) becomes predominant over the cation Na^+ . So, the effective change in particle size occurs due to counterions. Counterion iodine (I^-) can penetrate the hydrodynamic wall of the vesicles and causes immense interaction with the lipid. The variation of average vesicle size with different ion concentration for NaCl and NaI is given below.

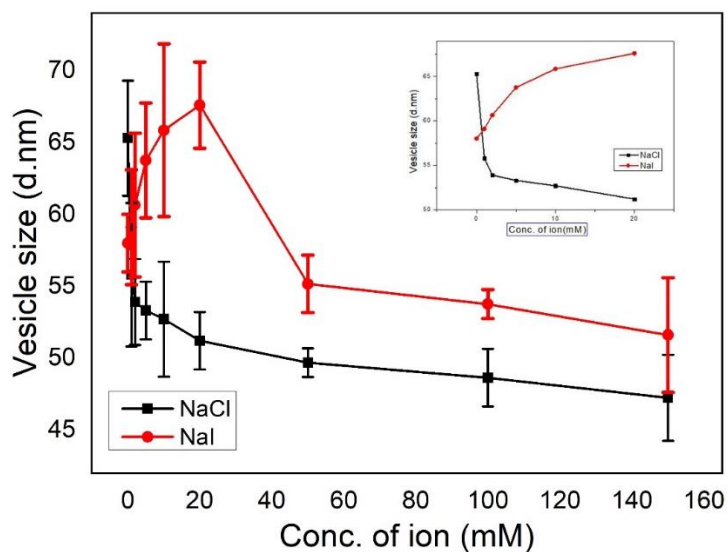


Fig. 5.1 Variation of average size of small unilamellar vesicles (SUVs) prepared from egg lecithin with ion concentration varying from 0 to 150 mM. Error bars are obtained from the average value of three different measurements.

5.3.2 Effect of alkali metal ions on zeta potential: -

Here we have systematically studied the effect of alkali metal ions (I^- & Cl^-) on the zeta potential distribution of vesicles for various ion concentration ranging from 0 mM to 150 mM. As expected, we can observe that zeta potential increases (negative value decreases) with increasing ion concentration.

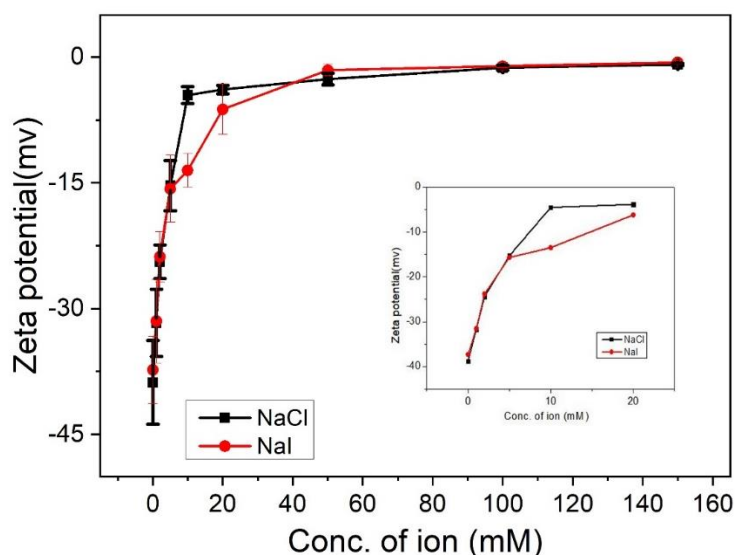


Fig. 5.2 Variation of zeta potential of SUVs made from egg lecithin (PC) with varying ion concentrations (indicated in figure legend). Error is determined from three different zeta potential measurements.

As observed from the experiment (fig. 5.2), for NaCl, the value of zeta potential varies from -39 mv to -0.9 mv for ion concentration ranging from 0 mM to 150 mM. To understand the effect of counterion Γ , we have also recorded the effect of NaI on the zeta potential distribution of egg lecithin. From this we can observe that for 0 mM of NaI, zeta potential given by zetasizer is -37 mv and for very high concentration of iodine i.e for 150 mM, it increases to -0.7 mv. So there is as such no ambiguity found in case of NaI, that means we got almost same effect for two different counterion Γ and Cl^- .

5.3.3 Effect of cholesterol on vesicle size and zeta potential distribution: -

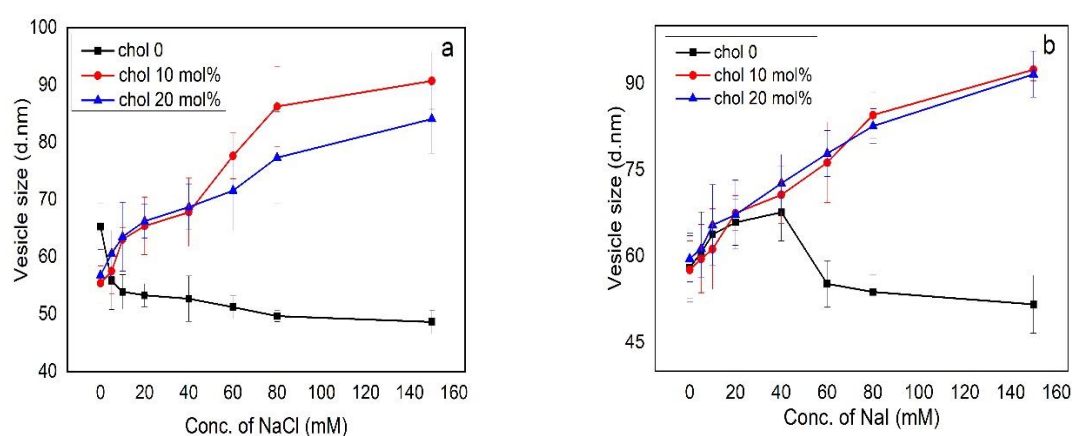


Fig. 5.3 Variation of vesicle size with different NaCl (a) and NaI (b) concentration in presence of cholesterol (0, 10 and 20 mol%) as indicated in the figure legend. Error bars are estimated from three consecutive measurements.

Variation of vesicle size with NaCl concentrations in the presence of cholesterol (0, 10, 20 mol%) is presented in the fig. 5.3. These results indicate that the vesicle size seems to decrease with increasing ion concentration for zero cholesterol concentration. But if we increase the cholesterol concentration (10 and 20 mol%) vesicle size decreases with the increase of NaCl concentration. Similar result has been observed, when the experiment has been performed with NaI.

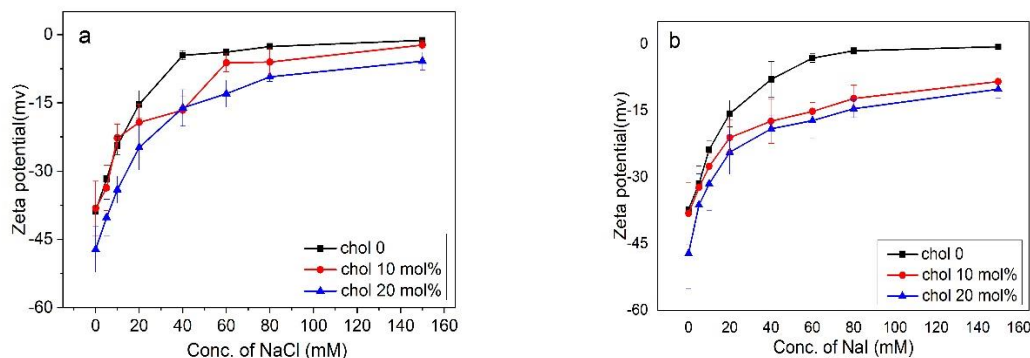


Fig. 5.4 Zeta potential of small unilamellar vesicles (SUV) was measured for mixture of egg lecithin and (a) NaCl and (b) NaI in presence of cholesterol concentrations (0, 10 and 20 mol%).

From the figure 5.4 it is clearly evident that zeta potential shows high negative value at all cholesterol concentration (X_C) in the absence of NaCl or NaI. Now, if we increase the salt concentration zeta value increases (becomes less and less negative) for all X_C . Interestingly, zeta value saturates close to zero, but never exceeds zero.

5.4 Effect of cholesterol on ion-binding in membrane: Gouy Chapman theory

Gouy- Chapman model is based on electrostatics double layer theory and is widely used to describe the electrostatic behaviour of charged surface in presence of ion. In this study, we used Gouy Chapman model to describe the distribution of ions in the vicinity of SUV in the form of electrostatic double layer followed by diffused layers which decays to a length known as screening length. Zeta potential (ζ) was measured for small unilamellar vesicles (SUVs), composed of lipid egg lecithin and cholesterol. It is clearly evident from the results of zeta potential (Fig 5.3) that the ζ shows a high negative value (-37 mV) in the absence of NaI for all cholesterol concentrations. Further, ζ decreases (negative value increases) lightly with increasing cholesterol concentrations for a particular ion concentration (Fig 5.3b). Now, if we increase the ion concentration gradually, zeta potential becomes less negative (the negative value decreases), which means zeta potential increases with the increase in ion concentration. However, variations in zeta potential can be distinguished for intermediate salt concentrations (> 20 mM). For example, zeta potential at 60 mM shows a much higher value (-17 mV) for a cholesterol concentration of 20 mol% than that without cholesterol (~ -47

mV). The underlying cause of partial charge compensation will be discussed later. Finally, zeta potential shows saturation at a similar zeta potential for all cholesterol concentrations. Interestingly, the zeta potential value saturates close to zero but never exceeds zero (fig. 5.5). A quantitative description of the lecithin-cholesterol binding process was done using the Gouy Chapman theory based on the concept of electrostatic double layer which is described in our previous papers (1; 17). Table 5.1(NaCl) and 5.2(NaI) summarises the electrostatic parameters estimated from the Gouy Chapman theory.

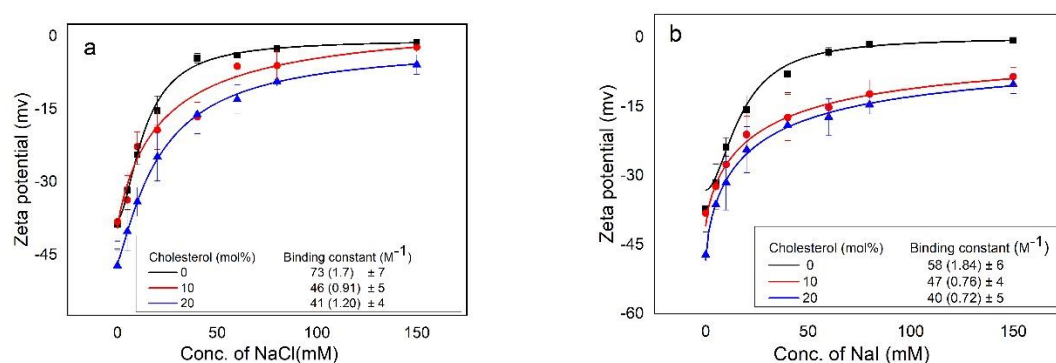


Fig. 5.5(a) Variation of zeta potential of egg lecithin vesicles with NaCl and (b) NaI concentrations for two different cholesterol concentration. Solid lines are obtained from the fit using Hill equation, describing the binding phenomenon. The binding constant obtained from the fit are presented in the inset of the figures. The number within the bracket represent the cooperativity index.

Table 5.1 (NaCl)

Electrostatic parameters obtained using the Gouy Chapman theory from the measured zeta potential of Small Unilamellar Vesicles (SUV) for different cholesterol concentration at 20 mM NaCl concentration. SUVs are prepared from binary mixture of egg lecithin and cholesterol.

Chol (mol%)	Surface potential (ψ_0) (mV)	Surface Charge (σ) (C/m^2)	Intrinsic concentration C_0 (M)	Binding constant (K) (M^{-1})
0	-16 \pm 4	-0.0011 \pm 0.0007	0.012 \pm 0.003	654 \pm 13
10	-21.2 \pm 3	-0.0070 \pm 0.0009	0.046 \pm 0.007	118 \pm 9
20	-27.3 \pm 5	-0.0092 \pm 0.0008	0.081 \pm 0.008	67 \pm 5

Table 5.2 (NaI)

Electrostatic parameters obtained using the Gouy Chapman theory from the measured zeta potential of Small Unilamellar Vesicles (SUV) for different cholesterol concentration at 20 mM NaI concentration

Chol (mol%)	Surface potential (ψ_0) (mV)	Surface Charge (σ) (C/m^2)	Intrinsic concentration C_0 (M)	Binding constant (K) (M^{-1})
0	-16.5 \pm 3	-0.0026 \pm 0.0008	0.017 \pm 0.007	747 \pm 9
10	-23.2 \pm 5	-0.0077 \pm 0.0005	0.049 \pm 0.006	168 \pm 8
20	-26.9 \pm 4	-0.0091 \pm 0.0007	0.057 \pm 0.009	69 \pm 6

As shown in table 5.1 and 5.2, the surface charge density decreases with cholesterol concentration at a particular salt concentration. As a consequence, the intrinsic binding constant of cations decreases with increasing cholesterol concentrations as shown in fig. 5.5. This result suggests that cholesterol reduces the binding affinity of the cations. We have not measured the value of the zeta potential for salt concentrations above 150 mM. This is due to the fact that measurement of zeta potential at very high salt concentrations causes electrolysis, leading to damage to the gold electrodes in the zeta cuvette. This is evident from the colour change of the solution at concentrations of electrolytes greater than 150 mM. For comparison, zeta potential as a function of salt concentration was also fitted to a Hill equation, originally developed for the binding of ligands to macromolecules. The values of the binding constant for different cholesterol concentrations are consistent with those obtained from the Gouy Chapman theory (Fig. 5.5). The difference in the numerical values may be due to simplified underlying assumptions in the Gouy Chapman theory. Further zeta potential is realised only for the charged component. Therefore, the change in zeta potential is only due to electrostatic contribution. However, entropic contribution plays a vital role in the binding process. This could also lead to difference in the binding constant obtained from Hill fit and Gouy Chapman theory. The variation of binding constants with cholesterol concentration for different salt concentration is represented through the curve shown in below (fig. 5.6).

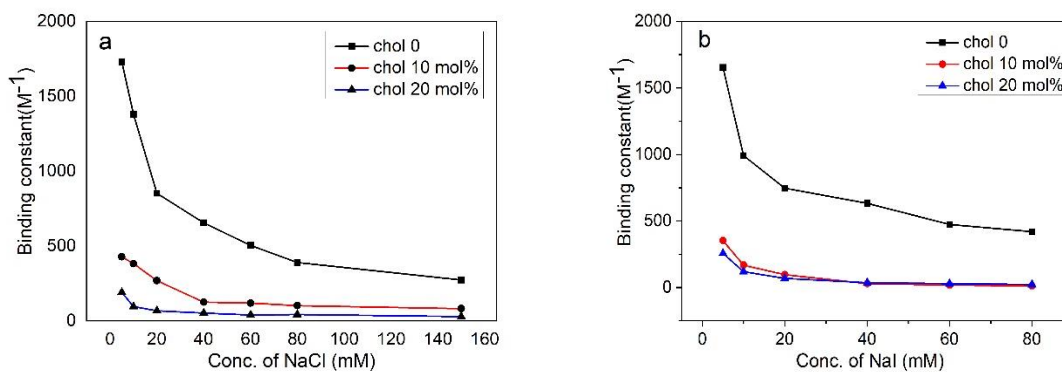


Fig. 5.6 Variation of binding constants with ion concentration NaCl(a) and NaI(b) for different cholesterol concentration shown in the figure legend.

Variation of different electrostatic parameters like surface charge density and intrinsic concentration in presence of NaCl and NaI for particular cholesterol concentration 10 mol% is given below (fig. 5.7).

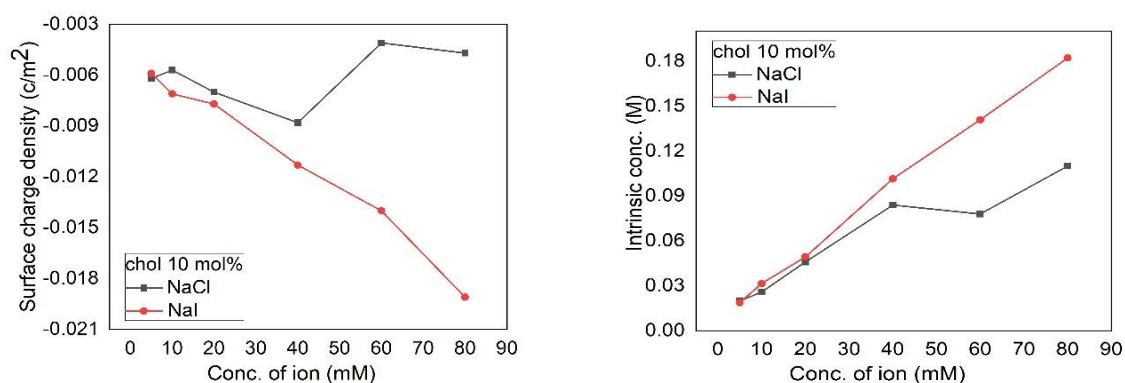


Fig. 5.7 Variation of surface charge density and intrinsic concentration with NaCl and NaI, for particular cholesterol concentration 10 mol%.

From the above curves (fig. 5.7), we can observe that negative surface charge density remains almost same for NaCl but it is continuously decreasing with increasing NaI concentration. These results are very helpful to understand the behaviour of different membrane parameters in presence of ion. On the other hand, the intrinsic concentration increases for both NaCl and NaI but for NaI it is more consistent than NaCl. To understand the effect of cholesterol on ion-membrane binding we have presented the binding constants for 10 mol% cholesterol in presence of NaCl and NaI.

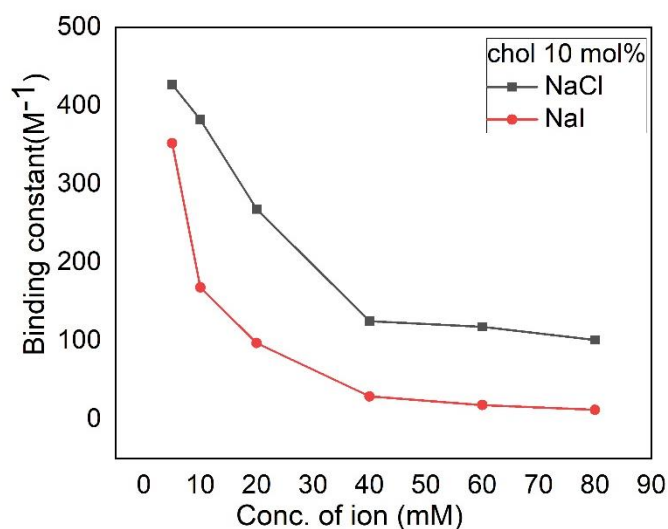


Fig. 5.8 Variation of binding constants with NaCl and NaI concentration for particular cholesterol concentration 10 mol%.

5.5 Discussion:

There is considerable evidence that cholesterol-lecithin interactions are important in certain biological and bio-medical systems. In particular, it has been recognized that these two compounds are major components of lipid fraction in cell membranes (34). In 1965, O'Brien discussed a model for myelin sheath membrane which involves van der Waals interaction in hydrocarbon portion and coulomb forces between the positively charged choline nitrogen of lecithin and the $-OH$ group of cholesterol (34). Lecithin has the ability to solubilize cholesterol and this interaction has many biological applications (33). Zull et al. obtained spectra of solid films of lecithin-cholesterol mixtures through attenuated total reflection of infrared spectroscopy technique and observed that presence of lecithin produces a low frequency shift of 150 cm^{-1} in the $-OH$ stretching absorption of cholesterol (33). But this interaction is not produced by other lipids which have same polar group that lecithin contains. The obvious interpretation to this $-OH$ shift is due to hydrogen bonding of cholesterol to some polar sites in the lecithin molecule. However, cholesterol-cholesterol polymeric association induced by lecithin may be an alternative interpretation but it seems unlikely (35). Experimental results in the size distribution of SUV using DLS clearly shows that vesicle size decreases with increasing ion concentration in the absence of cholesterol for NaCl. In case of NaI, we observe that initially vesicle size increases and after a certain ion concentration it

decreases. So, there is absorption of ion in the cholesterol-lecithin bilayer and that is why vesicle size is decreasing (3) with increasing ion concentration. In 1977 Yeagle et al. observed 40% nuclear overhauser effect (NOE) in pure egg PC bilayers. They also shown that presence of cholesterol disrupts (28) the intermolecular interaction in PC bilayers. Earlier studies suggested that in egg PC bilayers, the phosphorylcholine moiety is oriented parallel to the surface (28) and engaged in intermolecular interactions. They reached in a conclusion that zwitterionic dipole in sphingomyelin and phosphatidylcholine is oriented parallel to the bilayer surface and that cholesterol is capable of completely disrupting (28) the intermolecular association in bilayers. Dipole measurement predicts (29) that cholesterol slightly increases the hydration pressure, which is in qualitative agreement with the X-ray results. In our previous work (3) we have shown that due to presence of cholesterol, area per molecule decreases as cholesterol conc. increases. These observations are pertinent to cholesterol's role in vesicle adhesion and fusion which implies that cholesterol can alter the membrane binding (3), permeability of ions, drugs and metabolites. Russo et al. showed that lipid depletion in cholesterol enriched lipid vesicles is inversely proportional to the increasing amount of cholesterol in the vesicles. This actually occurs because cholesterol stiffens the phospholipid acyl chain packing of plasma membranes, increasing their resistance and reducing their permeability (30). Lund-Katz et al. used nuclear magnetic resonance (NMR) and monolayer methods to evaluate cholesterol physical state and interactions with phospholipid. They studied that rate of cholesterol desorption from the lipid-water interface depends on molecular packing in the bilayer and it follows the order unsaturated PC > saturated PC > sphingomyelin (SM). Their analysis suggests that variation in cholesterol-phospholipid van der Waals interaction energy is an important cause of different rate of cholesterol exchange from different host phospholipid (32). Cholesterol can interact with phosphatidylcholine on both the inner and outer surfaces of lipid bilayer vesicles. Huang et al. interpreted that up to 30%, there is homogeneous distribution of cholesterol in the egg lecithin bilayers but above 30%, cholesterol is asymmetrically distributed in favour of the inner bilayer. Egg lecithin, which consists of variety of polyunsaturated side chains, the side chains having greater number of double bonds are preferentially displaced by higher concentrations of cholesterol, but such preferential displacement by cholesterol doesn't occurs for saturated dipalmitoyl lecithin (31). Like dipalmitoyl lecithin, egg lecithin also forms liquid expanded monolayers but with a larger limiting area than that of dipalmitoyl lecithin (1). Van Deenen (2) has reported that because of shorter chain lengths, intermolecular cavities are smaller and they are unable to accommodate cholesterol

molecules. Thus, addition of cholesterol causes increase in the area of mixed monolayers (25). From the variation of vesicle size with sodium salts (NaCl and NaI), we observe that in presence of cholesterol vesicle size increases and this rate of increase is high for NaI. As a result of this area of the mixed monolayers increases. Now from the measurement of zeta potential we observe that, zeta potential has a high negative value for all cholesterol concentration and with the increase of ion negative zeta potential increases (becomes less negative). As a result of this surface zeta potential decreases (negative value increases) with the increase of cholesterol concentration as shown in the table. Shah and Schulman have previously (26) shown that presence of 25 mol% or more cholesterol in mixed monolayers prevents the binding of Ca^{2+} ions to egg lecithin. Similarly, in our work we have systematically studied the effect of cholesterol on the interaction of saturated egg lecithin with NaCl and NaI. Here we also observe that due to increase in cholesterol concentration, binding of Cl^- and I^- decreases. When there is no cholesterol, Cl^- binds more than I^- with the membrane but if we increase cholesterol (for 10 mol%) I^- binds more than Cl^- . In egg lecithin, the phosphate group interacts with the counter ion and the presence of cholesterol causes a small net increase (25) in the spacing between the phosphate group which eventually reduces the ionic repulsion between polar groups and strengthens the internal salt linkage. Consequently, mixed monolayers of lecithin-cholesterol binds less with I^- and Cl^- . So it is clearly evident from the tabular data that cholesterol prevents the binding of ion with the membrane.

References:

1. D. O. Shah and J. H. Schulman, J. Lipid Res 8, 215-226(1967).
2. Van Deenen, L. L. M, editor. Pergamon press, New York 8(pt1): 14, 59(1965).
3. Kalyan Kumar Banerjee, Pabitra Maity, Surajit Das and Sanat Karmakar, Chem. Phys. Lipids, 254, 105307(2023).
4. B. D. Ladbroke, R. M. Williams and D. Chapman, Biochim. Biophys. Acta, 150, 333(1968).
5. B. D. Ladbroke and D. Chapman, Chem. Phys. Lipids, 3, 304(1969).
6. J. C. A. Offringa, R. Plekkenpol and D. J. A. Crommelin, J. Pharm. Sci. 76, 821(1987).
7. M. R. Morrow and J. H. Davis, Biochemistry, 27, 2024 (1988).

8. M. A. Singer and L. Finegold, *Biophys. J.*, 57, 153 (1990).
9. M. Bourges, D. M. Small and D. G. Dervichian, *Biochim. Biophys. Acta*, 137, 157(1967).
10. A. Darke, E. G. Finer, A. G. Flook and M. C. Philips, *J. Mol. Biol.*, 63, 265 (1972).
11. R. A. Demel and B. de Kruffy, *Biochim. Biophys. Acta*, 457, 190(1976).
12. M. C. Philips and E. G. Finer, *Biochim. Biophys. Acta.*, 356, 199(1974)
13. E. Oldfield and D. Chapman *FEBS Lett.*, 23, 285(1972).
14. M. R. Vist and J. H. Davis, *Biochemistry*, 29, 451(1990).
15. M. B. Sankaram and T. E. Thompson, *Biochemistry*, 29, 10676(1990).
16. S. Mabrey, P. L. Mateo and J. M. Sturtevant, *Biochemistry*, 17, 2464(1978).
17. H. J. Hinz and J. M. Sturtevant, *J. Biol. Chem.*, 247, 3697(1972).
18. H. Lecuyer and D. G. Derivichian, *J. Mol. Biol.*, 45, 39(1969).
19. T. Nishihata, *Int. J. Pharmaceut.*, 40, 125(1987).
20. M. Fujii, H. Terai, T. Muri, Y. Sawada and M. Matsumoto, *Chem. Pharm. Bull.*, 36, 2186(1988).
21. H. Maclean and I. S. Maclean, Longman's Green and Co. Ltd., London, 1-11.
22. Y. Hirotsu, Y. Arakawa, Y. Maeda, A. Yamaji, A. Kamada and T. Nishihata, *Chem. Pharm. Bull.* 35, 3049(1987).
23. T. Nishihata, M. Sudho, A. Kamada, M. Keigami, T. Fujimoto, S. Kamide and N. Tatsumi, *Int. J. Pharmaceut.*, 33, 181(1986).
24. T. Nishihata, M. Sudho, A. Kamada, M. Keigami, T. Fujimoto, S. Kamide and N. Tatsumi, *Int. J. Pharmaceut.*, 42, 251(1988).
25. D. O. Shah and J. H. Schulman, *J. Lipid Res.*, 8, 227-233(1967).
26. D. O. Shah and J. H. Schulman, *J. Lipid. Res.*, 6, 341(1965).
27. S. P. Wrenn, E. W. Kaler, *J. Lipid Res.*, 40, 1483-1494(1999).
28. Yeagle et al, *Biochemistry* vol. 16, 20 (1977).
29. T. J. McIntosh, A. D. Magid and S. A. Simon., *Biochemistry* 28, 1(1989).

30. G. Russo, J. Witos, A. H. Rantamaki and S. K. Wiedmer., BBA-Biomembranes 1859, 12 (2017).
31. C. Huang, J. P. Sipe, S.T. Chow and R. B. Martin, PNAS 71(2), 359-362 (1974).
32. S. L. Katz, H. M. Laboda, L. R. McLean and M. C. Phillips., Biochemistry 27, 3416-3423 (1988).
33. J. E. Zull, S. Greanoff and H. K. Adam., Biochemistry 7, 12 (1968).
34. O'Brien, J. S., Science 147,1099 (1965).
35. O'Brien, J. S., and Sampson, E. L., J. Lipid Res. 6, 537 (1965).
36. M. I. Khan and I. G. Tucker., Chem. Pharm. Bull. 40(11), 3056-3061(1992).
37. N. J. Cho, L. Y. Hwang, J. J. R. Solandt, C. W. Frank, Materials, 6, 3294-3308 (2013).
38. R. Hunter, Zeta Potential in Colloids Science, Academic Press, New York, 1981.
39. S. Karmakar, U. K. Sur (Ed.) , Recent Trends in Materials Physics and Chemistry, Studium Press (India) Pvt Ltd, ISBN: 978-93-85046-32-2, 117-159(2019).
40. A. Sannigrahi, P. Maity, S. Karmakar, K. Chattopadhyay, J. Phys. Chem. B 121, 1824-1834(2017).

Chapter 6

Effect of cholesterol on the interaction of alkali metal salt with cationic vesicles

6.1 Introduction

In the previous chapters, we have discussed how cholesterol affects the interaction of alkali metal salts NaCl and NaI with unsaturated phospholipid DOPC: DOPG, saturated phospholipid DMPC: DMPG and egg lecithin. Positively charged lipid bilayer has drawn a lot of attention in DNA and mRNA transfection research and nonviral vector for gene delivery into a target cell (2). Although cationic lipids are not abundant in nature, the cationic lipid-DNA complex is extensively used to transfer DNA into the defective cell to recover infectious diseases such as heart disease, genetic defects etc. (31, 32, 33). Further, cationic lipids are well known to overcome the antitoxicity problem for gene therapy (34).

In this chapter, we have systematically investigated the interaction of different monovalent alkali metal salts with cationic membrane, composed of 1, 2-dioleoyl-sn-glycero-3-phosphocholine (DOPC)/ 1,2-dioleoyl-3-trimethylammonium-propane (DOTAP) in the presence of cholesterol. From the experimental results, we observed that for zero cholesterol vesicle size slowly increases and with the increase of cholesterol, vesicle size decreases. Similarly, without cholesterol, there is a decrease in zeta potential with ion concentration but for higher cholesterol concentration, zeta potential increases. So, both the zeta potential and average size of vesicles show an opposite trend in presence of cholesterol. The increase in size of vesicles without cholesterol is due to aggregation of vesicles, as evidenced by microscopy of giant unilamellar vesicles (GUV). However, the presence of cholesterol seems to inhibit the aggregation. The decrease in zeta potential without cholesterol indicates the adsorption of anions on the cationic membrane. But the presence of cholesterol increases the zeta potential, suggesting the adsorption of Na^+ onto the membrane and preventing the binding of halide ions. We have summarised earlier studies in section 6.2. Detailed experimental results are given in section 6.3. We have concluded the chapter in section 6.4.

6.2 Earlier Studies

From the past decades giant unilamellar vesicles have become an extremely versatile model system that can be used in a wide range of biomedical applications (4). One can get GUVs of different size ranging up to few tens of micrometers from this method depending on variable experimental condition. Therefore, GUVs can serve as excellent model system to mimic freestanding lipid bilayer. Lipid bilayer, composed of positively charged lipid has drawn significant attention in DNA, mRNA transfection research and non-viral gene delivery (2) into a target cell. During the last decades, transfer of therapeutic gene (3) into the disordered cells by using non-viral gene carriers had achieved great attention in the field of biomedical and material sciences (4). Though cationic lipids are generally not encountered in nature, they have drawn much attention due to their potential for biomedical applications such as gene delivery. Although viral gene delivery is more efficient than non-viral, toxicity of the viral delivery is a serious issue. Cationic vesicles are nontoxic and bio compatible carriers of gene. Therefore, stability of these vesicles in a cellular environment would be important to enhance the efficiency of gene transfer. For safe and efficient gene delivery, developing new non-viral gene carriers with merit of low cytotoxicity (6) and high gene transfection performance (7) is regarded as major task. Till date, a number of cationic lipids (8–14), cationic polymers (15–19) and nanoparticles (20, 21) were developed as new non-viral gene carriers for gene delivery. Recent researches had revealed that the cytotoxicity, gene transfection efficiency and intercellular trafficking on non-viral gene carriers depend strongly on the molecular architectures (22). The cationic vesicles themselves can act as antimicrobial agents toward bacteria and fungi at concentrations that scarcely affect eukaryotic cells (5). Previous studies have revealed that different molecular factors such as presence of ions, cholesterol can influence the lipid-DNA complex and also change the antimicrobial activity of cationic vesicles (2). Na^+ and K^+ are the most abundant cations in the cellular fluid. Anions like Cl^- , Br^- and I^- are also found in all living organisms and play a vital role in maintaining hydration, balancing cations in the extracellular fluid for electrical neutrality in cellular fluid (2). Recent study revealed that presence alkali metal ions significantly affect the membrane integrity and hence stability of the system. Therefore, in the present study we intend to improve the stability of these vesicles by introducing cholesterol to the membrane. Cholesterol, is one of the natural-based lipids often participates in many biological processes including membrane formation, lipid transportation and so on (3). Cholesterol in a bio-membrane plays a significant role in many cellular events and is well known to regulate the

functional activity of protein and ion-channel. Inhomogeneous distribution of cholesterol, so called rafts has led to large number of studies on lipid-cholesterol membranes. Membrane cholesterol and partitioning of cholesterol in the membrane domains are also known to regulate ion-channel. Cholesterol can change the surface charge and electrostatic behaviour of the membrane. Within the membrane it can significantly alter elastic properties and permeability of the membrane (23). It has been developed as hydrophobic building block for the construction of functional cationic lipids (24). Earlier researches revealed that cholesterol derived cationic lipids could improve gene transfection efficiency. This motivates us to study the effect of cholesterol on the interaction of monovalent sodium salts with cationic membranes. Although a large number of studies on the interaction monovalent sodium salts with cationic, anionic or neutral membrane has been done already but the effect of cholesterol is overlooked in the literature studies. Further development of cationic vesicles as nonviral vectors and their biological implications is highly important. As discussed earlier both cholesterol and sodium salts have great effect on gene delivery process, gene transfection efficiency, so a systematic and detailed study needs to be elucidated. We have investigated systematically the interaction of different monovalent alkali metal salts with cationic membrane, composed of 1,2-dioleoyl-sn-glycero-3-phosphocholine (DOPC) / 1,2-dioleoyl-3-trimethylammonium-propane (DOTAP) in the presence of cholesterol. Unilamellar vesicles serve as excellent model system to study biological membrane. As model systems, we have prepared large unilamellar vesicles (LUV) and giant unilamellar vesicles (GUV) using extrusion and electroformation techniques. LUV will be used to study the interaction of membrane containing cholesterol with ions using dynamic light scattering and zeta potential study. Owing to the large size (diameter of GUV 10 – 100 μm), GUVs are directly visible under phase contrast optical microscope and as well as fluorescence microscope. Therefore, the present study can be utilized in a wide range of biophysical fields as well as the cell biology including biomedical applications.

6.3 Results

6.3.1 Effect of monovalent sodium salts on the size distributions of cationic vesicles

As model membranes, small unilamellar vesicles (SUV) have been prepared to study the ion-membrane interaction. The size distributions of the SUV in the presence of salts have been

monitored by dynamic light scattering (DLS). The average hydrodynamic radius of SUV for various concentrations of salt is depicted in fig. 6.1. In all cases, the polydispersity index is much less than 0.7, indicating SUVs are fairly monodisperse. We have shown the variation of average vesicle size with NaCl concentrations (fig 6.1a) and with NaI concentrations (fig. 6.1b) ranging from 0 to 100 mM in presence of different cholesterol concentrations (0, 5 and 10 mol%). From the results we can observe that, for both NaCl and NaI, average vesicle size increases with the increase of ion concentration when there is no cholesterol. But for 5 and 10 mol% cholesterol, vesicle size decreases with the increase of ion concentration. The increase in average size of the vesicles without cholesterol may be occurring due to aggregation of vesicles. However, in presence of cholesterol vesicle size is decreasing, which proves that cholesterol inhibits vesicle aggregation. It is known that reorientation of the DOPC head group occurs in the presence of cationic lipid which could also increase the hydrodynamic radius in the vicinity of the membrane.

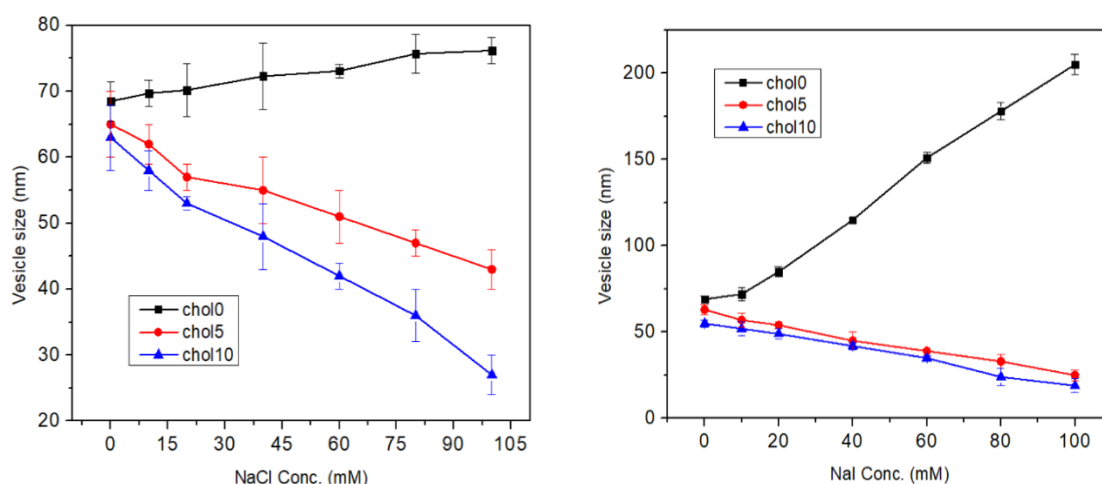


Fig. 6.1 Size distribution of SUV composed of DOPC-DOTAP (4:1) vesicles for different concentration of sodium salts (a) NaCl and (b) NaI at different cholesterol concentration (0, 5 and 10 mol%). Error bars were obtained from three independent measurements. Solid lines are intended as a guide to the experimental points.

6.3.2 Effect of cholesterol on zeta potential: Binding of ion with vesicles

Zeta potential can be a good approximation of surface potential at a moderate electrolyte concentration (10 - 100 mM). We have also estimated the binding constant of anions with positively charged vesicles using well known Gouy-Chapman theory. Without NaCl, the zeta

potential of positively charged vesicles composed of DOPC – DOTAP (4:1) was found to be 63 mV. In the presence of different sodium salts (NaCl and NaI), the positive zeta potential gradually decreases with increasing concentration of salt as shown in Fig.6.2. In case of anionic lipid, we have observed that zeta potential decreases with increasing cholesterol content even in the absence of monovalent ions. Without NaCl, the value of zeta potential at 5 mol% cholesterol is 67 mv and at 10 mol% cholesterol is 69 mv. So, in case of cationic lipid complex, zeta potential increases with increase in cholesterol content. The difference in such behaviour of anionic and cationic membranes could be due to the strong interplay between PC and TAP head groups, where the PC group reorients in the presence of TAP group [28]. This conjecture is supported by an earlier simulation study which shows that such an interplay leads to reorientation of the PC head group which gives rise to the significant change of the electrostatic properties of the membranes [29]. Here in the figure 6.2, we have observed that zeta potential decreases with the increase in ion concentration, when there is no cholesterol. This indicates adsorption of anions into the cationic membrane. However, the presence of cholesterol increases the zeta potential, suggesting the adsorption of Na^+ on to the membrane and preventing the binding of halide ions (fig. 6.2). In summary, the interaction of salt with the DOPC-DOTAP vesicles in presence of cholesterol shows entirely different behaviour relative to DOPC-DOPG vesicles. Therefore, besides electrostatic attraction, there are other factors, such as size of the ions, ion correlation, solvation, hydrophobic force, structure of water around the vesicles and ion hydration plays important role in the ion-membrane interaction.

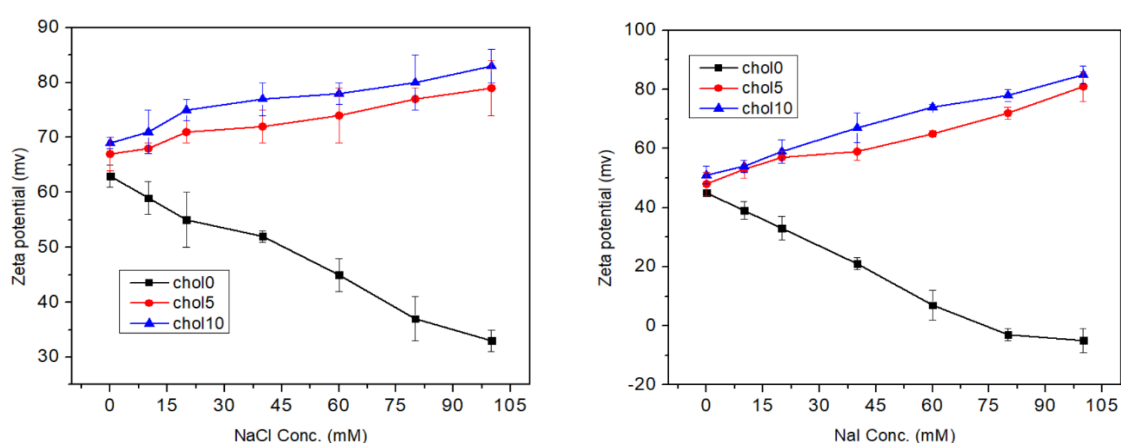


Fig. 6.2 The zeta potential of SUV obtained from a mixture of DOPC and DOTAP (4:1) for different concentration of sodium salts (a) NaCl and (b) NaI in the presence of various cholesterol

concentration. Solid lines are intended as guide points and not obtained from the fit. Errors in zeta value were obtained from three independent measurements.

The summary of the binding parameters of anions obtained from the zeta potential using Gouy Chapman theory has been presented in table 6.1. Detailed theory and procedure to obtain the intrinsic binding constant (K_{int}) has been described in chapter- 2 (experimental techniques) in the context of cation binding to the anionic membranes.

Table 6.1

Electrostatic parameters obtained from Gouy Chapman theory from the measured zeta potential for DOPC: DOTAP (4:1) in presence of cholesterol at a particular NaCl and NaI concentration 20 mM. SUVs are prepared from binary mixture of DOPC-DOTAP (4:1) and cholesterol.

NaCl				
Chol (mol%)	Surface potential (ψ_0) (mV)	Surface Charge (σ) (C/m^2)	Intrinsic concentration C_0 (M)	Binding constant (K) (M^{-1})
0	59	0.029	0.34	15.6
05	77	0.038	0.45	33.4
10	88	0.049	0.59	48.2
NaI				
Chol (mol%)	Surface potential (ψ_0) (mV)	Surface Charge (σ) (C/m^2)	Intrinsic concentration C_0 (M)	Binding constant (K) (M^{-1})
0	38	0.011	0.21	71.3
05	65	0.018	0.39	125.7
10	77	0.023	0.51	279.6

In the table 6.1, we have shown the variation of surface potential, surface charge density, surface concentration and binding constant with cholesterol concentration (ranging from 0 to 10 mol%) for particular ion concentration 20 mM. Both positive zeta potential and surface charge density increases with the increase of cholesterol concentration. When there is no cholesterol, the value of surface potential for 20 mM NaCl is 59 mv and for 20 mM NaI is 38 mv. As cholesterol conc. increases, surface potential increases for both the salts NaCl and NaI. The variation of surface charge density (σ), as shown in table 6.1, is known to have important biological implications in regulating immune responses of the human body. As the ion-membrane interaction alters significantly the electrostatics of the membranes, the

quantitative knowledge of surface potential, surface charge as well as intrinsic affinity towards ions has an important implication for optimizing the adjuvant effect of cationic vesicles and enhancing the efficacy of liposome-based vaccines.

6.3.3 Phase contrast microscopy of GUV exposed to various concentration of ion: Effect of cholesterol

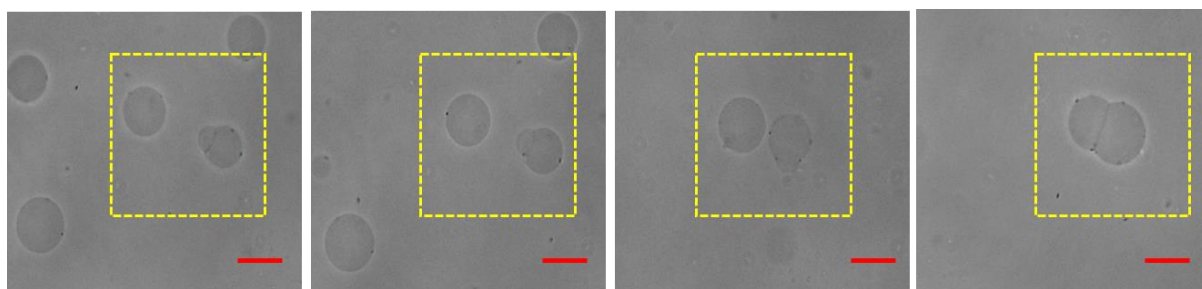
GUVs composed of cationic lipid composition DOPC-DOTAP (4:1) exhibits significant membrane-membrane interactions leading to the aggregation of vesicles. Further some vesicles are undergoing the process of pore formation and burst too. We will now discuss the pore formation, aggregation and membrane disruption induced by ion and effect of cholesterol on these phenomena. Since we are observing a single GUV in presence of other GUVs of different size, it can be considered that ion binding and distribution of cholesterol might have significant variations from vesicle to vesicle. The kinetics of pore formation and aggregation dynamics may also vary due to the different sizes of the vesicles.

- **Formation of transmembrane pores induced by cholesterol: Kinetics of pore formation**

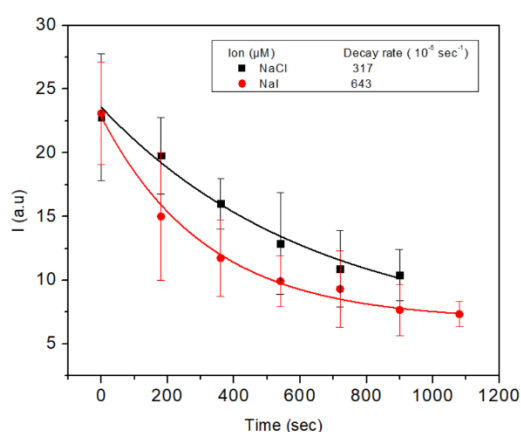
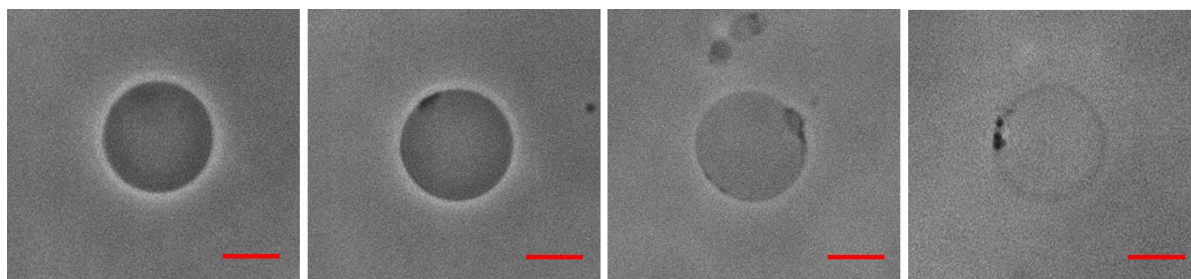
We have used phase contrast microscopy to observe the evidence of transmembrane pores in giant unilamellar vesicles (GUV) in presence of cholesterol. The pore formation activity was studied for various concentrations of cholesterol (0, 5 and 10 mol%). Fluorescence spectroscopy as well as microscopy were widely used to study the pore formation kinetics (36). The major drawback of this process is using fluorescence probe may affect and alter the membrane properties. There we have adopted a non-fluorescence based method phase contrast microscopy to investigate the membrane pores in giant vesicles. Due to their large size, GUVs can be observed and hence leakage or exchange of liquid between the interior and exterior of fluid can be seen with respect to time from phase contrast micrographs. The contrast of GUV images was enhanced by preparing GUV in sucrose and diluting it in a glucose solution maintaining the osmolality. Fig. 6.3 shows the phase constant micrographs taken against time from GUV made with DOPC-DOTAP lipid composition in presence of cholesterol. Initially GUV shows a halo region which indicates the good contrast between interior and exterior of the vesicles. The contrast in the halo region arises due to different refractive indices of glucose and sucrose solution. It is clearly evident from the micrographs that halo region in GUV images gradually disappears with time, and subsequently GUV looks like one without halo i.e GUV with similar external and internal fluids. The loss of contrast in

the halo region is occurring due to exchange between internal and external fluids through transmembrane pores. Here we have presented the effect of cholesterol on kinetics of pore formation. In the curve we have drawn the variation of I_{ptp} with time. This curve is characterised by decay rate constant whose value is decreasing with increasing cholesterol concentrations. The typical decay rate constants are given in the inset of figures.

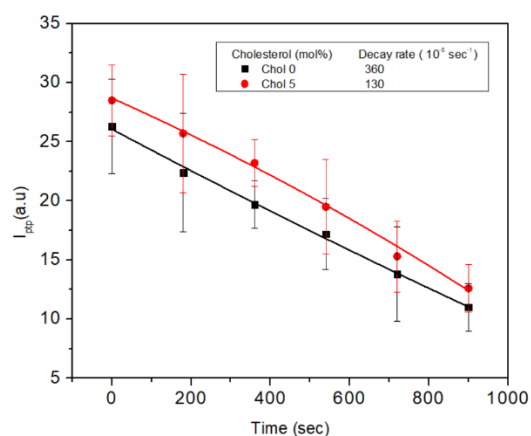
(a)



(b)



(c)



(d)

Fig.6.3 Phase contrast micrographs of GUV composed by DOPC-DOTAP (4:1) and NaI for different cholesterol concentrations (a) 0 & (b) 5 mol%. Figure (c) & (d) shows decrease in I_{ptp} with time, actually indicating kinetics of pore formation. Rate constants derived from the fit using single exponential decay are given in the inset of figure. Scale bar is 30 μm .

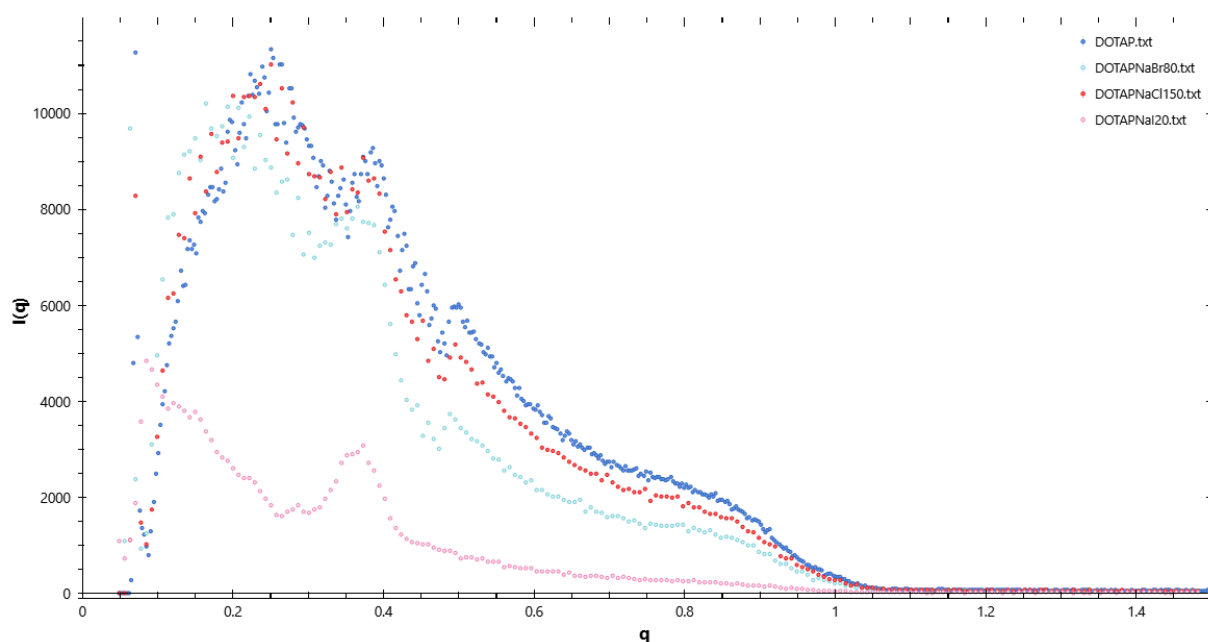
6.3.4 Small angle X-ray scattering (SAXS) studies

Aqueous solution of surfactant lipid complex DDAB-DOPC (4:1) and cationic –zwitterionic lipid complex DOPC-DOTAP (4:1) were studied using small angle x ray scattering (SAXS). Previously, Maity et al. studied the interaction of monovalent sodium salts with cationic lipid membranes. They systematically investigated effect of alkali metal ions on pure DOTAP and DOPC-DOTAP complex. In case of pure DOTAP, LUV solution becomes turbid, indicating the formation of aggregates for a particular concentration of salts. (> 80 mM for NaBr >150 mM for NaCl and >10 mM for NaI). Similarly, we have observed turbid solution of surfactant lipid complex in case of pure DDAB. However, no such aggregation was found for DDAB-DOPC complex. As already discussed, SAXS is a very important technique to study the structural details of macromolecules. Therefore, lipid and surfactant mixture using SAXS will be highly informative in terms of structure of the membrane. Variation of X-ray scattered intensity $I(q)$ as a function of scattering vector (q) upon exposure to salt concentrations at which solution becomes turbid is shown in the figure 6.4(a). The corresponding Guinier plot is shown in the figure 6.4(b). From the Guinier plot, radius of gyration R_g and $I(0)$ in the reciprocal space for pure DOTAP is estimated with the help of ATSAS 2.7.1 software package. Comparison of values of R_g and $I(0)$ for both pure DOTAP and DOTAP with salts is given in tabular form. During finding radius of gyration and $I(0)$ from the Guinier plot we have assumed the particle size to be globular and the system is taken as polydisperse sphere. From the pair distribution function $p(r)$ for pure DOTAP and DOTAP with ions we found that for the both the cases nature of distribution function is almost similar bell-shaped curves with peak at 4 \AA having maximum particle diameters (D_{\max}) 240 \AA for pure DOTAP and 215 \AA for DOTAP with ions (NaCl). As the value $D_{\max}^* S_{\min}$ is greater than the polydispersity index (PDI), so we can infer possibility of aggregation among vesicles.

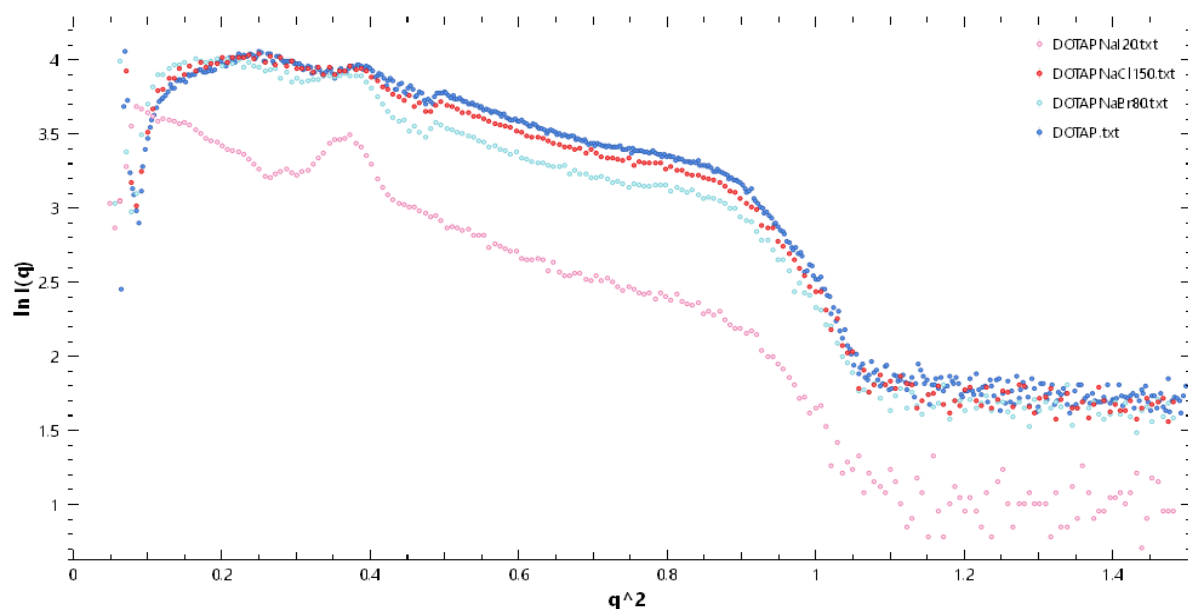
Table 6.3 Values of radius of gyration R_g and $I(0)$ obtained from the guinier plot of pure DOTAP and DOTAP-ion mixture using ATSAS 2.7.1 software package.

Solution	R_g (\AA)	$I(0)$
DOTAP	2.81 ± 0.10	11990 ± 273.05
DOTAP+150 mM NaCl	2.92 ± 0.15	11882.10 ± 376.87
DOTAP+80 mM NaBr	3.54 ± 0.18	11776 ± 306.96
DOTAP+10 mM NaI	6.94 ± 0.28	5103.29 ± 145.38

To understand the effect of DOPC on the interaction of cationic membrane with ions (2), it is desirable to study pure DOTAP as well as increasing concentration of DOPC in DOTAP/DOPC mixture. A significant increase in the mean diameter of DOTAP LUV with increasing NaI concentration has been observed.



(a)



(b)

Fig. 6.4 (a) Variation of X-ray scattered intensity $I(q)$ as a function of scattering vector (q in nm^{-1}) and (b) corresponding guinier plot of fig. (a).

Though for NaI, concentration is > 10 mM but for NaCl and NaBr, large aggregation has been found at high concentration of salt. At this particular concentration transparent vesicle solution becomes turbid. Such aggregation or turbid solution is only observed for pure DOTAP or pure DDAB solution. The large average size and high PDI of the distributions of pure DOTAP or pure DDAB vesicles for salt concentrations > 10 mM for NaI > 80 mM for NaBr and > 150 mM for NaCl are due to aggregation or the formation of nonlamellar dispersion of lipids. Previously it has been reported by Pokorna et al. (36) from time resolved fluorescence spectroscopy (TCSPC) as well as molecular dynamics simulation that Br^- is found to strongly and specifically absorb in the DOTAP head group region which causes lipid clustering via formation of $\text{TAP}^+ - \text{Br}^-$ ion complexes. In our experiment we also got similar ion complexes for I^- study. The volume and molecular weight of the lipids have been further enumerated from the porod plot that shows the variation of $q^4 I(q)$ as a function of q . We have observed from DLS results that without cholesterol, vesicle size is increasing. This might be happening due to aggregation of vesicles as evidenced from microscopy images of giant unilamellar vesicles. Similarly, from the SAXS study, we observe that without cholesterol there is an increase in radius of gyration for particular NaCl, NaBr and NaI concentration which is also indicating turbid or aggregation of vesicles. So, SAXS results are in agreement to the results from DLS and microscopy images. Further studies are underway to understand the phase and structures of aggregate in detail using SAXS.

References:

1. C. Herold, G. Chwastek, P. Schwille and E. P. Petrov. *Langmuir*, 28, 5518-5521(2012).
2. P. Maity, B. Saha, G. S. Kumar and S. Karmakar. *Langmuir*, 34, 9810-9817(2018).
3. R. Sheng, T. Luo, H. Li, J. Sun, Z. Wang and A. Cao. *Colloids and Surfaces B: Biointerfaces*, 116, 32-40(2014).
4. C. Herold, P. Schwille, P. E. Petrov., *Phy. Rev. Lett.* 101, 148102(2010).
5. B. D. Viera, M. A. Carnona-Ribeiro. Cationic lipids and surfactants as antifungal agents: mode of action. *J. Antimicrob. Chemother.*, 58, 760-767(2006).
6. D. Putnam, *Nat. Mater.* 5, 439–451(2006).

7. J.L. Santos, H. Oliveira, D. Pandita, J. Rodrigues, A.P. Pego, P.L. Granja, H. Tomas, J. Controlled Release 144, 55–64(2010).
8. S. Bhattacharya, A. Bajaj, Chem. Commun. 4632–4656(2009).
9. A. Bajaj, P. Kondiah, S. Bhattacharya, J. Med. Chem. 50, 2432–2442(2007).
10. D. Zhi, S. Zhang, B. Wang, Y. Zhao, B. Yang, S. Yu, Bioconjugate Chem. 21, 563–577(2010).
11. R. Mukthavaram, S. Marepally, M.Y. Venkata, G.N. Vegi, R. Sistla, A. Chaudhuri, Biomaterials 30, 369–2384(2009).
12. A. El-Aneed, J. Controlled Release 94, 1–14(2004).
13. X. Guo, F.C. Szoka, Acc. Chem. Res. 36, 335–341(2003).
14. J.J. Green, R. Langer, D.G. Anderson, Acc. Chem. Res. 41, 749–759(2008).
15. S.Y. Wong, J.M. Pelet, D. Putnam, Prog. Polym. Sci. 32, 799–837(2007).
16. M. Morille, C. Passirani, A. Vonarbourg, A. Clavreul, J.P. Benoit, Biomaterials 29, 3477–3496(2008).
17. H. Cheng, J.L. Zhu, X. Zeng, Y. Jing, X.Z. Zhang, R.X. Zhuo, Bioconjugate Chem. 20, 481–487(2009).
18. M.S. Shim, C.S. Kim, Y.C. Ahn, Z. Chen, Y.J. Kwon, J. Am. Chem. Soc. 132, 8316–8324(2010).
19. M.V. Yezhelyev, L. Qi, R.M. O'Regan, S. Nie, X. Gao, J. Am. Chem. Soc. 130, 9006–9012 (2008).
20. R.I. Mahato, Adv. Drug Delivery Rev. 57, 699–712(2005).
21. S. Chesnoy and L. Huang, Annu. Rev. Biophys. Biomol. Struct, 29, 27-47 (2000).
22. L. Waunga and D. Hoekstra, Journal of Controlled Release 116, 255-264(2006).
23. K. K. Banerjee, P. Maity, S. Das and S. Karmakar. Chem. Phys. Lipids, 254, 105307(2023).
24. M.A. Mintzer, E.E. Simanek, Chem. Rev. 109, 259–302(2009).
25. Angelova, M. I.; Dimitrov, D. S. Faraday Discuss. 81, 303–311(1986).

26. D. Ibraheem, A. Elaissari and H. Fessi. *International Journal of Pharmaceutics* 459, 70-83(2014).
27. Martina Havlíková, Jana Szabová, Ludmila Mravcová, Tereza Venerová, Chien-Hsiang Chang, Miloslav Pekař, Adam Jugl and Filip Mravec *Langmuir* 37, 2436-2444(2021).
28. A. A. Gurtovenko, M. Miettinen, M. Karttunen, I. Vattulainen, *J. Phys. Chem. B*, 109, 21126-21134 (2005).
29. A. A. Gutovenko, M. Patra, M. Karttunen, I. Vattulainen., *Biophys. J*, **86**, 3461-3472 (2004).
30. Godbey, W. T.; Mikos, A. G. Recent progress in gene delivery using non-viral transfer complexes. *J. Controlled Release*, 72,115–125 (2001).
31. Simberg, D.; Weisman, S.; Talmon, Y.; Barenholz, Chemistry, Biophysics, and Transfection. *Crit. Rev. Ther. Drug Carrier Syst.* 21, 257–317(2004).
32. Clark, P. R.; Hersh, E. M. *Curr. Opin. Mol. Ther.* 1, 158(1999).
33. Safinya, C. Structures of lipid-DNA complexes: supramolecular assembly and gene delivery. *Curr. Opin. Struct. Biol.* 11, 440–448(2001).
34. Lv, H.; Zhang, S.; Wang, B.; Cui, S.; Yan, J. Toxicity of cationic lipids and cationic polymers in gene delivery. *J. Controlled Release* 114, 100–109(2006).
35. Schröder-Born, H.; Willumeit, R.; Brandenburg, K.; Andra, J. *Biochim. Biophys. Acta* 1612, 164-171(2003).
36. Pokorna, S.; Jurkiewicz, P.; Cwiklik, L.; Vazbar, M.; Hof, M.; *Faraday Discuss*, 160, 341-358 (2013).

List of publications

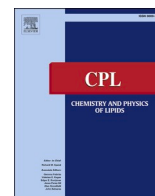
(Included in the thesis)

1. **Kalyan Kumar Banerjee**, Pabitra Maity, Surajit Das, Sanat Karmakar, *Effect of cholesterol on the ion-membrane interaction: Zeta potential and dynamic light scattering study*, *Chem. Phys. Lipids*, 254(2023), 105307. (Impact factor: 3.4)
2. **Kalyan Kumar Banerjee**, Pabitra Maity, Surajit Das, Sanat Karmakar, *Cholesterol modulates the interaction of sodium salt with negatively charged phospholipid membrane*, *Biophysical Chemistry*, 317(2025), 107354. (Impact factor: 3.3)
3. **Kalyan Kumar Banerjee**, Surajit Das, Sanat Karmakar, *Interaction of alkali metal ions with phospholipid membranes: Effect of cholesterol*. Submitted to *Journal of surface science and technology*.
4. **Kalyan Kumar Banerjee**, Surajit Das, Sanat Karmakar, *Cholesterol affects significantly on the interaction of alkali metal salt with cationic vesicles*. To be submitted.

Other publications

5. Sanat Karmakar, Surajit Das and **Kalyan Kumar Banerjee**, *Interaction of antimicrobial peptides with model membranes: a perspective towards new antibiotics*, EPJ ST, 233(2024), 2981-2996. (Impact factor: 2.6)
6. Surajit Das, Rajeev Jain, **Kalyan Kumar Banerjee**, Sanat Karmakar, *Cholesterol-driven modulation of membrane-membrane interactions by an antimicrobial peptide, NK-2, in phospholipid vesicles*, BBRC, 741(2024), 151021. (Impact factor: 2.5)
7. Surajit Das, Rajeev Jain, **Kalyan Kumar Banerjee**, Pabitra Maity, Krishnananda Chattopadhyay & Sanat Karmakar, *Cholesterol affects the pore formation and the membrane-membrane interaction induced by an antimicrobial peptide, NK-2, in phospholipid vesicles*, J. Membr. Biol., 258(2025) 237-252. (Impact factor: 2.3)

Reprint of Papers ...



Effect of cholesterol on the ion-membrane interaction: Zeta potential and dynamic light scattering study

Kalyan Kumar Banerjee, Pabitra Maity, Surajit Das, Sanat Karmakar^{*}

Soft matter and Biophysics Laboratory, Department of Physics, Jadavpur University, 188, Raja S. C. Mallick Road, Kolkata 700032, India

ARTICLE INFO

Keywords:

Phospholipids
Cholesterol
Bio-membrane
Alkali metal ions
Zeta potential
DLS

ABSTRACT

Cholesterol in a bio-membrane plays a significant role in many cellular event and is known to regulate the functional activity of protein and ion channel. In this study we report a significant effect of cholesterol on the ion-membrane interaction. We prepare large unilamellar vesicles, composed of zwitterionic lipid DOPC and anionic lipid DOPG with different cholesterol concentration. Electrostatics of anionic membranes containing cholesterol in the presence of NaCl has systematically been explored using dynamic light scattering and zeta potential. Negative zeta potential of the membrane decreases its negative value with increasing ion concentration for all cholesterol concentrations. However, zeta potential itself decreases with increasing cholesterol content even in the absence of monovalent ions. Electrostatic behaviour of the membrane is determined from well-known Gouy Chapmann model. Negative surface charge density of the membrane decreases with increasing cholesterol content. Binding constant, estimated from the electrostatic double layer theory, is found to increase significantly in the presence of cholesterol. Comparison of electrostatic parameters of the membrane in the presence and absence of cholesterol suggests that cholesterol significantly alter the electrostatic behaviour of the membrane.

1. Introduction

Cholesterol is a ubiquitous component of all animal cell membranes. It plays a vital role in maintaining structure and regulating functions and properties of membranes (Finegold, 1993). Inhomogeneous distribution of cholesterol, so called rafts, has led to large number of studies on lipid-cholesterol membranes (Subczynski et al., 2017; de Meyer and Smit, 2009; Rivel et al., 2019; Simons and Ikonen, 1997). Membrane cholesterol and partitioning of cholesterol into the membrane domains are also known to regulate ion channel (Levitani et al., 2014). Activity of the ion channel is highly influenced by the level of membrane cholesterol. For example, increase in the cholesterol level leads to suppression of ion-channel activity (Levitani et al., 2010). Besides ion transport, ions in the membrane regulate the surface charge which in turn affect the efficiency of the drug delivery liposome with the immune system (Klausen et al., 2016; Melcrová et al., 2016). Ions also alters the interaction of peripheral membrane protein (Boes et al., 2021). Studies on the effect of various ions, especially alkali metal ions on the phospholipid membranes has received a significant attention in view of understanding ion transports and other biological functions (Deplazes et al., 2020; Catte et al., 2016; Binder and Zschornig, 2002). Recently we have

explored effect of alkali metal ions on the electrostatic and thermodynamics properties of the membranes (Maity et al., 1858, 2016). As cholesterol regulates the ion transports across the membranes, we intend to investigate the effect of cholesterol on the ion-membrane interaction.

A variety experimental techniques along with computer simulation has been employed in order to gain insights into the ion-membrane interaction (Friedman, 2018; Melcr et al., 2018; Deplazes et al., 2019). Ion-membrane interaction has an important role in restructuring of macromolecules, such as proteins, peptides, etc. at the membrane-solvent interface and in modulating the membrane properties (Friedman, 2018; Kunz et al., 2014). For example, asymmetric binding of Na⁺ and Cl⁻ showed significant influence on the ion transport across the bilayer (Lee et al., 2008). Among all different monovalent ions, present in the intra-cellular and extra cellular fluid, Na⁺, K⁺ are most abundant cations. Recently binding of these cations with different lipids have been studied in details (Melcr et al., 2018). Na⁺ has higher binding affinity than K⁺ and all other alkali metal ions except Li⁺ (Klasczyk et al., 2010). However, the measurement of binding affinity for different ions to the phospholipid membranes is incredibly complex, and there is considerable variation of binding affinities even for a particular ion to a specific lipid bilayer (Catte et al., 2016). Anions such as Cl⁻ also plays a

^{*} Corresponding author.

E-mail address: sanat.karmakar@jadavpuruniversity.in (S. Karmakar).



Cholesterol modulates the interaction of sodium salt with negatively charged phospholipid membrane

Kalyan Kumar Banerjee, Pabitra Maity, Surajit Das, Sanat Karmakar *

Soft matter and Biophysics Laboratory, Department of Physics, Jadavpur University, 188, Raja S. C. Mallick Road, Kolkata 700032, India

ARTICLE INFO

Keywords:

Membrane

Cholesterol

NaI

ITC

Zeta potential

Fluorescence spectroscopy

ABSTRACT

We present a systematic study on how alkali metal salts, like NaCl and NaI, affect negatively charged phospholipid vesicles using a range of experimental methods. Our goal was to find out how chain saturation and cholesterol affect the interaction between the ions and the membrane. An isothermal titration calorimetry study on large unilamellar vesicles made from dimyristoyl phosphatidylcholine (DMPC) revealed that Na^+ shows higher binding affinity to the gel phase at 15 °C compared to the fluid phase at 30 °C. Further, cations also show stronger affinity to the membrane in the fluid composed of saturated lipids than that of unsaturated lipids. The binding affinity of Na^+ with anionic vesicles prepared from a mixture of DMPC and DMPG was found to decrease significantly with increasing cholesterol as well as salt concentrations, as revealed by the zeta potential study. Besides the binding constant, the Gouy Chapman theory based on the electrostatic double layer shows that cholesterol reduces the surface charge density without altering the significant area per molecule. Further, the effect of counterions was investigated using fluorescence spectroscopy of an environment-sensitive lipophilic dye, Nile red. Although cholesterol alters the emission properties of Nile red significantly, there is no significant change in the presence of ions. This result suggests that anions do not bind significantly to anionic vesicles. The main striking feature of the ion-membrane interaction in the presence of cholesterol is that membranes with saturated lipids exhibit a completely opposite trend from membranes with unsaturated lipids.

1. Introduction

The lipid bilayer is the structural basis of all biological membranes. Unilamellar vesicles, which are single bilayer shell, serve as an excellent model system to study the structure and function of biological membranes. Studies on ion-membrane interaction, for example, yield significant insights into the effect of ions on the membrane's transport properties. The presence of ions, especially alkali metal ions, leads to a significant alteration of the electrostatic properties of the membrane [1,2]. For example, the rate of lipid flip-flop dynamics is greatly influenced by ions in the membranes. The asymmetric binding of Na^+ and K^+ causes the transmembrane potential. Ion-induced defects are known to regulate permeation processes, diffusion mechanisms, and the free energy barrier [3,4]. Anions and cations in the membranes are capable of modifying the membrane surface potential [5] and dipole potential [6]. The distribution of ions at the membrane-water interface plays an important role in substantially modifying the structure and dynamics of the membranes [7]. For instance, head group conformational fluctuations, such as changes in tilt angle, are a determining factor in structural

rearrangements upon adsorption of ions onto the membrane [8].

It has been shown that the water layer, i.e., the hydration layer, plays an important role in the ion-membrane interaction. Therefore, low hydration or partial hydration in the gel phase prevents ion penetration into the core of the bilayer as compared with the bilayer in the liquid-crystalline phase. Weak binding of Na^+ ions in the gel phase was explained by low hydration and less penetration or exchange of ions due to the more compact structure of the bilayers in this phase. Besides the anionic membrane, neutral vesicles made from phosphatidylcholine (PC) can also interact significantly [5]. Entropic contribution and water dynamics at the membrane interface may play an important role in determining the interaction of ions with the zwitterionic membrane [9]. However, the question remains: does chain saturation play any role in the ion-binding process? There are many earlier reports that showed the binding affinity of Na^+ ions with DOPC and DOPG membranes. It was generally overlooked to study saturated lipids due to their higher chain melting transition. In this study, we have investigated the effect of chain saturation and compared it with that of unsaturated lipids.

Cholesterol is an essential and ubiquitous component of all plasma

* Corresponding author.

E-mail address: sanat.karmakar@jadavpuruniversity.in (S. Karmakar).

<https://doi.org/10.1016/j.bpc.2024.107354>


Received 26 July 2024; Received in revised form 13 November 2024; Accepted 13 November 2024

Available online 19 November 2024

0301-4622/© 2024 Published by Elsevier B.V.



Interaction of antimicrobial peptides with model membranes: a perspective towards new antibiotics

Sanat Karmakar^a , Surajit Das^b, and Kalyan Kumar Banerjee^c

Department of Physics, Jadavpur University, 188, Raja S. C. Mullick Road, Kolkata, West Bengal 700032, India

Received 29 September 2023 / Accepted 22 January 2024 / Published online 19 February 2024
© The Author(s), under exclusive licence to EDP Sciences, Springer-Verlag GmbH Germany, part of Springer Nature 2024

Abstract Antimicrobial peptides (AMPs), found in both animals and plants, are used to fend off a wide variety of invading pathogens, such as bacteria, fungi, protozoa, viruses, etc. Their widespread distribution and defensive activity towards all different microbes lead to the successful evolution of complex multicellular organisms. In particular, AMPs target bacterial membranes and disrupt the membrane via the formation of transmembrane pores without interacting with any specific receptors. It is known that different antimicrobial peptides use different mechanisms to disrupt the membrane by forming transmembrane pores. The interaction of the antimicrobial peptide with the membrane depends on peptide charge, hydrophobicity, membrane composition, etc. Therefore, to get insights into the mechanisms of membrane disruption, it is useful to study the model membrane, as biological membranes are complex and regulated by various other proteins, cholesterol, etc. In the present review, we will primarily describe the interaction of antimicrobial peptides with phospholipid membranes, which mimic the bacterial membrane, in view of understanding the mechanism of action, various factors affecting their activity, application prospects in drug therapeutics, etc.

1 Introduction

Antimicrobial peptides (AMPs) are a diverse group of molecules that are evolutionarily conserved components of the innate immune response in the animal and human body against invading pathogens, such as viruses, fungi, bacteria, protozoa, etc [1, 2]. Prolonged use of conventional antibiotics leads to resistance to the spectrum of bacteria and other invading pathogens. Hence, there is an urgent need for alternatives to the common antibiotics [3]. Therefore, the current research focuses on the development of novel methods to get rid of the inevitable resistance that develops with conventional antibiotics [4–6]. A large number of recent studies have suggested that AMPs have the potential to act as excellent antibiotic toward a broad-spectrum of Gram-positive and Gram-negative bacteria [7]. The unique mode of action with less bacterial resistance than conventional antibiotics has led to a new possibility in the development of AMPs as human therapeutics [8].

A total of 3569 antimicrobial peptides have been reported in the Antimicrobial Peptide Database (<https://aps.unmc.edu>). AMPs mostly contain 10–60 amino acid residues. Almost all of them are cationic, and a few AMPs are found to be anionic in nature [9]. AMPs, which are a unique and diverse group of molecules found in bacteriolytic substances, basic antimicrobial proteins, and basic linear tissue polypeptides, are classified on the basis of their source, amino acid composition, structural characteristics, such as size, sequence, charge, conformation and structure, hydrophobicity, amphipathicity, etc. [1, 7]. Classes of AMPs are summarised in Table 1 [1]. In the present review, we are not elucidating the details of the various classes of AMP. However, some details can be found in Ref. [1] and references therein. Current research focuses on host-derived antimicrobial molecules, particularly antimicrobial fragments of large proteins, which are identified as possible alternatives to therapeutics for the treatment of antibiotic-resistant bacterial infections [10, 11].

AMP-mediated cell killing may be rapid or may take several minutes (~ 15 –90 min). Further, different AMPs use different mechanisms to destroy cellular integrity. It is extremely difficult and technically challenging to unravel

^a e-mail: sanat.karmakar@jadavpuruniversity.in (corresponding author)

^b e-mail: surajitphys@gmail.com

^c e-mail: kalyanbanerjee802@gmail.com



Cholesterol-driven modulation of membrane-membrane interactions by an antimicrobial peptide, NK-2, in phospholipid vesicles

Surajit Das^a, Rajeev Jain^{b,c}, Kalyan Kumar Banerjee^a, Krishnananda Chattopadhyay^{b,c}, Sanat Karmakar^{a,*}

^a Soft Matter and Biophysics Laboratory, Department of Physics, Jadavpur University, 188, Raja S. C. Mullick Road, Kolkata, 700032, India

^b Structural Biology & Bio-Informatics Division, CSIR, Indian Institute of Chemical Biology, 4, Raja S. C. Mullick Road, Kolkata, 700032, India

^c Academy of Scientific and Innovative Research (AcSIR), CSIR- Human Resource Development Centre, (CSIR-HDRC) Campus, Ghaziabad, Uttar Pradesh, 201 002, India

ARTICLE INFO

Keywords:

Vesicles
Membrane
Antimicrobial peptide
Cholesterol
Phase contrast microscopy

ABSTRACT

Antimicrobial peptides (AMPs) are essential components of the innate immune system, demonstrating their antimicrobial effects primarily through the creation of transmembrane pores that result in membrane disruption. Cholesterol within the membrane can significantly affect the interaction between AMPs and the membrane, as it is known to alter both the permeability and elastic properties of the membrane. In this study, we have investigated the influence of cholesterol on the interaction of the AMP, NK-2 with phospholipid vesicles. We prepared giant unilamellar vesicles (GUVs) composed of DOPC-DOPG and Egg PC, varying the cholesterol concentrations, and analyzed them using phase contrast microscopy. The aggregation of vesicles is evident in the phase contrast microscopy observations of GUVs. The aggregation of GUVs with cholesterol ultimately leads to a collapse state, a condition not typically seen in GUVs lacking cholesterol. Furthermore, the aggregation kinetics were determined from the analysis of phase contrast micrographs. This biophysical investigation offers valuable insights into how cholesterol affects the interactions between membranes induced by antimicrobial peptides.

1. Introduction

Antimicrobial peptides (AMPs) constitute a crucial component of the innate immune response found in both animals and humans, providing defense against various invading pathogens, including viruses, fungi, and bacteria. These peptides function by directly compromising the integrity of bacterial membranes, rather than engaging with specific receptors. They specifically target the negatively charged regions of bacterial membranes, inducing defects such as pore formation, which ultimately results in membrane disruption [1]. The extended and excessive use of conventional antibiotics can lead to the emergence of bacterial resistance. Consequently, to address the unavoidable resistance that arises from the use of conventional antibiotics, it is essential for the development of peptide antibiotics [2]. A significant distinction between bacterial and eukaryotic cell membranes lies in the substantial presence of cholesterol within eukaryotic cell membranes, whereas bacterial cell membranes lack cholesterol entirely. Therefore, An important question that needs to be addressed is: does cholesterol play a role in bacterial selectivity?

The primary goal of the present research is to investigate the effect of cholesterol on the antimicrobial activity of the peptide NK-2 in the model membrane. The highest density of cationic core region (residues K39–K65) of NK-lysin yields NK-2, a potent antimicrobial peptide known to kill cancer cells [3]. It also exhibits antimicrobial activity against bacteria, such as *E. coli* and fungi [4], as well as against the protozoan parasites *Trypanosoma cruzi* [5] and *Plasmodium falciparum* [6]. Studies on model membranes demonstrated that cholesterol significantly reduces the binding of AMP and is also known to prevent the disintegration of the lipid bilayer [7–9]. Cholesterol is known to enhance the stiffness of the membrane, which subsequently elevates the bending rigidity as well as membrane permeability [10,11]. Such an increased stiffness may inhibit the formation of pores by an antimicrobial peptide (AMP), thereby preventing membrane disruption [12,13].

One must contemplate whether the reduction in antimicrobial activity results from a direct interaction between cholesterol and the antimicrobial peptide (AMP) or if it is a consequence of changes in membrane properties induced by the presence of cholesterol. Earlier studies on the model membrane revealed that cholesterol showed a

* Corresponding author.

E-mail address: sanat.karmakar@jadavpuruniversity.in (S. Karmakar).

<https://doi.org/10.1016/j.bbrc.2024.151021>

Received 14 November 2024; Accepted 18 November 2024

Available online 21 November 2024

0006-291X/© 2024 Elsevier Inc. All rights are reserved, including those for text and data mining, AI training, and similar technologies.



Cholesterol Affects the Pore Formation and the Membrane–Membrane Interaction Induced by an Antimicrobial Peptide, NK-2, in Phospholipid Vesicles

Surajit Das¹ · Rajeev Jain^{2,3} · Kalyan Kumar Banerjee¹ · Pabitra Maity¹ · Krishnananda Chattopadhyay^{2,3} · Sanat Karmakar¹

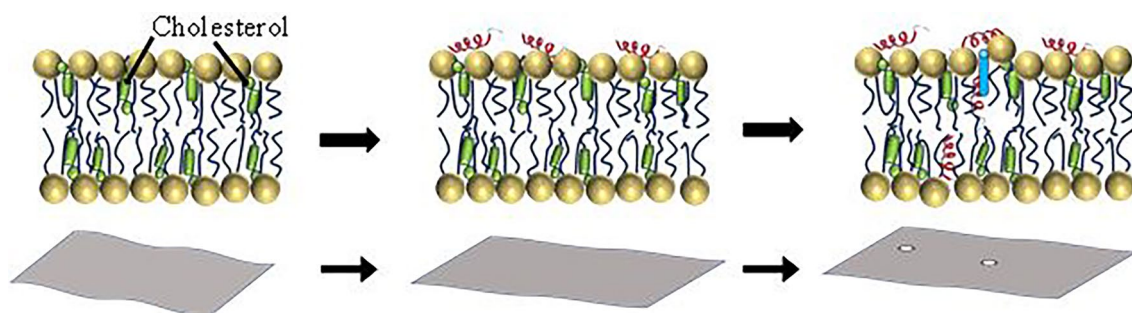
Received: 16 February 2025 / Accepted: 21 April 2025 / Published online: 3 May 2025

© The Author(s), under exclusive licence to Springer Science+Business Media, LLC, part of Springer Nature 2025

Abstract

Antimicrobial peptides are part of the innate immune response and show their antimicrobial activity by forming pores, followed by disintegration of the membrane. Cholesterol in the membrane can affect the pore formation process, as cholesterol is known to alter the permeability and elastic properties of the membrane. The present research systematically explores the role of cholesterol in modulating the interaction of the antimicrobial peptide NK-2 with phospholipid membranes, as well as the processes of pore formation induced by NK-2 within the membrane. Large unilamellar vesicles (LUVs) and giant unilamellar vesicles (GUVs) made from DOPC-DOPG and Egg PC with varying cholesterol concentrations have been studied using a variety of experimental techniques. The present study revealed that both the magnitude of zeta potential and surface charge density diminished as cholesterol concentrations increased at an intermediate NK-2 concentration. The proliferation of the size distributions of LUVs containing cholesterol when exposed to NK-2 indicates the occurrence of vesicle aggregation. The phase contrast micrographs of GUVs as well as the calcein release experiments on LUVs show evidence of pores. Notably, the incorporation of cholesterol into the membrane was found to have a significant effect on both the permeability of the membrane and the kinetics of the pore formation process. This biophysical research contributes essential knowledge regarding the role of cholesterol in influencing the antimicrobial efficacy of the membrane.

Graphical Abstract



Keywords Vesicles · Membrane · Antimicrobial peptide · Cholesterol · Phase contrast microscopy

Introduction

Antimicrobial peptides (AMPs) are part of the innate immune response in all animals and humans against invading pathogens, like viruses, fungi, and bacteria. AMPs are

known to act by directly destabilizing target bacterial membranes without interacting with specific receptors. They target the negatively charged surface of bacterial membranes and create defects, such as pores, leading to disruption of the membrane (Brogden 2005; Karmakar et al. 2024). The prolonged and excessive use of conventional antibiotics can

Extended author information available on the last page of the article